

# Reactive power control during power system restoration and HVDC investigation



---

**André Petersson**  
**Christian Bergstrand**

Division of Industrial Electrical Engineering and Automation  
Faculty of Engineering, Lund University

# Abstract

As the society gets more and more dependent on electrical energy, it is highly desirable to ensure power supply at all times. In case of events of natural disasters, simple technical faults or human mistakes, any power system or a large part of it can suffer a blackout. An electrical shutdown is a crisis situation where recovery should happen as quickly as possible.

During the restoration after the blackout in Sweden and Denmark on 23 September 2003, one problem that delayed restoration was reactor hunting.

This thesis suggests a method to avoid hunting and decrease the time of restoration. The result consists of an equation, which uses a variable that describes the strength of the net and with this equation new settings for the *Extreme Voltage Automatics (EVA)* in the system can be calculated.

The method is tested through simulations of NORDIC32 in ARISTO. Many restoration sequences are tested and reactor hunting is avoided in all of them.

Further investigations on how *VSC-HVDC* connections can assist in power restoration have been made. The conclusion is that it works and that it also is possible to energize lines. It is shown that a system is less sensitive to voltage fluctuations, when HVDC is used. That means shunt reactors can be used with existing automatics during power restoration with HVDC.

**Keywords:** Power restoration, reactor hunting, reactive power control, VSC-HVDC.

# Sammanfattning

Samhället blir mer och mer beroende av elektricitet och det är mycket önskvärt att säkerställa att produktionen alltid fungerar. Vid eventuell naturkatastrof, tekniskt fel eller mänskligt misstag kan det Svenska elnätet drabbas av ett elavbrott. Ett sådant avbrott är en krissituation där återstart måste ske så fort som möjligt.

Under återstarten efter strömavbrottet i Sverige och Danmark den 23 september 2003, var ett av problemen som försenade återstarten reaktorpumpning.

Det här examensarbetet föreslår en metod att undvika *reaktorpumpning* för att minska återstartstiden av elnätet. Resultatet består av en ekvation, med en variabel som beskriver styrkan i elnätet, och med ekvationen beräkna nya inställningar till *extremspänningsautomatiken* som finns i systemet.

Metoden är testad med simuleringar av NORDIC32 i ARISTO. Många återstartssekvenser har testats och reaktorpumpning undviks i samtliga.

Vidare undersökningar har gjorts på hur *VSC-HVDC* anslutningar kan stödja under återstart. Slutsatsen är att det fungerar och att det är möjligt att elektrifiera ledningar. Det visas att ett system är mindre känsligt för spänningsvariationer när *VSC-HVDC* är anslutet. Det betyder att shuntreaktorer kan användas med befintlig automatik under återstart av ett elnät med HVDC.

# **Acknowledgement**

We would like to thank our supervisor Reza Safari for all his support. With his knowledge and feedback he has been a big help during the whole project. During difficulties he has been leading us towards the right path. We also wish to thank our examiner Olof Samuelsson for his guidance and support. His experience with master theses has laid a solid foundation for our work. Further we want to thank Lars Lindgren for helping us with the ARISTO software and for valuable discussions. Lastly we thank our contact at Svenska Kraftnät, Barbro Andersson, for her answers and feedback to our questions regarding power restoration.

# Abbreviations

**Ssc** – Short circuit capacity

**EVA** – Extreme voltage automatics

**VSC-HVDC** – Voltage source converter - high voltage direct current

**TSO** – Transmission system operator

**Hunting** – Reactor hunting

**PWM** – Pulse width modulation

**ARISTO** – Advanced real time interactive simulator for training and operation

# Contents

Abstract .....	i
Sammanfattning.....	ii
Acknowledgement.....	iii
Abbreviations .....	iv
Contents .....	v
1 Introduction.....	1
1.1 Background.....	1
1.2 Scope of thesis.....	2
Reactor hunting .....	2
VSC-HVDC performance .....	2
1.3 Previous work .....	2
1.4 Aims .....	3
Reactor hunting .....	3
VSC-HVDC .....	3
1.5 Contribution .....	3
Reactor hunting .....	3
VSC-HVDC .....	4
1.6 Applications .....	4
1.7 Outline of the thesis .....	4
2 Theory.....	5
2.1 Voltage profile .....	5
2.1.1 Transmission line .....	5
2.1.1 The Ferranti effect.....	6
2.1.2 SIL-Surge Impedance Loading.....	6
2.2 Voltage regulation .....	7
2.2.1 Shunt Reactor .....	7
2.2.2 Reactor Hunting.....	8
2.3 HVDC transmission .....	8
2.3.1 VSC – Voltage Source Converter .....	9
2.3.2 Control system VSC-HVDC.....	10
2.4 Future HVDC links.....	11

2.4.1 SydVästlänken .....	11
2.4.2 The Gotland Link.....	12
2.4.3 NordBalt .....	13
2.4.4 Overview of other HVDC projects .....	13
2.5 Restoration .....	14
2.5.1 Islands in power systems.....	14
2.5.2 The Process of Restoration.....	15
2.5.3 Reactive power compensation and net strength .....	15
2.5.5 Cold load pickup .....	16
3 Programs and models.....	18
3.1 Nordic32 Model.....	18
3.2 Aristo .....	19
3.3 Power Factory.....	19
4 Method for avoiding reactor hunting.....	20
4.1 Process to solution. ....	20
4.1.1 Determine short circuit capacity .....	20
4.1.2 Experimental method for determining Short circuit capacity.....	21
4.1.3 Tolerance band shunt automatics.....	22
4.1.4 Over voltage vs. under voltage.....	23
4.1.5 Finding the weakest restoration strategy .....	23
4.2 Simulations .....	24
4.2.1 Initial system.....	24
4.2.2 Method used for gathering data .....	25
4.3 Verification of thresholds .....	26
4.4 Restoration of whole grid with load and generation .....	27
4.5 Theoretical analysis of method .....	27
5 Method HVDC investigation .....	29
5.1 HVDC Modelling .....	29
5.2 HVDC simulation.....	30
6 Results on avoiding reactor hunting.....	33
6.1 Relationship between Ssc and tolerance band of automatics .....	33
6.1.1 Experimental determination of Ssc .....	34
6.1.2 Weakest power restoration strategy .....	35
6.1.3 Data gathering to find relation between Ssc and $\Delta V$ .....	37

6.2 Theoretical result .....	40
7 Results HVDC .....	47
7.1 HVDC performance.....	47
7.2 Energizing with VSC-HVDC and connecting shunt.....	51
8 Verification .....	53
8.1 Verification of results in 6.1 .....	53
8.2 Restoration of whole grid with load and generation .....	61
8.3 Larger blackout.....	63
8.4 Northern blackout .....	65
9 Discussion and conclusion .....	67
9.1 Reactor hunting.....	67
9.1.2 Reliability of verification.....	67
9.3 Discussion on theoretical analysis of Ssc.....	68
9.4 HVDC performance.....	69
9.6 Future work .....	70
References.....	72
Appendix A .....	73
Paths for gathering data.....	73
Appendix B .....	76
DC cable parameters .....	76





# 1 Introduction

The Swedish power system has several times been exposed to massive power system faults, referred to as *blackouts or outages*. It is impossible to predict where and when this power fault will occur. Therefore even if great efforts are made to avoid blackouts it is necessary to also prepare for restoring the system after any blackout

Components that regulate the voltage with reactive power may delay the restoration process. In this thesis it will be investigated a method to eliminate this problem and shorten the restoration time after a major blackout.

This thesis will also investigate how HVDC can assist after an event of a power system blackout. HVDC with voltage source converters (VSC-HVDC) should theoretically be able to regulate voltage with reactive power in an AC grid.

## 1.1 Background

A blackout refers to when electrical energy is inaccessible in the electric power grid due to a fault in generation, components, transmission lines etc. Large electric power system blackouts have occurred in Sweden several times, with the most recent ones in 1983 and 2003. When the blackouts extend nationally or regionally they have immediate and big impact on society. Economically this can be described with Energy Not Supplied (SEK/not delivered kWh). According to the report [1] made after the blackout 2003 the cost was 50 SEK/not delivered kWh. The total estimated cost for the blackout was 500 million SEK. This impact motivates transmission system operators (TSOs) to give high priority to avoiding blackouts. But since blackouts cannot be entirely avoided and thus will happen it is important to try minimizing the duration of the blackout once it occurs.

The restart of the grid after a blackout is called the restoration process. The voltage in the grid is regulated with reactive power. Reactive power can be either consumed or injected into the grid by generators and by reactive shunt components. These components consist of shunt reactors and shunt capacitors that are controlled by EVA. One issue during the restoration of the grid is the phenomenon called *reactor hunting*, which is normally handled by turning off the EVA. That leaves the reactive shunts in manual operation, which slows down the restoration process. In this work a solution to the problem with reactor hunting is developed and proposed by changing the EVA so it does not have to be turned off, and automatic operation of shunts can continue.

The growth of renewable energy together with new HVDC connections between countries' power systems has given the Swedish TSO new control options. The most recent HVDC converters are resources that can be used during power system restoration. There will be a new HVDC connection between Sweden and Lithuania of 700 MW. One challenge lies in finding a way to use this new dynamic feature of the grid.

Power control can effectively be made with power electronics at the HVDC converter station from DC to AC. The technology is called VSC (voltage source converter) and enables instant control of both reactive and active power, without affecting each other. Using this technology during a power restoration can speed up the procedure and assist to avoid hunting by decreasing the voltage deviation

## **1.2 Scope of thesis**

This thesis is about solving the problem with reactor hunting and investigating the use of VSC-HVDC during power system restoration.

### **Reactor hunting**

To automatically control reactive components (shunt reactors) in the network, it is necessary to have reliable control parameters. One idea is to let the control parameter depend on the strength of the network. One possible indicator of this is the short circuit capacity. This work investigates if the short circuit capacity can be used to improve the reactive component control.

More specifically this thesis aims to prove the concept that short circuit capacity can be used to change of tolerance band of the automatics of the reactive components. There is a manual verification part in this thesis, which proves that the explained relationship is strong enough to control the reactive components. An automatic implementation has not been done.

### **VSC-HVDC performance**

In this part of the thesis there will be simulations investigating HVDC performance together with a simplified grid. It is desirable to verify and confirm if the HVDC can energize a line and what advantages that come with it.

## **1.3 Previous work**

There have been some studies on automatic shunt switching. In the MSc. thesis of M.Larsson [2], he studied how the voltage stability could be improved by changing the EVA switch delay time of shunt components that connects to the grid. His studies show that improvement can be achieved by shortening the delay time but that this causes problems in other situations. He suggests further studies on automation of shunt components when in situation with high risk of reactor hunting.

Another MSc. thesis from 2005 [3] made a study on how sensitive the power system is to the hunting phenomenon. Several simulations with varying network strength were made. The thesis shows that changing delay time of the shunt switching can prevent hunting, by extending the time. However, as

the simulations were made on nets with different strength and the adjustment of delay time was made specifically for each simulation, no single solution was found for the general net.

Lars Lindgren made a study on fully automatic power restoration [4]. He proposes a simple heuristic algorithm to black-start the power system.

There is also one study [5], performed at Uppsala University, about how to implement HVDC in Aristo. However, that work is mainly a preparation and nothing was actually implemented in PowerFactory.

## 1.4 Aims

The first and largest focus will be on managing the shunt reactors to avoid hunting. The work on VSC-HVDC in this thesis is more of an investigation, rather than problem solving.

### Reactor hunting

Until now there has been no success in finding an automatic system for switching shunt reactors that is simple and eliminates the risk of reactor hunting during restoration. Therefore the Swedish transmission system operator is turning off the extreme voltage automatics (EVA) during the restoration process. The aim of this thesis is to find a way to avoid reactor hunting. The automatics to the shunt reactors are controlled with a tolerance band of voltage level. This thesis suggests the use of a variable tolerance band that changes with network strength. If that is a known factor one can control the shunt automatics with how the tolerance band needs to be changed ( $\Delta V$ ) in every node. The change of control consists of changes in the EVA. This means changing the threshold values in voltage at which the switching occurs. A system like that adapts to both strong and weak power systems, which is necessary during restoration.

### VSC-HVDC

This part will be similar to the part about reactor hunting. The investigation will try to prove that reactive power can be controlled with VSC-HVDC during power system restoration. It is desirable to verify and confirm on how the HVDC can consume and supply reactive power to regulate voltage. Can the VSC-HVDC assist in avoiding hunting during power restoration?

## 1.5 Contribution

### Avoiding reactor hunting

In this work the automatics that control the shunt reactors in the Nordic power system will be improved. Compared with the previous work in the area of reactor hunting, this work will use a new

angle to try to solve the problem. The earlier work has mostly focused on changing the delay timings of the relays that connects the shunt reactors. Our angle consists of using the short circuit capacity as a basis for controlling how the shunt reactors are connected. Instead of changing delay times, we will change the tolerance band limits for the relays to try avoiding hunting. This work will also try to find a connection between the short circuit capacity and the width between the lower and the upper limits in the tolerance band.

### **VSC-HVDC during restoration**

The contribution from our work on VSC-HVDC will mainly be a confirmation that the used VSC-HVDC in our simulations behaves like expected according to theory. We will show that our model can both supply and consume reactive power during power system restoration.

## **1.6 Applications**

The results of this work can be used as a starting point for improving or developing new automatics for the shunt reactors that could possibly remove the hunting issue completely. The results can also be used as a tool for operators to get a better understanding for the hunting phenomenon. The operators can then avoid hunting by predicting the voltage change and set the tolerance bands manually.

Our HVDC investigations can be a foundation for further investigation on power restoration with HVDC connections. The HVDC model used in our simulations has the abilities for voltage regulation during power restoration. The model can be implemented with a large power grid.

## **1.7 Outline of the thesis**

The second chapter explains necessary theory that is used in this thesis. Chapter three covers the simulation software used, and how the network model is constituted. Chapter four describes the method used regarding solving the reactor hunting issue. Chapter five is further description of the method, here for how the HVDC investigation is made. Chapter six presents the results found regarding chapter four. Chapter seven, gives the results from the HVDC investigation. Chapter eight is a verification of the results in chapter six. Finally chapter nine contains the conclusion and discussion of the thesis.

## 2 Theory

To get a complete understanding of this work, it is necessary to explain certain theory to the reader. The transmission lines in the power system have an effect on the voltage. How this works and how it can be controlled is explained in this chapter. Further it is explained how reactor hunting can occur during restoration of a power system. Also how VSC-HVDC works and an overview of future HVDC projects is presented. Lastly, the restoration process is explained.

### 2.1 Voltage profile

The behavior of the voltage is highly dependent on characteristics of the transmission lines. The line reactance has an impact on how much the voltage will rise due to the Ferranti effect. Depending on how a transmission line is loaded it can produce or consume reactive power.

#### 2.1.1 Transmission line

Due to its inherent reactance and capacitance, a power transmission line can both generate and consume reactive power. This can be seen by the standard pi-model that is used to describe a transmission line (seen in figure 2.1). In reality L and C is distributed along the line, the pi-model is a simplification of the distributed parameters.

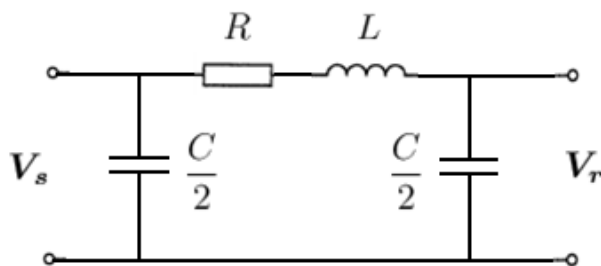


Figure 2.1 Model of a transmission line.

The amount of reactive power generated and consumed is described by the equations 2.1 and 2.2.

$$Q_{loss} = j\omega LI^2 \quad (\text{eq. 2.1})$$

$$Q_{gen} = j\omega CV_s^2 \quad (\text{eq. 2.2})$$

### 2.1.1 The Ferranti effect

The Ferranti effect is an increase in voltage level at the receiving end in a long transmission line. This happens when there is light or no load at the receiving end. The effect is caused by the natural line capacitance and inductance. The length of the line has a quadratic effect on the voltage rise. During the restoration process of a power system this can be seen when energizing the transmission lines without load or production at the receiving end. The effect is shown in figure 2.2

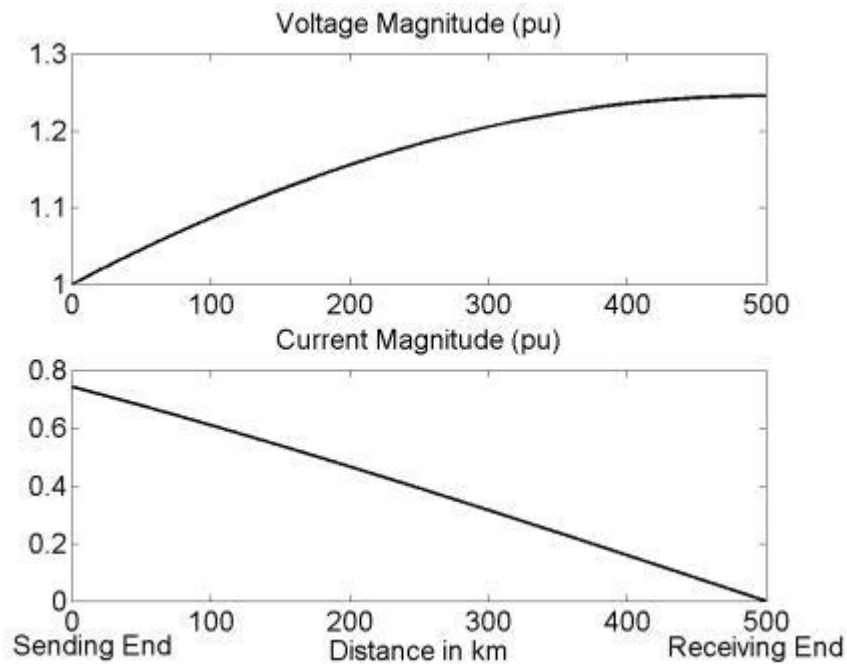


Figure 2.2. Principle of the Ferranti effect for a line with arbitrary distributed parameters, ( $C=F/\text{km}$  and  $L=H/\text{km}$ )[15].

### 2.1.2 SIL-Surge Impedance Loading

Transmission lines produce reactive power due to their charging capacitance. The amount of power produced depends on the line capacitive reactance  $X_c$  and the voltage at which the line is energized. Equation 2.3 shows the relation.

$$\text{var produced} = \frac{V^2}{X_c} \quad (\text{eq. 2.3})$$

The transmission lines also consume reactive power to support their magnetic field. The strength of the field is dependent on the current flow in the line and the inductive reactance  $X_l$  of the line. The relation is shown in equation 2.4.

$$\text{var used} = I^2 X_l \quad (\text{eq. 2.4})$$

The surge impedance loading point (SIL) is when the amount of produced reactive power is equal to the used amount. This is the optimal point of loading a transmission line. If the equations above is

rearranged and it's noted that  $X_L = 2\pi fL$  and  $X_C = 1/2\pi fC$ . Then the impedance ratio can be written as equation 2.5 below.

$$\frac{2\pi fL}{2\pi fC} = \sqrt{\frac{V^2}{I^2}} \quad (\text{eq.2.5})$$

Which gives the *impedance*  $= \frac{V}{I}$  and the *surge impedance*  $= \sqrt{\frac{L}{C}}$ . The practical use of the surge impedance is to calculate the SIL with equation 2.6. The result can tell you that if a line is loaded above SIL it will act as a shunt reactor and absorb reactive power. If it's loaded below SIL it will act like a shunt capacitor.

$$SIL = \frac{V^2}{\text{Surge impedance}} \quad (\text{eq.2.6})$$

## 2.2 Voltage regulation

As the voltage level in the grid can vary for reasons described in 2.1, it needs to be controlled. The voltage can be regulated with shunt reactors that consume reactive power and with synchronous generators and VSC-HVDC that can both consume and inject reactive power.

### 2.2.1 Shunt Reactor

Shunt reactors are used to compensate for reactive power produced by the transmission lines[6]. The reactors lower the voltages by consuming reactive power. Following equation 2.7 describes the change in voltage ( $\Delta U$ ) when consuming reactive power ( $Q_c$ ) with the shunt reactor in a network with short circuit capacity ( $S_{sc}$ ). The normal rating of a shunt reactor is 100-200 MVAR.

$$\Delta U(\%) = \frac{Q_c \cdot 100}{S_{sc}} \quad (\text{eq. 2.7})$$

The shunt reactors in the grid is connected or disconnected automatically by EVA when the voltage at the node which the reactor is located, exceeds a high or low limit. The default tolerance band is most often 420-380 kV. The voltage needs to stay past the limit for a period of time before any action is made, in this work this intentional delay is set to two seconds, which is the standard time used in the Swedish transmission system. In figure 2.3 this is illustrated with an example of a node voltage. Some unknown event forces the voltage to rise above the upper limit, after two seconds the shunt reactor at the node is connected and the voltage is stabilized inside the tolerance band.



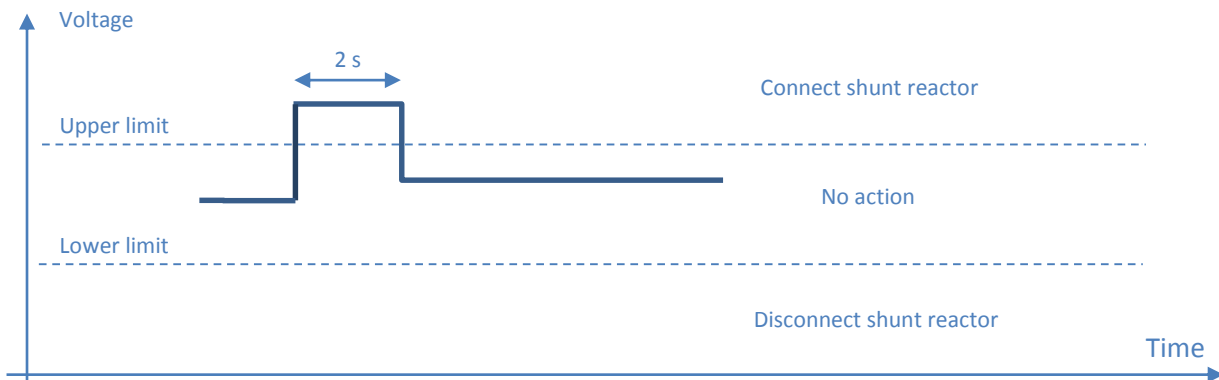


Figure 2.3 Example of shunt extreme voltage automatics with limits. Normal voltage fluctuations have been disregarded in this example.

### 2.2.2 Reactor Hunting

When the power system is weak the connected or disconnected shunt reactor has a larger impact on the voltage [2]. Which means that when the voltage is too low automatic control tries to increase the system voltage to stay within the tolerance band by disconnecting a reactor, the voltage could rise above the upper limit. The control system then connects a reactor and the voltage decreases below the lower limit again thus creating an oscillating behaviour. This is referred to as a reactor hunting phenomenon, see figure 2.4.

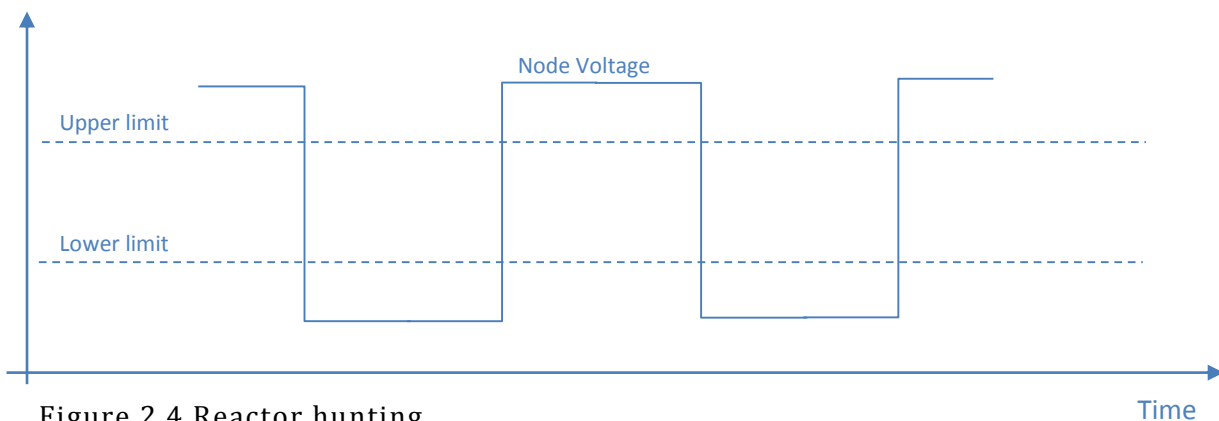


Figure 2.4 Reactor hunting

## 2.3 HVDC transmission

High voltage direct current (HVDC) can transmit high power with low losses over long distances. One advantage compared to ac transmission is that one can use a HVDC-cable under ground and water as well as an overhead line. HVDC allows two separated power systems to exchange power without being synchronised.

The HVDC can be implemented with voltage source converters (VSC), which can control reactive and active power independently on the AC side. That attribute is highly desirable during a restoration process.

### 2.3.1 VSC – Voltage Source Converter

The VSC is a controllable voltage source, which can control the reactive and active power instantly. The simplest case is a back-to-back system seen in figure 2.5, from the MSc. thesis by Woldeyesys Shire and Tamiru. 2009 [7].

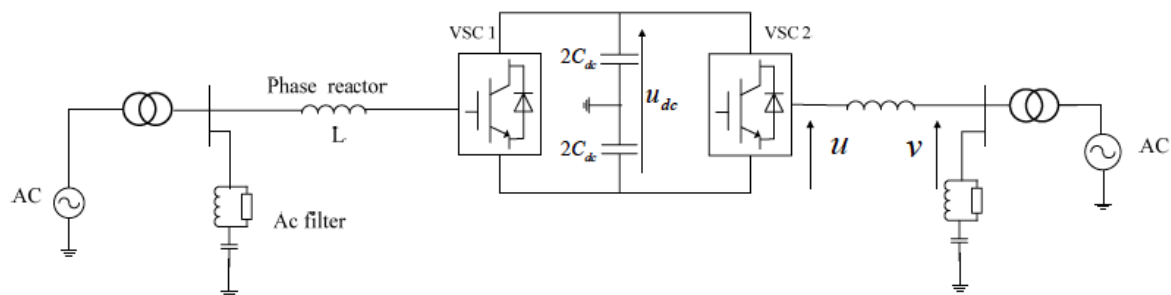


Figure 2.5 Back-to-back VSC system with DC-link capacitors

The VSC system works in both directions. The DC-link capacitors maintain the voltage level over the DC-cable (disregarded in the back-to-back case) at each VSC converter.

The VSC consists of multiple modules in which every module is built with many IGBT transistors, which are connected in series. They are connected in series to reach a high blocking voltage, higher than the AC –voltage. Otherwise the IGBT would conduct even when it is not desired. What limits the VSC power characteristic is mainly the current running through the IGBTs in a VSC module. It can be described with the diagram in fig 2.6 [7].

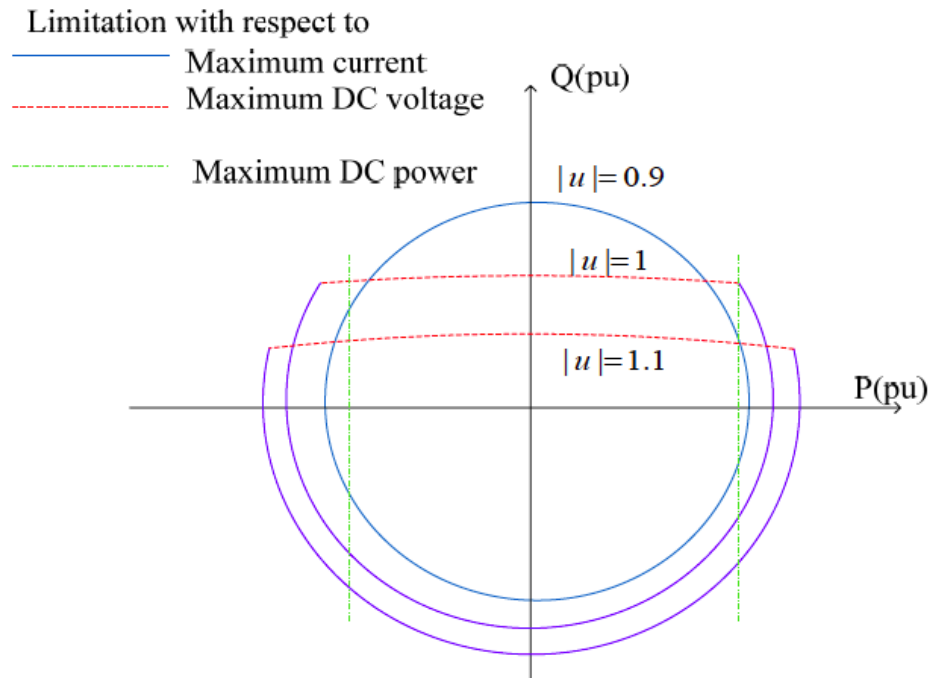


Figure 2.6 Power limits due to the IGBT current [7].

Another limitation is the maximum DC-voltage. As the DC-voltage limits the possible AC-voltage generation it will have direct impact on the reactive power, which depends on the difference between the generated AC-voltage ( $u$  in Fig 2.5) and the AC-voltage of the grid ( $v$  in Fig 2.5).

The third limitation is the maximum current through the DC-cable. The maximum DC-cable current sets the maximum active power of the cable. Both consumed and injected power.

### 2.3.2 Control system VSC-HVDC

The control system of VSC makes it possible to control the transfer of energy through the DC-cable. The active power and the reactive power can be independently controlled.

The reactive power flow can be controlled at both ends of the DC-cable, in each converter. What controls the reactive power flow is the AC-current. The AC-current can be set without changing the DC-voltage. The active power is controlled by the difference in DC-voltages on the DC-sides of the converters.

The control system consists of an inner loop control and an outer loop control. The inner control loop has a current reference, which is provided by the outer loop control, and controls the ac current with a PWM. The outer control loop consists of a DC-voltage controller, AC-voltage controller, active power controller and a reactive power controller. See fig. 2.7 for block schedule.

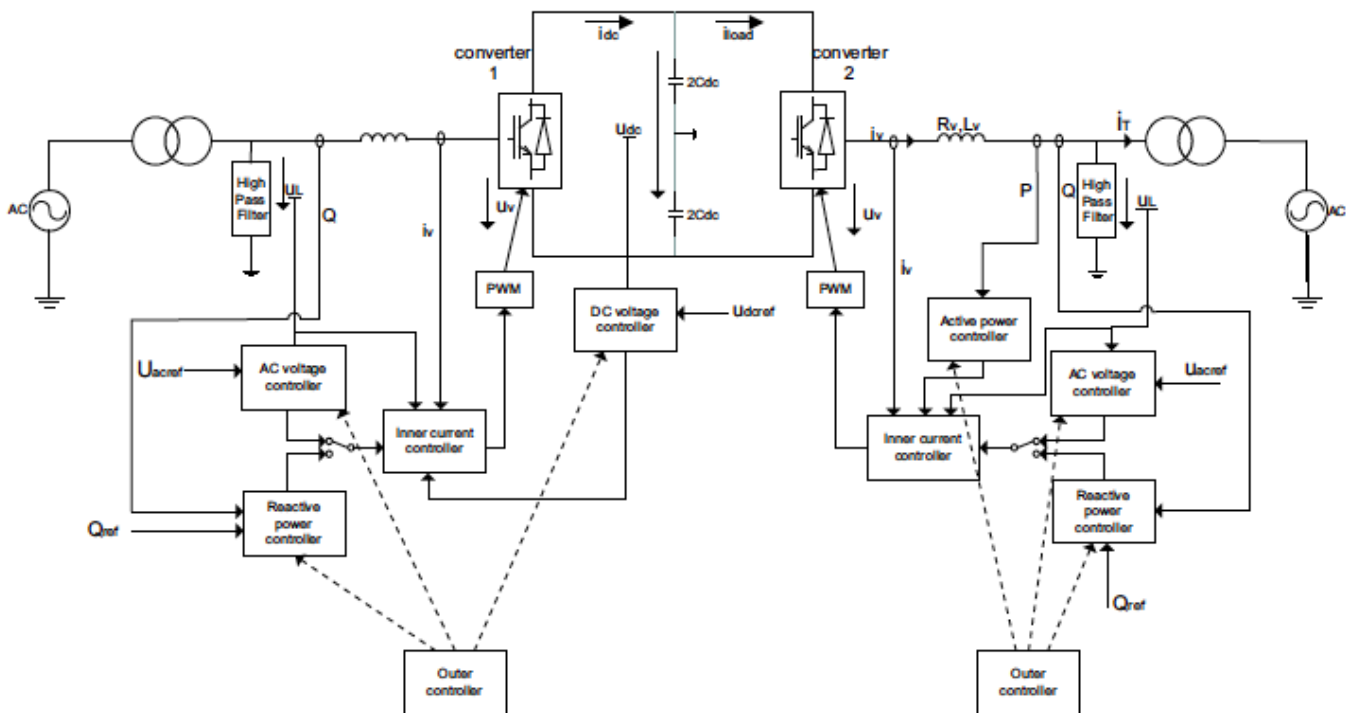


Figure 2.7 Block scheme of control system of a VSC-HVDC [7].

In fig. 2.7 the first VSC-converter uses AC-voltage control, reactive power control and DC-voltage control. The second converter uses active power control instead of DC-voltage control. What is clear in the picture is that the outer loop controllers supply parameters for the inner loop control, which proved the PWM, which controls the IGBTs in the converter. The AC-current reference is derived from the DC-voltage controller and the active power controller.

## 2.4 Future HVDC links

Here follows some examples of on-going and future HVDC projects. Where SydVästlänken and the Gotland Link is within Swedish borders and Nordbalt is an international connection.

### 2.4.1 SydVästlänken

SydVästlänken is an AC and DC link from the middle to the southern Sweden. The link will be completed in early 2015 [8]. The northern part of the link between Hallsberg and Barkeryd is 400 kV overhead AC. The southern part between Barkeryd and Hurva is 300 kV DC, where most parts are in the ground, see figure 2.8.



Figure 2.8 Location of SydVästlänken in Sweden [12]

### 2.4.2 The Gotland Link

A second HVDC connection between Gotland and the mainland is planned, see figure 2.9. The reason for this link is to be able to build and connect large wind power plants on Gotland in the future. The link capacity is 500 MW. The estimated completion time is during 2018.

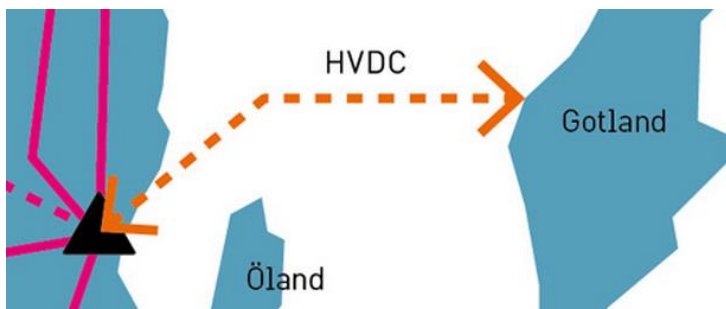


Figure 2.9 Gotland link location. [12]

### 2.4.3 NordBalt

The link, see fig 2.10, between Sweden and Lithuania is under construction. The link will have a voltage level of 300 kV and a capacity of 700 MW. This will connect the Baltic nations with the Nordic power system. Today there is only one cable between Estonia and Finland. This new link enables the Baltic nations to be integrated with the Nordic electricity market.

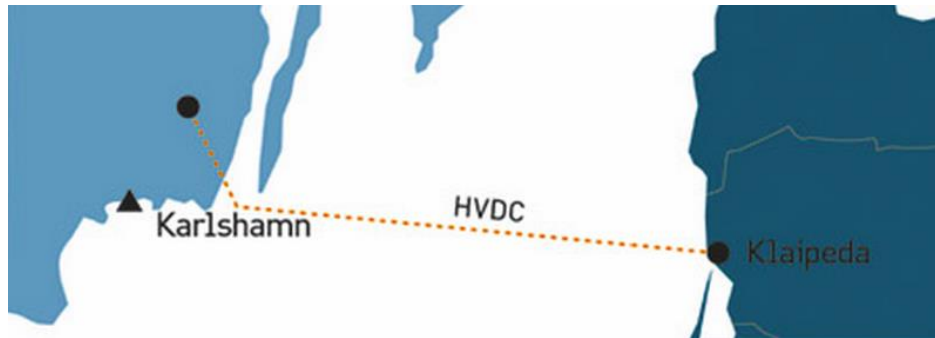


Figure 2.10 Nordbalt location [12]

### 2.4.4 Overview of other HVDC projects

The use of HVDC is growing in general. In Europe there are several HVDC projects planned to be completed before 2020. Germany has decided to build four “corridors” through their grid. There is plans to build a “super grid” in the Nordic sea for future offshore wind power plants. A link between Denmark and the Netherlands is planned. Norway and UK plan to connect via a very long cable and also an expansion of the link from Norway to Denmark is planned. This is a selection of projects to show that a lot is happening in the HVDC area. In figure 2.11 below the medium to large existing and planned HVDC connections are shown.

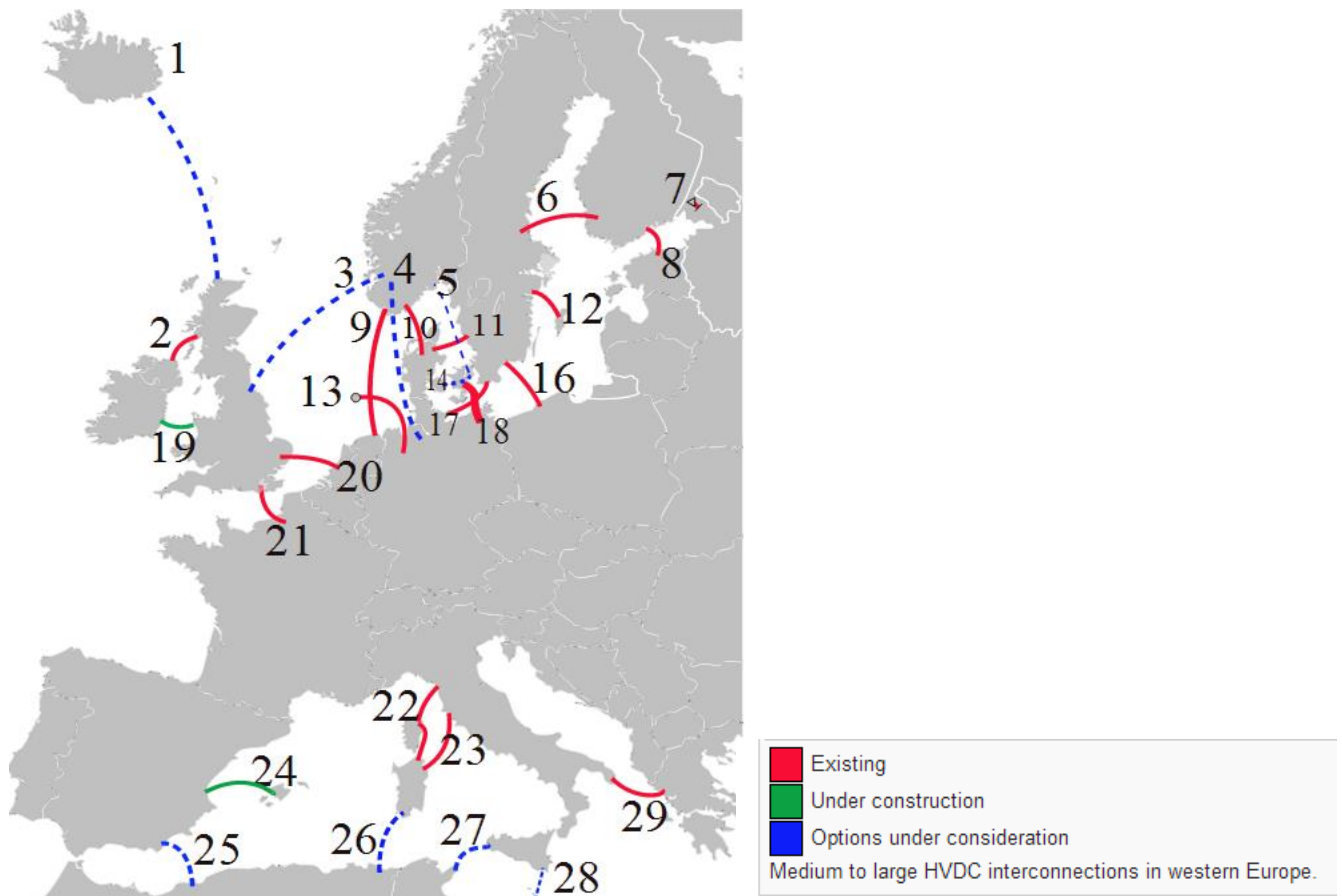


Figure 2.11 HVDC projects overview. [11]

## 2.5 Restoration

The process of recovering from a blackout is called power system restoration. A restoration strategy is normally used to restore the system in an effective way. Due to the Ferranti effect the voltage is high at the remote end of the line as it is energized. Shunt reactors are used to bring down the voltage. As the net is under restoration the network is very weak and shunt reactors might impact too much and lower the voltage. Then there is high risk of hunting to occur.

### 2.5.1 Islands in power systems

An island in an electrical power system refers to an isolated part of the system that can sustain itself without support from other parts. Islands can be created when a fault occurs that splits a big system into smaller ones. In order to connect the islands together again, they need to be synchronized. I.e. they need to have similar phase angles at the moment of connection.

### 2.5.2 The Process of Restoration

The first step of the restoration process is to know the system status. This includes knowing which parts of the system still works, if there is any islands and which generators that have successfully transferred to “household operation”. Meaning that they disconnect from the grid and supply only the power necessary to keep the power station operating. This enables it to connect considerably faster to the grid again compared to a generator that as stopped totally. Any lines or other equipment that sustained damage needs to be identified as soon as possible and the transfer limits needs to be known for the functioning lines in order to create a safe restoration plan. If there was a total blackout, available black start resources should be identified.

When the status is known, a build strategy should be chosen. There are mainly two different strategies: “build-up” and “build-down”. The first means that you start by reenergizing the low voltage level (local level) in multiple smaller islands. Then a build up towards higher voltage levels is made by interconnecting the islands together. To do this the islands needs to be synchronized. The process creates growing islands that in the end become the complete restored grid. The build-down strategy is used in Sweden because of our big resources of hydropower. The strategy consists of first energizing the high voltage grid and then successively energizing the regional and lastly the local voltage grids. In this work the build-down strategy is used.

When the grid is energized with either of the strategies, generation should be added continuously. At the point where the complete grid is energized the load restoration begins. This includes alternating between generation increases and connection of loads so that the frequency and voltage keeps acceptable levels. This procedure is continued until supply has been restored to all customers.

### 2.5.3 Reactive power compensation and net strength

As the voltage level will be fragile during restoration reactive power compensation could be needed.

The purpose of reactive power compensation is to reduce the amount of reactive power transported over the lines, and thereby reduce active as well as reactive losses. The power system is simplified with a Thévenin equivalent, as in figure 2.12. In this figure the source resistance is also simplified with  $R=0$ . Then the approximate amount of shunt compensation necessary to lower/raise the voltage level is calculated from equation 2.8. This describes how sensitive the bus is to injection of reactive power.



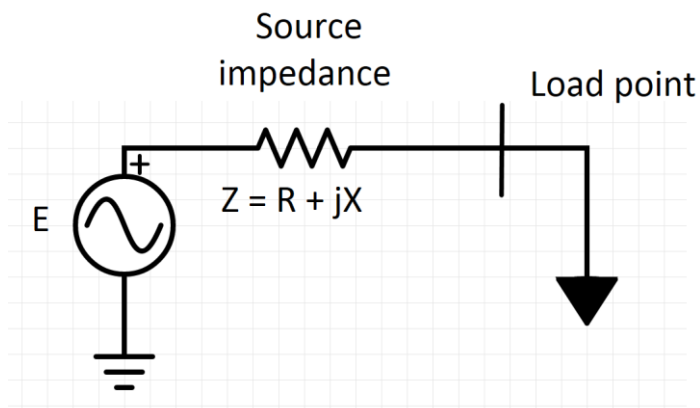


Figure 2.12 Thévenin equivalent of a power system,  $R=0$

$$\frac{\partial V}{\partial Q} = \left(\frac{\partial V}{\partial Q}\right)^{-1} = \left(\frac{E}{X} \cos\delta - \frac{2V}{X}\right)^{-1} \quad (\text{eq. 2.8})$$

$$\left(\frac{E}{X} - \frac{2V}{X}\right)^{-1} = -\frac{X}{E} \approx -X_{(p.u.)} \approx -\frac{1}{S_{sc(p.u.)}} \quad (\text{eq. 2.9})$$

When the equivalent system is unloaded  $\delta = 0$  and  $E = V = 1$  and the p.u. short-circuit capacity is  $S_{sc}=1/X$ . The equation can be simplified to eq. 2.9. In this work a concept of net strength is used. The point is to have a parameter that in some way describes how strong a node in a net is. The short circuit capacity is a possible parameter. Equation 2.8 and 2.9 lead to equation 2.10, which can be used to approximate the “strength” of the nodes in the net.

$$S_{sc(p.u.)} = -\frac{\Delta Q_{(p.u.)}}{\Delta V_{(p.u.)}} \quad (\text{eq. 2.10})$$

It is important to remember that eq. 2.10 is an approximation.  $S_{sc}$  is defined as in equation 2.11.

$$S_{sc(p.u.)} = V_{th} \cdot I_{sc}$$

Where  $V_{th}$  is the Thévenin voltage and  $I_{sc}$  the short circuit current.

### 2.5.5 Cold load pickup

As described in previous sections, there are problems with the reactive power during restoration. However, there are also issues with active power. When a load is reconnected to the power system after an outage, it is referred to as cold load pickup. This reconnected load will act significantly different compared to before the outage, both in size and character. Industrial loads will have

considerably lower consumption due to processes that needs to restart. This time can vary between hours to days, depending on the size and sensitivity of the process. However in the residential sector the load will normally be significantly higher than pre-disturbed situation. Thermostatically controlled loads are the main reason for this increase in power, this includes e.g. electrical heating, refrigerators, heat pumps, water heating and air condition. The reason why these equipment use more power is because they have lost their diversity and are almost always put in an "on" state when they are reconnected.

The amount of increased active power consumption depends on the time of the outage and the outdoor temperature. It can reach a peak that can be higher than the power used under the most heavy steady state conditions. When restoring a system this needs to be considered to avoid overloading lines that could lead to new disturbances

# 3 Programs and models

Two different software have been used for the simulations in this work, ARISTO (Advanced real time interactive simulator for training and operation)[16] and DIGSILENT PowerFactory [14]. The model of the Swedish power grid, which is used in both programs, is called Nordic32 [13].

## 3.1 Nordic32 Model

In Sweden there are four main voltage levels. They are grouped as follows: Transmission (220-400 kV), Subtransmission 50-130 kV, medium voltage (10-40 kV) and low voltage (400 V) [9]. Most generation is connected to the transmission and subtransmission level via transformers that raise the voltage. Heavy electricity-consuming industries are connected at the medium level. Loads such as homes are connected to the low level.

The Nordic32 is a test model that consists of 32 nodes and is a simplification of the Swedish transmission system. It is created to react in the same way as the real Swedish power system. The model is created for simulation with real life scenarios. It follows the characteristics with most production in the northern part and most of the consumption in the southern part. The node names are invented and have nothing to do with the geographic location. In figure 3.1 the model is used in Aristo. In every switchyard in the used model, there are two or three bus bars connecting the transmission lines. The practical use of multiple bars is to have more possibilities to connect the lines when a fault occurs.

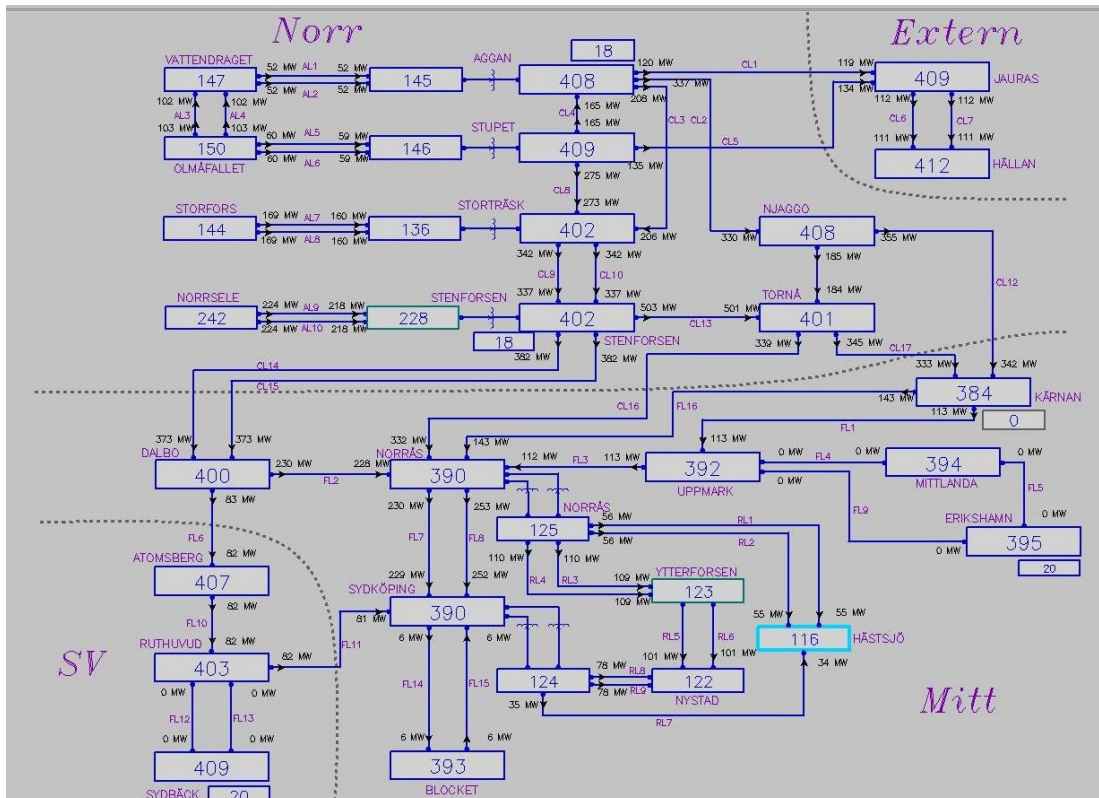


Figure 3.1 The Nordic32 model in Aristo

## 3.2 Aristo

ARISTO is used by the Swedish TSO Svenska Kraftnät and is a real-time simulator. This simulator has been mainly developed for training operators to handle the restoration process of the power system. This means that there aren't that many tools for developing and adding parts to the system, compared to other software. However, a link between ARISTO and Matlab has been developed and this makes it possible to create new functionalities. ARISTO is also good for monitoring the system and for manual control of breakers, generators etc.

## 3.3 Power Factory

PowerFactory is more widespread and used by several TSO's in Europe. It's not in real-time like Aristo where one can interact during simulations. Compared to ARISTO this simulator has some more ways of performing analysis and for adding functionality to the system models. Small model simulations in PowerFactory take little time and larger models take more time. Which makes PowerFactory a powerful tool for small models.

# 4 Method for avoiding reactor hunting

The main idea is to find the short circuit capacity in the nodes that are being energized, as it describes the strength of a node. This will be done for several paths to collect data. The hunting phenomena will occur in weak nodes and to avoid hunting the tolerance band in the automatics of the shunt reactors must be changed. Simulations are made to find out how much the tolerance band of the shunt automatics must be changed to avoid hunting. With the collected data of the short circuit capacity ( $S_{sc}$  in eq. 2.7) and needed change of tolerance band a relation can be used to control the automatics. The found relation must be verified to ensure that it works for a general net. The goal is to, with this formula, completely restore a net after blackout with loads and generation without reactor hunting.

## 4.1 Process to solution.

Here follows how  $S_{sc}$  is found and how the tolerance band is changed. It also describes how to find the weakest path.

### 4.1.1 Determine short circuit capacity

To be able to change the EVA tolerance band, it's needed to know how much the voltage will change when connecting a node. The change can be found with different methods. There are essentially four possible methods of determining the  $S_{sc}$  that will in turn give the voltage difference. These possible methods are shown in figure 4.1.

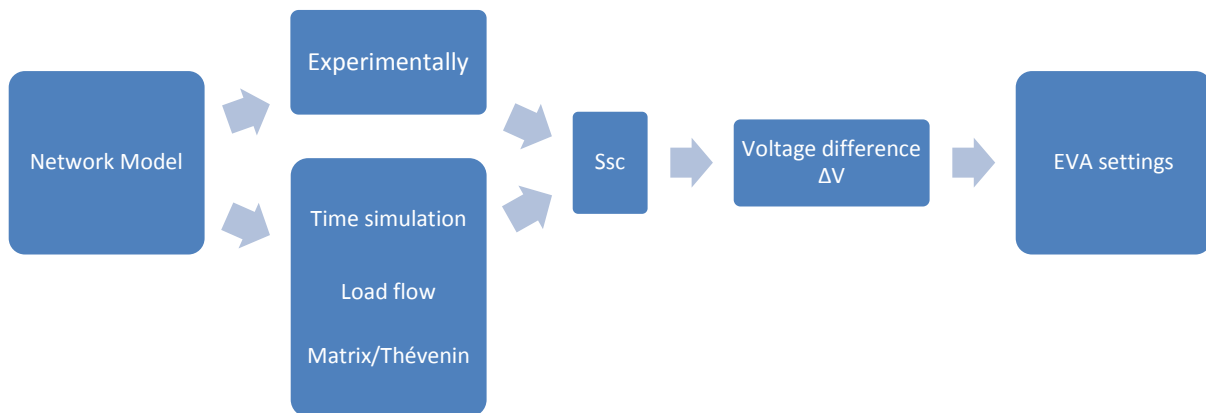


Figure 4.1. Process to change the EVA settings

The experimental method is carried out on the real net. The experimental method can alternatively be made with simulations in e.g. ARISTO or PowerFactory. However, this will decrease accuracy due to the fact that the network model always is a simplification of the real net. Some simulators can produce admittance matrices, from which one can calculate Ssc. The easiest method is to simplify the network model to an approximate model and create a Thévenin equivalent in which one can make hand calculations. However, it can be hard to make an accurate Thévenin estimation of the real net.

In ARISTO there is no easy way to determine the Ssc. For this you would need the admittance matrices for the Nordic32 model in the different stages (when something is connected/disconnected). This would be equal to finding the Thévenin equivalent for the whole system and then the Ssc could be calculated. However, these matrices are not available in ARISTO. Instead the Ssc is derived from eq. 2.7 and the parameters are found in the real-time simulation as explained below.

#### 4.1.2 Experimental method for determining Short circuit capacity

In the first scenario the whole power system is intact. To determine the short circuit capacity (Ssc) the shunts at the node which is investigated is first disconnected. The voltage at the node is then noted. The second step is to connect all the shunt reactors, and measure the voltage again and also the reactive power drawn by the shunts. This gives values of the change in voltage and reactive power. With these the short-circuit power can be calculated with equation 2.10. This process is repeated for all the stations in the part of the grid that will be blacked out in the restoration scenario, i.e. the southern nodes.

In the case of determining the Ssc for the stations when the southern part is blacked out, the process is a bit harder. The stations that are closest to the functioning grid is energized and investigated one at a time. The order that the nodes are energized can be chosen in many ways, we have chosen to take a number of different paths. The energizing node is made to have a voltage around 410 kV and

all shunts are chosen to be 350 MVAR. When choosing a different path to energize the net, the resulting  $S_{sc}$  becomes different. This is because the system, seen from the latest connected node, has a different Thévenin equivalent. This determines the level of the voltage at the node and thus will impact on the value of  $S_{sc}$ .

#### **4.1.3 Tolerance band shunt automatics**

The hunting phenomenon can only occur when the extreme voltage automatics (EVA) is turned on. Therefore to study the phenomenon it is required that the automatics are turned on when the specific node is connected. The default tolerance band is most often 420-380 kV. If hunting occurs with the default tolerance band, it is desirable to increase the tolerance band until the threshold for avoiding hunting is found. The most important parameter in this work regarding EVA settings is the change of tolerance band  $\Delta V$  (kV). See figure 4.2 for a description of the definition of  $\Delta V$ . That is the relative change from the lower default limit to the set new lower limit. Note that the upper tolerance limit is also changed to 440 kV in all cases to create a safer margin for avoiding hunting. Voltages above 440 kV is not desirable during restoration due to the fact that the voltage will rise even higher when connecting a new node (because of the Ferranti effect). Additionally In the same figure it is shown how the hunting phenomenon looks like with default tolerance band, when the shunt reactor is connected the voltage is lowered too much and the shunt is disconnected again. It should be true that a strong node can handle a narrower tolerance band than a weak node.

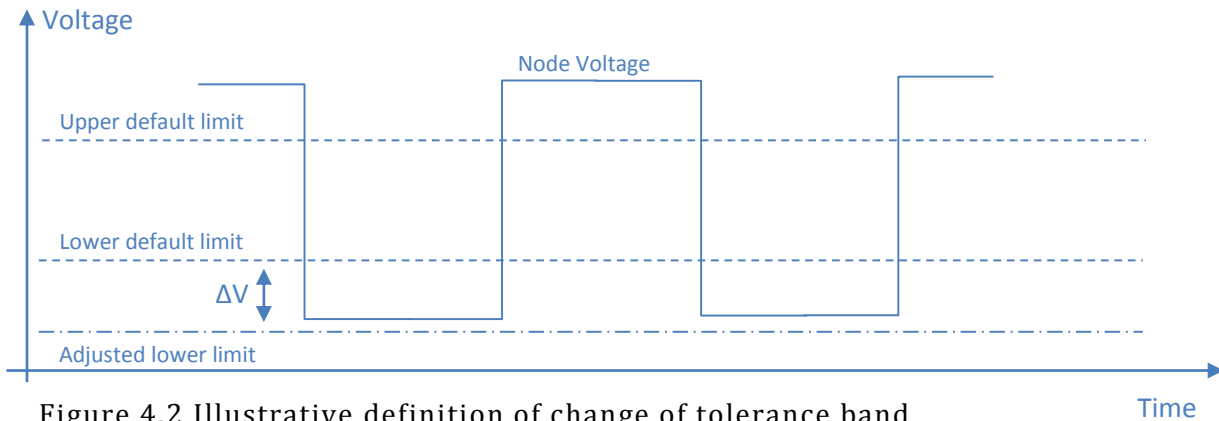


Figure 4.2 Illustrative definition of change of tolerance band

#### 4.1.4 Over voltage vs. under voltage

When the voltage level on the transmission lines is around 10% over or under the nominal voltage level, we are talking about over/under voltage. It is interesting to know which one is more preferable. If the nominal voltage is 400kV and there is a 500kV over voltage and 300kV under voltage. Both are a 25 % change from the nominal value.

At high voltages the current is low and at low voltages the current is high. When high current the power system suffers from more energy losses. Which results in an increase of energy production. The components in a power system are designed for high voltages and low currents, so a high current will perform a high strain on the components and there will be risk of damages. That can result in parts of the power system without energy, due to disconnection. If the voltage level is low during an energising restoration process, there will be problems connecting loads to the energized node. As the load will lower the voltage even more.

On the other hand a high voltage can produce arcs in substation. This means that a flashover occurs from one bus bar to the next one. The instant heat increase at such events can melt components. The higher voltage, the longer can the arc be from one node to another.

During restoration it is desirable to stabilize at or below nominal voltage (400 kV). This is because the voltage level will rise when connecting a new node, due to the Ferranti effect. If i.e. the node where the energizing starts from has an over voltage, the next node will get an even higher voltage.

#### 4.1.5 Finding the weakest restoration strategy

With information about the Short circuit capacity in each node, the weakest restoration strategy can be found. By only connecting to the weakest of all possible nodes the net will be built up in the weakest way. The method for calculating the strength of the node uses the difference in reactive power consumption. Therefore it's necessary to add an artificial shunt reactor to all nodes without shunt reactors. The Ssc can be calculated with delta V and delta Q, see equation 2.8.



In Aristo it's a bit complicated to add components. Therefore already existing components will be used to implement shunt reactors. In nodes with only loads the settings for the load can be modified relatively simple by increasing the reactive part of the load and totally eliminating the active part. Then the load will appear like a shunt reactor.

## 4.2 Simulations

First data is collected, later the result is verified. The simulations finish with an example of complete restored net.

### 4.2.1 Initial system

The system used as start point when testing different strategies are in figure 4.3 below. This represents the power system after a blackout, which should be restored. The rectangular boxes represents switchyards. A Colored outline means that the switchyard is energized and a gray color means that the switchyard is blacked out. The diagram shows that all the nodes below the horizontal dotted except for Dalbo, are blacked out.

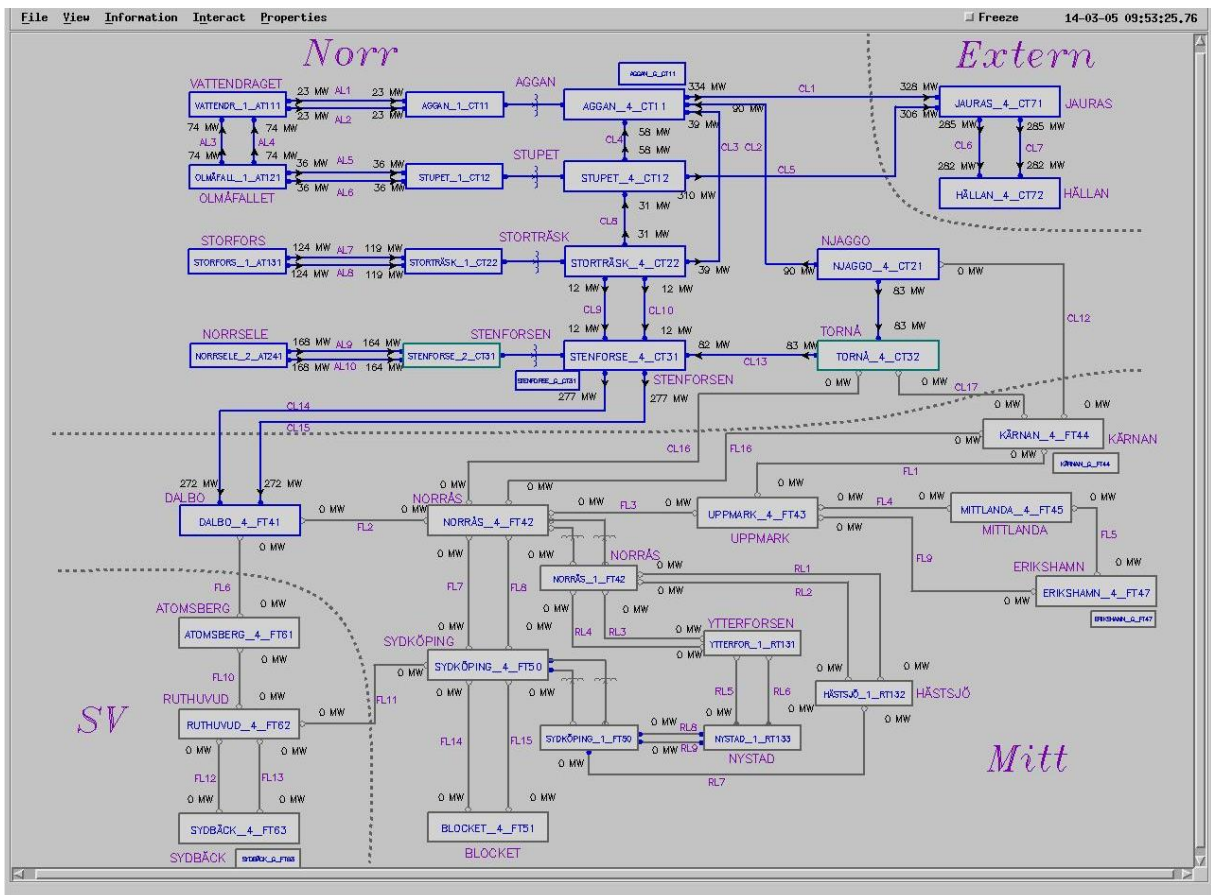


Figure 4.3 Diagram of initial system

### 4.2.2 Method used for gathering data

A test scenario that uses similar conditions at every node was desired. This eliminates some parameters that makes the system unnecessary complex. It was decided that all shunts should have the same capacity, that only one line should be used between nodes and that the voltage at the node which the energizing starts from should be 410kV. The latter was obtained by turning off/on shunts in different nodes.

Four different paths for energizing the net were used to gather data. These are shown in table 4.1-4.4. For figures of the paths, see appendix A. The first path, the weakest strategy is obtained in the same way as the strongest strategy explained in section 4.1.4, but instead of choosing the strongest available next node, the weakest is chosen in each step. The Random strategy is a path randomly selected to get more measurements.

Table 4.1. Path 1, the weakest strategy

Weakest restoration strategy	
1.	Kärnan from Njaggo
2.	Norrås from Kärnan
3.	Sydköping from Norrås
4.	Ruthuvud from Sydköping
5.	Sydbäck
6.	Blocket
7.	Atomsberg from Ruthuvud

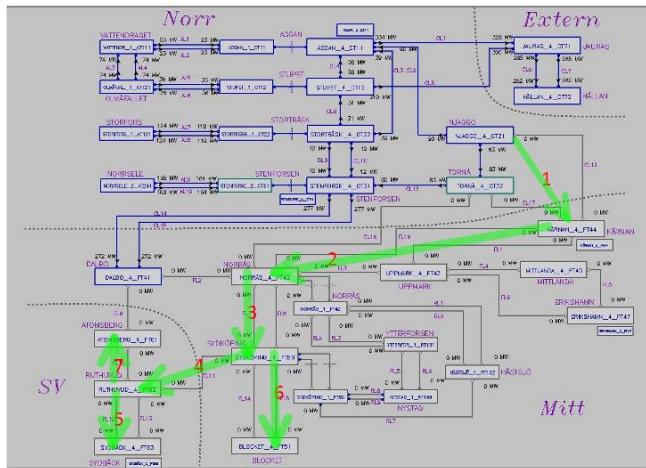


Table 4.2 Path 2, random strategy 1

Order	Node
1	Atomsberg
2	Ruthuvud
3	Kärnan from Njaggo
4	Sydköping
5	Blocket
6	Norrås from Tornå

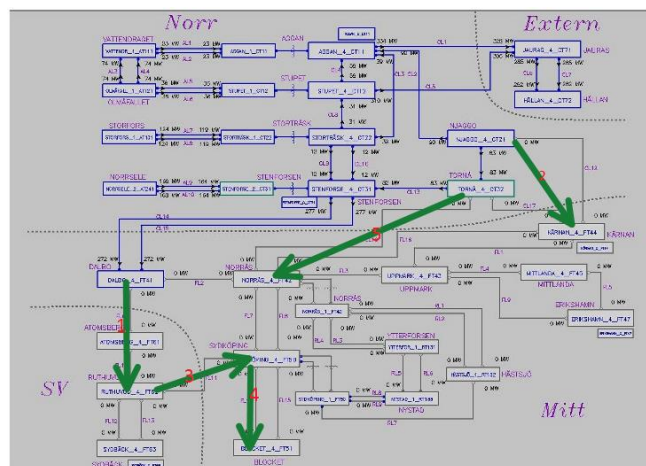


Table 4.3 Path 3, random strategy 2

Order	Node
1	Kärnan from Tornå
2	Norrås from Kärnan
3	Sydköping
4	Ruthuvud from Sydköping
5	Blocket

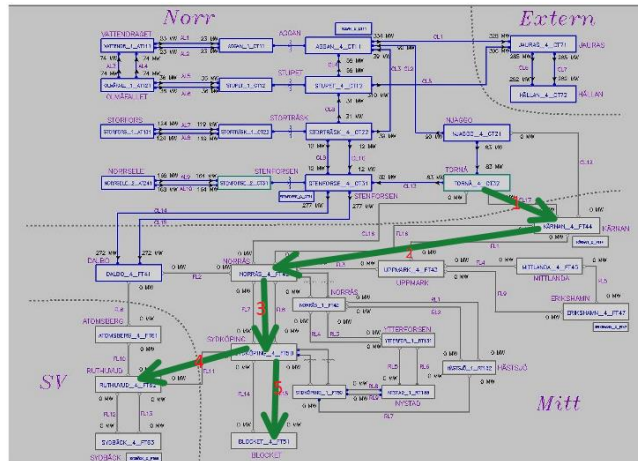
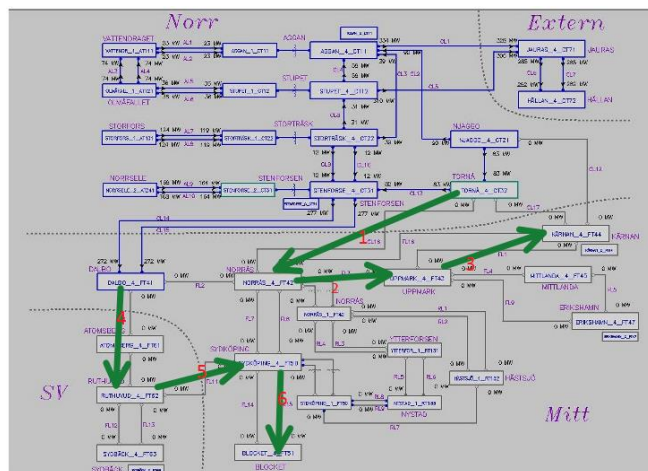


Table 4.4. Path 4, random strategy 3

Order	Node
1	Norrås from Tornå
2	Uppmark from Norrås
3	Kärnan from Uppmark
4	Ruthuvud from Atomsberg
5	Sydköping from Ruthuvud
6	Blocket



In each path the Ssc was determined for every node with the experimental method described in section 4.1.2. The necessary change of tolerance band for the shunt automatics to avoid hunting was also determined for all shunts. The results are shown in section 5.1.3

### 4.3 Verification of thresholds

If a relation between Ssc and the change of the tolerance band can be found, this should be verified by testing random paths to energize the system. The found relation should then set the tolerance band and if no hunting occurs the relation is valid.

The new tolerance bands from the change of tolerance band values determined in section 4.2.1 were tested in a scenario where all automatics were turned on. The nodes were energized in the four different paths shown in above section. If no hunting could be observed in a node, the next node was energized. If no hunting occurred in any of the nodes in a path, the thresholds are verified.

## 4.4 Restoration of whole grid with load and generation

With the previous section of this chapter a relation between  $S_{sc}$  and change of tolerance is desired. A full restoration with loads and generators is to be performed with the possible relation.

When the net is fully energized, it is desirable to reset the tolerance bands for the shunt reactors to their default values. 420-380 kV. During load pick up and connection of generators, a voltage level around nominal of 1 p.u. is required. If the voltage level is low when connecting a big load a collapse might occur. Due to synchronisation issues frequency must be 50Hz and voltage level at nominal level when connecting a generator. ARISTO uses a function called "unit panel" to start up the generators. It automatically ramps up the power and synchronizes to the grid. This function was used to start the generation in the southern nodes. When the frequency in the southern nodes where starting to get slightly above 50 Hz, The smallest loads where connected. After the frequency stabilized additional loads were connected and then more generation could be started. This process was repeated until the whole system where restored to the point before the blackout.

## 4.5 Theoretical analysis of method

The experimental method to determine the  $S_{sc}$  is to be compared to theory to further improve the reliability of the used method. This is done by using the gathered data from section 4.2.2 and trying to find a relation with a PI-model, where the  $S_{sc}$  is calculated as it is defined in eq. 2.11.

The approximation in equation 2.10 can be rewritten as equation 4.1. This relation has been used to find  $S_{sc}$  on experimental way. But as it is an approximation it is interesting to see how well it corresponds to the real  $S_{sc}$ .

$$\frac{\Delta V_{(p.u)}}{\Delta Q_{(p.u)}} = - \frac{1}{S_{sc}(p.u)} \quad (\text{eq. 4.1})$$

The  $\Delta V$  increases with a weaker network (smaller  $S_{sc}$ ). To visualize this, a simple model is investigated. The model can be seen in fig 4.4. The model consists of a voltage source with the internal reactance  $X_s$  (s for source), a transmission line (PI-model) and a shunt reactor that can be disconnected. If the voltage  $V_{th}$  (E) is kept, one can say that  $X_s$  affect the network strength, as  $S_{sc} = I_{sc} \cdot V_{th}$  and  $I_{sc}$  can easily be found as  $I_{sc} = V_{th} / X_s$ . That gives a weaker network as  $X_s$  increases. One could say that a larger  $X_s$  means that the generation moves further away from the consumption.

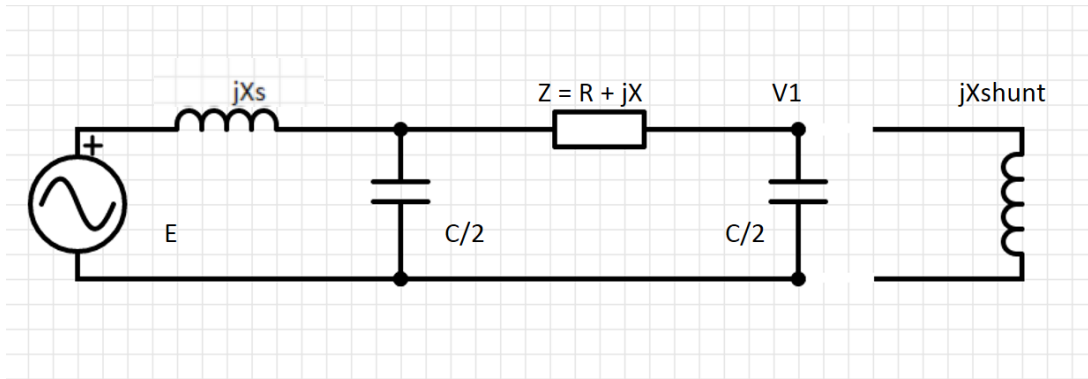


Figure 4.4 Simple model circuit with source, line and shunt reactor.

The parameters in the PI model are taken from Nordic32 in the specific line between Tornå and Kärnan, to keep the model as realistic to the model as possible. By changing network strength and looking at the voltage difference before after the shunt reactor is connected one can confirm the theory.

A similar model is also built in PowerFactory. The same parameters are used as for the model in fig 4.4. With PowerFactory one can simulate and see how the voltage changes when the shunt is connected. As for in fig. 4.4 one can only get instant values.

The simple model in PowerFactory is seen in fig. 4.5.

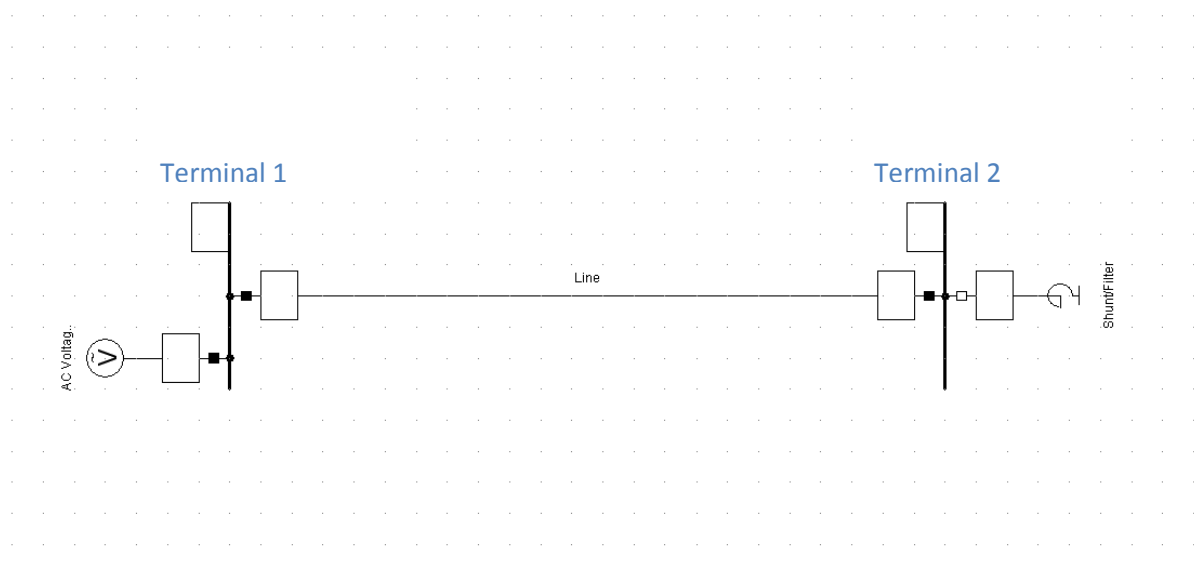


Figure 4.5 Simplified model of source, transmission line and shunt reactor.

What is desired in the simulation is that from figure 4.5, the voltage difference should be larger when energising from a weaker network. To create a weaker network, the internal reactance ( $X_s$ ) is changed in the AC voltage source, as with the Matlab model.

# 5 Method HVDC investigation

To investigate how HVDC can contribute in power restoration a set of EMT (electro mechanical transient) simulations will be run in PowerFactory. First needed is an HVDC-model built in PowerFactory. In this case a simplified PI-model is used to represent a transmission line. A theoretical analysis will be done to prove the performance of the HVDC in the simplified model.

## 5.1 HVDC Modelling

The HVDC model in this work is built in DIGSILENT PowerFactory by using existing components of the software. The structure will be as described in section 2.3.1. The PWM modulated converters are used to rectify/invert the voltage at the HVDC station. The DC cable parameters are set accordingly to the Sydvästlänken. For parameter values, see appendix B.

The model in fig 5.1 was used in the simulations and suggested by DIGSILENT. The parameters of the converter controller is already pre-set by DIGSILENT.

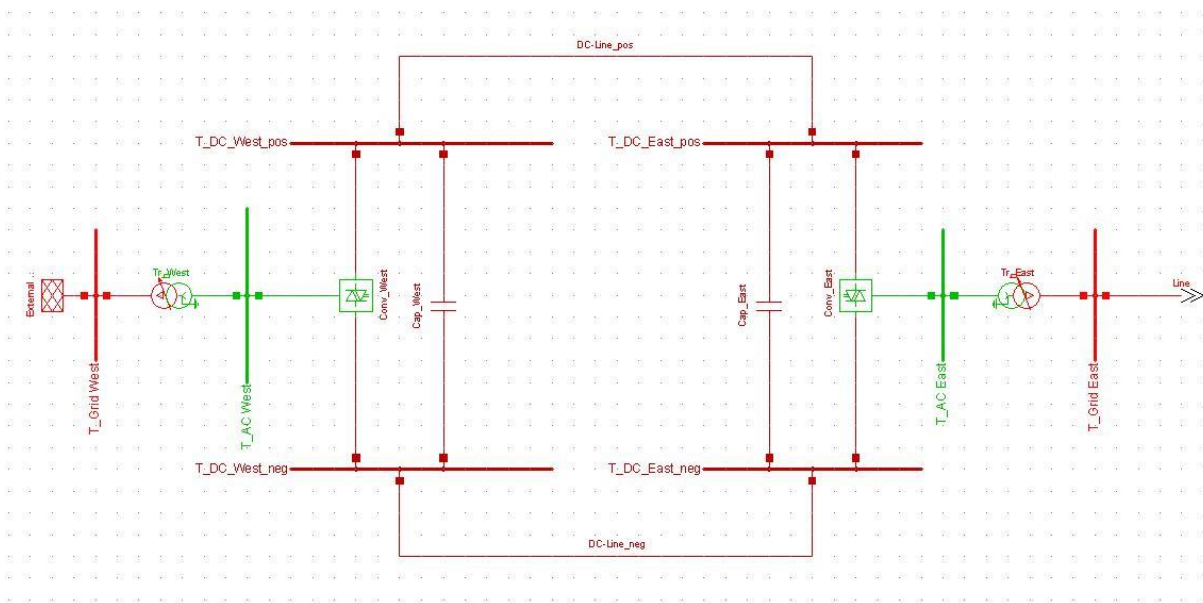


Figure 5.1 The VSC-HVDC model in PowerFactory.

Each converter is set to PV-controlled or PQ-controlled. In this system the eastern converter is PV-controlled as the voltage level should be controlled in the node connected to the grid. The western node is a PQ-controlled converter. The control system of the VSC can be viewed in the following block diagram in fig. 5.2.

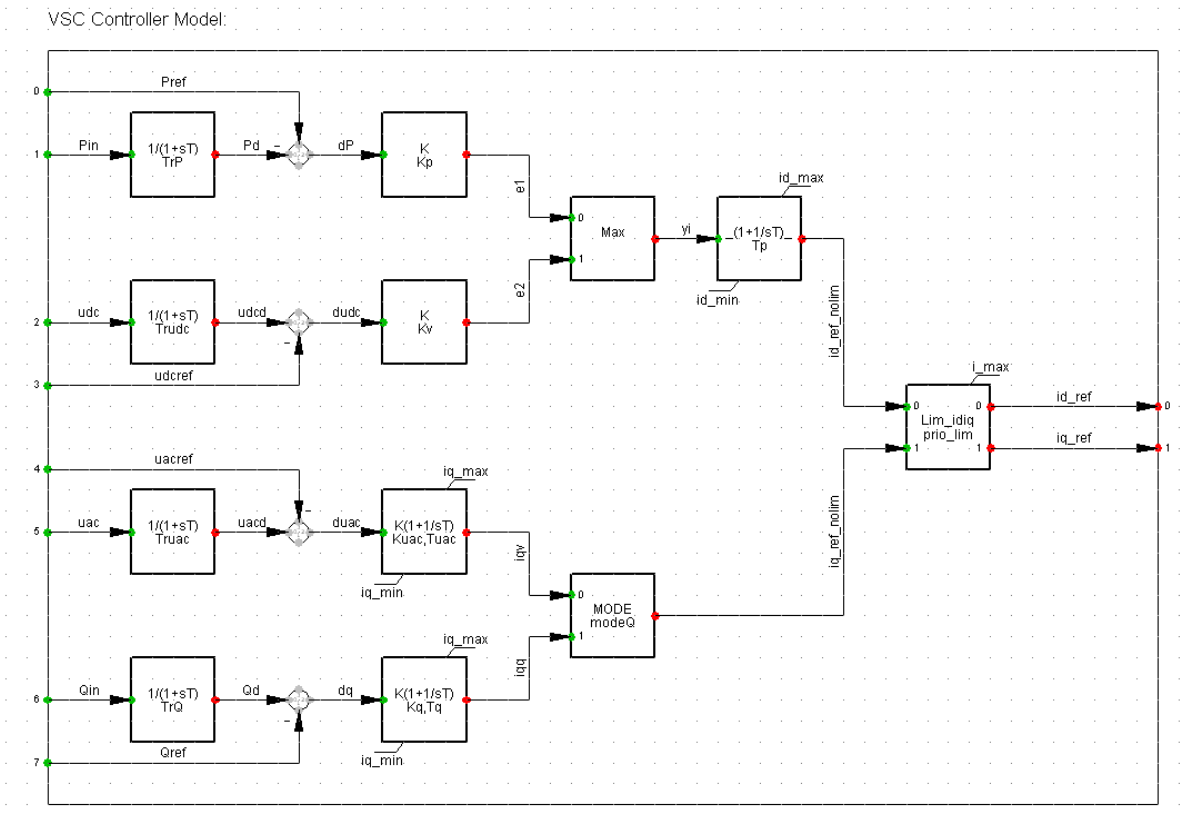


Figure 5.2 Block diagram of the converter control system.

## 5.2 HVDC simulation

The HVDC performance is investigated by implementation with the already presented PI-model in the previous chapter. A shunt reactor is connected to the same terminal as the HVDC. The complete model to be run in PowerFactory is presented below in fig. 5.3.

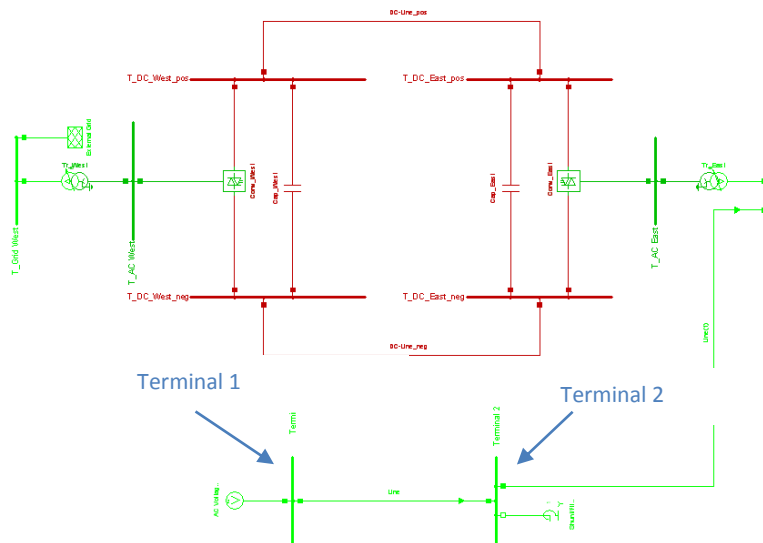


Figure 5.3 HVDC connected with PI-model in PowerFactory.

With simulations on this model the HVDC ability to compensate with reactive power can be proven. There will be a voltage difference when connecting and disconnecting the shunt reactor. The voltage differences supposed to be smaller when HVDC is connected. In this type of simulation the HVDC will only supply reactive power and no active power.

To show the ability that the HVDC can consume reactive power a simulation without the shunt reactor will be done. One can run the PI-model without the HVDC and connect it after some time. In a simulation like that the Ferranti effect will increase the voltage in terminal 2 in figure 5.3 and when the HVDC is connected it will consume reactive power, which will decrease the voltage in terminal 2 to the desired voltage level.

In another simulation the HVDC will alone energize the PI-model. PowerFactory has some limitations on how to initialize the system and therefore one will have to work around that. The simulation will be run on the following model, see fig. 5.4.



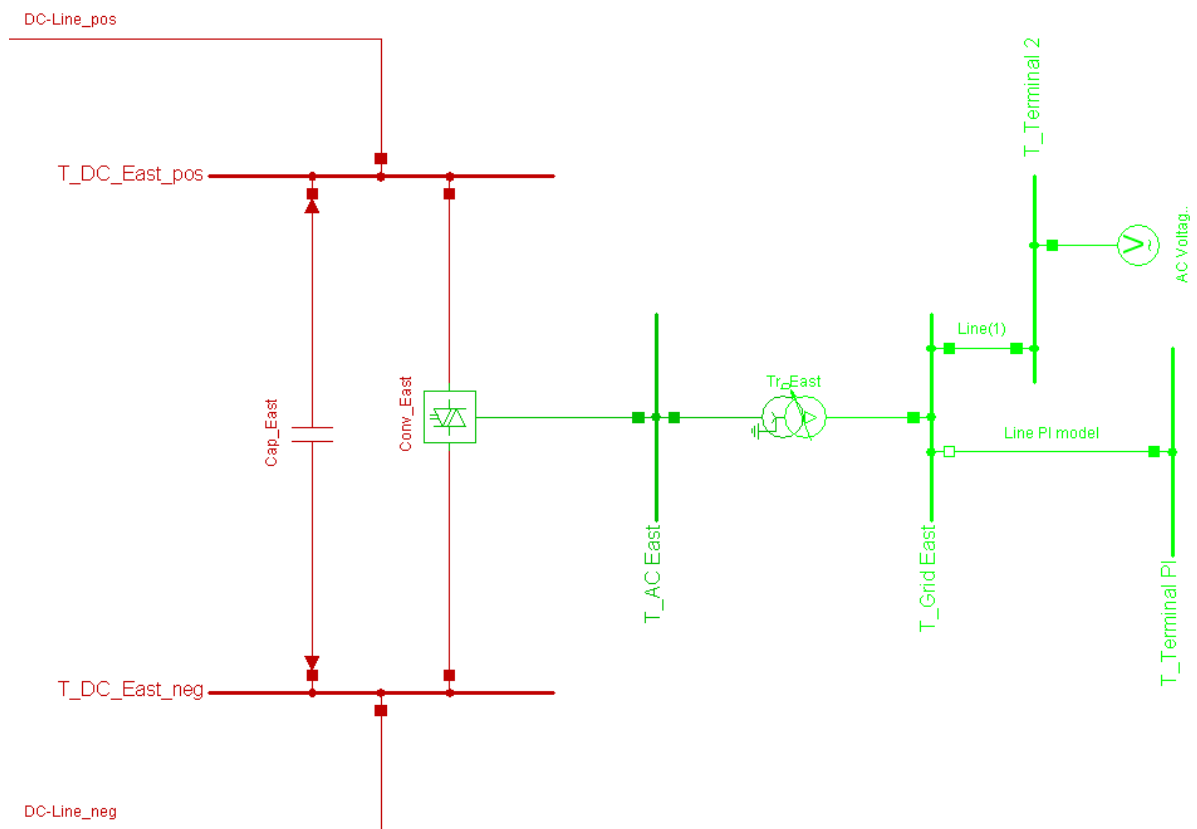


Figure 5.4 HVDC energizing PI-model in PowerFactory.

In the Initialisation the PI-model is disconnected and a voltage source is connected with the HVDC. Then during simulation the voltage source is disconnected, which forces the HVDC to energize the node T\_Grid East. When the HVDC is energising alone, the PI-model is connected to T\_Grid East.

# 6 Results on avoiding reactor hunting

Results from experiments on how the strength of the net ( $S_{sc}$ ) is related with hunting. To improve the validity of these results a theoretical comparison is made with a simple PI model in Matlab.

## 6.1 Relationship between $S_{sc}$ and tolerance band of automatics

There have been three steps of measurements and calculations to reach a conclusion regarding a relationship between a node's  $S_{sc}$  and the required change of tolerance band to avoid hunting. Each step is presented with results and evaluation. The first step proves the fact that the method used to calculate  $S_{sc}$  is valid. The  $S_{sc}$  should be higher in a functioning grid than in a net during restoration.

The second step is about finding the weakest strategy regarding connecting nodes. If a weak path can be identified, a data collection can be done to find extreme values of tolerance band change. If we know what is characteristic for a weak path it will be easier to choose random paths that are rather weak than strong. In that way more valuable data can be obtained. The random paths are used in step three. In this part the relation between  $S_{sc}$  and change of tolerance band of the shunt automatics is presented.

In figure 6.1 a plot with the consumed reactive power and the change of tolerance band has been made. This is to show one example of possible relations that could have been used in the investigation of how to avoid hunting.

The MVA base in this chapter is always 1000 MVA and the voltage base is 400 kV.

### 6.1.1 Experimental determination of Ssc

Below are calculated short circuit capacities for all nodes in the southern part of the grid. Table 6.1 shows high values of short circuit capacity when in a complete functioning grid. Tables 6.2-6.4 show significantly lower values of the short circuit capacity, during the restoration after a partly black out. Tables 6.2-6.4 have different starting nodes to be able to find a comparison between different possibilities to start the restoration process. The results give an indication about what node is most suitable for being the start node in a restoration process.

Table 6.1. Measured  $\Delta Q$ ,  $\Delta V$  and the calculated short circuit capacity Ssc of nodes in the southern part of the grid with shunt reactors in an intact network

	Q2(MVAR)	Vbefore(kV)	Vafter(kV)	Ssc(pu)
Ruthuvud 3X	267	413	409	26,7
Norrås 3X	300	406	398	15
Kärnan 3X	350	410	399	12,73
Blocket 1X	100	410	406	10
Sydköping 2X	250	408	397	9,1

Table 6.2. Measurements during the restoration process with Kärnan as starting node

Column1	Q2(MVAR)	Vbefore(kV)	Vafter(kV)	Ssc(pu)
Norrås 3X	303	442	406	3,37
Kärnan 3X	332	478	429	2,71
Ruthuvud 3X	420	530	436	1,79
Sydköping 2X	242	445	387	1,67
Blocket 1X	137	502	468	1,6

Table 6.3. Measurements during the restoration process with Norrås as starting node

	Q2(MVAR)	Vbefore(kV)	Vafter(kV)	Ssc(pu)
Norrås 3X	300	464	427	3,24
Kärnan 3X	330	441	380	2,16
Sydköping 2X	241	445	387	1,66
Blocket 1X	132	492	460	1,65
Ruthuvud 3X	364	499	408	1,6

Table 6.4 Measurements during the restoration process with Atomsberg as starting node

	Q2(MVAR)	Vbefore(kV)	Vafter(kV)	Ssc(pu)
Kärnan 3X	460	477	442	5,26
Norrås 3X	318	466	412	2,36
Sydköping 2X	282	485	428	1,98
Blocket 1X	130	490	455	1,49
Ruthuvud 3X	262	480	345	0,78

If to choose a starting node there are three different options: Norrås, Kärnan or Atomsberg (next node after Atomsberg with shunts would be Ruthuvud). It's desirable to start with a node that has the highest chance to avoid hunting. It appears that Norrås or Kärnan are the two strongest nodes, as Ruthuvud appears very weak when connecting from Atomsberg first, which increases the possibility for hunting. If starting either with Kärnan or Norrås, the result shows that Norrås is the strongest node. Norrås has a larger Ssc in both table 6.2 and 6.3.

### 6.1.2 Weakest power restoration strategy

The Ssc marked in red, in table 6.5, is the next node to connect with lowest Ssc. Same procedure is done for the selected node until the entire transmission level grid is connected. The resulting weakest strategy based on short circuit capacity is seen in table 6.6.

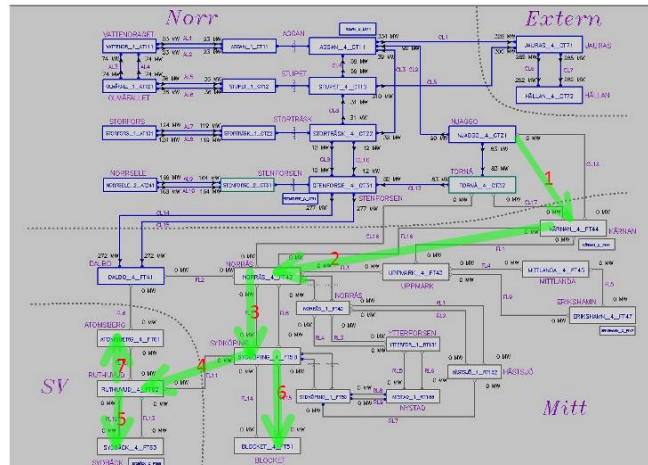
Table 6.5. Finding the weakest strategy

Node	Next node	Q(MVAR)	Vb(kV)	Va(kV)	Ssc(pu)
0. North					
	Kärnan (Njaggo)	280	473	357	0,97
	Kärnan (Tornå)	272	428	350	1,39
	Norrås (Dalbo)	268	411	350	1,76
	Norrås (Tornå)	269	441	350	1,18
	Atomsberg	274	417	330	1,26
1. Kärnan					
	Norrås (Kärnan)	175	377	283	0,74
	Norrås (Dalbo)	269	411	349	1,74
	Norrås (Tornå)	272	444	352	1,18
	Uppmark	177	373	285	0,80
	Atomsberg	280	424	333	1,23
2. Norrås					
	Uppmark (Kärnan)	130	312	243	0,75
	Uppmark (Norrås)	108	290	222	0,64
	Atomsberg	280	420	328	1,22
	Sydköping (Norrås)	111	305	225	0,56
3. Sydköping					
	Uppmark (Kärnan)	105	275	219	0,75
	Uppmark (Norrås)	80	240	191	0,65
	Atomsberg	289	419	323	1,20
	Ruthuvud	71	307	180	0,22
	Blocket	68	254	175	0,34
4. Ruthuvud					
	Blocket	60	235	165	0,34
	Atomsberg (Dalbo)	291	417	320	1,20
	Sydbäck	50	175	550	0,17
5. Sydbäck					
	Blocket	65	248	172	0,34
6. Blocket					
7. Atomsberg					
8. Uppmark					

Blocket is the evident weakest node when connecting from Sydbäck. No further measurements are needed. As there are no shunt reactors connected to neither Atomsberg nor Uppmark, it is not interesting to find the weakest node between them. All nodes with shunt reactors are already connected and further connections will not affect the experimental result.

Table 6.6. Resulting weakest strategy

Weakest restoration strategy
1. Kärnan
2. Norrås
3. Sydköping
4. Ruthuvud
5. Sydbäck
6. Blocket
7. Atomsberg
8. Uppmark



### 6.1.3 Data gathering to find relation between Ssc and ΔV

The following data was achieved while implementing 4 different strategies for power restoration. With different strategies a wider range of data can be obtained, see tables 6.7-6.10 for the different strategies.  $V_b$  is the voltage when the node is energized but without shunt elements,  $V_a$  is when the shunt elements have been connected.  $\Delta V$  is, as explained in section 4.1.3, the change in tolerance band with respect to the lower default limit 380kV. Table 6.11 contains the collected data from the 4 different experiments.

Table 6.7. Nodes with shunt reactors and corresponding short circuit capacity and change of tolerance band for random strategy 1.

Nodes	Q2(MVAR)	V <sub>b</sub> (kV)	V <sub>a</sub> (kV)	Ssc(pu)	Δ V(kV)
Ruthuvud	234	430	327	0,91	53
Kärnan	292	484	365	0,98	15
Sydköping	232	586	324	0,35	56
Blocket	166	519	276	0,27	104
Norrås	286	455	361	1,22	19

Table 6.8. Nodes with shunt reactors and corresponding short circuit capacity and change of tolerance band for strategy 2

Nodes	Q2(MVAR)	V <sub>b</sub> (kV)	V <sub>a</sub> (kV)	Ssc(pu)	Δ V(kV)
Kärnan	291	443	364	1,47	16
Norrås	97	428	396	1,21	0
Sydköping	223	435	319	0,77	61
Ruthuvud	230	591	325	0,35	55
Blocket	212	475	312	0,52	68

Table 6.9. Nodes with shunt reactors and corresponding short circuit capacity and change of tolerance band for strategy 3

Nodes	Q2(MVAR)	Vb(kV)	Va(kV)	Ssc(pu)	$\Delta V$ (kV)
Norrås	286	456	362	1,22	18
Kärnan	218	427	316	0,79	64
Ruthuvud	233	429	325	0,90	55
Sydköping	230	582	325	0,36	55
Blocket	161	539	271	0,24	109

Table 6.10. Nodes with shunt reactors and corresponding short circuit capacity and change of tolerance band for the weakest strategy

Nodes	Q2(MVAR)	Vb(kV)	Va(kV)	Ssc(pu)	$\Delta V$ (kV)
Kärnan	291	485	365	0,97	15
Norrås	221	437	318	0,74	62
Sydköping	202	439	303	0,59	77
Ruthuvud	215	651	316	0,26	64
Blocket	194	497	298	0,39	82

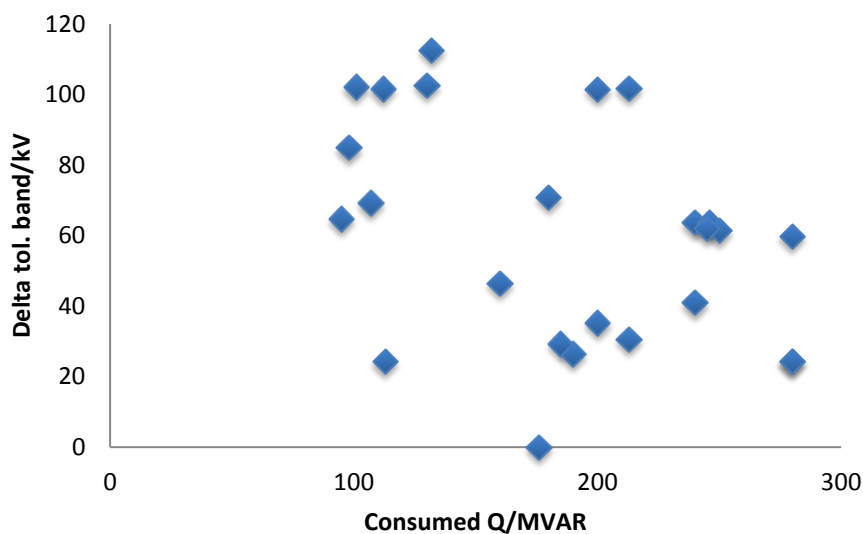


Figure 6.1. Consumed reactive power with needed change of tolerance band to avoid hunting.

No relation can be found between the consumed reactive power of a shunt in a node and the change of tolerance band to avoid hunting. The points in figure 6.1 are scattered with no obvious connection. This enhances the focus on the relation between Ssc and the change of tolerance band. It might seem rare that the consumed reactive power is different even though every node is equipped with the same size of shunt reactor with aspect to reactive power (350 MVAR). But the reactive power is not constant and it can't be with a varying voltage. Instead it is the inductance

(Xshunt) that is constant and the same in every, although reactive power is what define the size of a shunt reactor. The reactive power consumption will vary as we have different voltage levels when connecting the shunts see eq. 2.4 for how the Qloss depends on the current I (which can be described as U/Xshunt).

Table 6.11. Collected data for short circuit capacity and corresponding change of tolerance band

Strategy	Ssc(pu)	$\Delta V(kV)$
Random 1	0,91	53
	0,98	15
	0,35	56
	0,27	104
	1,22	19
Random 2	1,47	16
	1,21	0
	0,77	61
	0,35	55
	0,52	68
Random 3	1,22	18
	0,79	64
	0,90	55
	0,36	55
	0,24	109
Weakest	0,97	15
	0,74	62
	0,59	77
	0,26	64
	0,39	82

With the data in table 6.11, a plot could be made to visualize the evident increase of tolerance band change for weaker nodes (lower short circuit capacity). See figure 6.2.

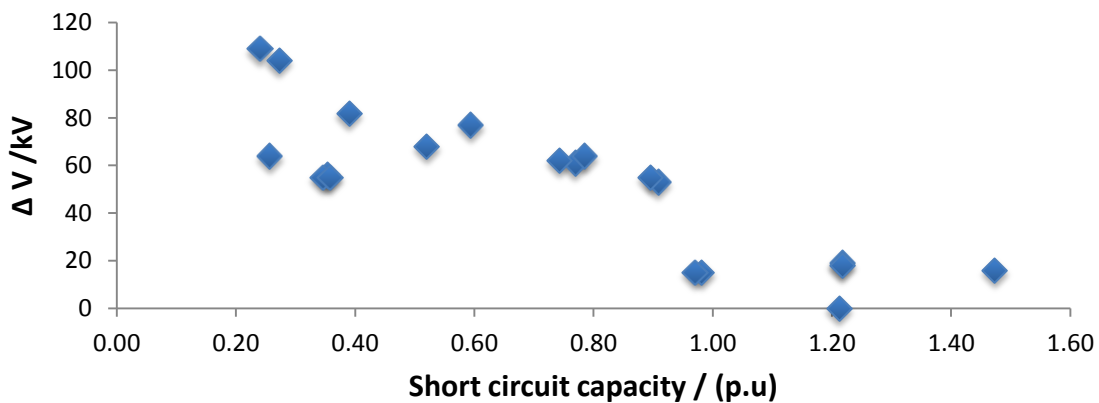




Figure 6.2. Plotted result from table 6.11

To prevent hunting, all points in figure 6.2 need to be below a possible relation-curve. This relation curve is implemented in figure 6.3. It is made by a linearization between the point with highest change of tolerance band and the point with highest short circuit capacity. That line is then raised with a five percent margin. Eventual points above the line would cause hunting for their corresponding node.

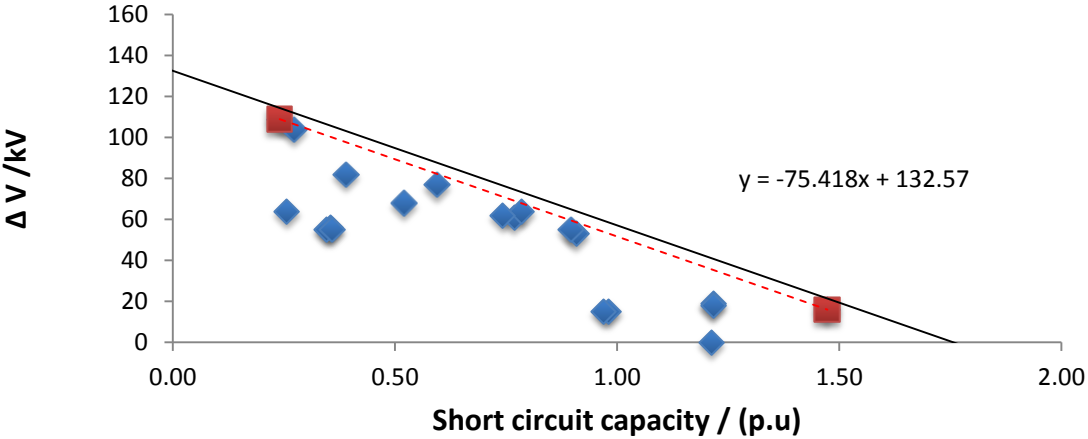


Figure 6.3 Linearization between two points creating a relation that will prevent hunting.

The minimum change of tolerance band can be calculated from the equation in fig. 6.3. It will not generate the minimum tolerance band for every specific node, but the minimum tolerance band for every possible node with the corresponding Ssc. The result is obtained by using the three paths, which are explained in section 4.2.1. This includes the weakest possible path that has the lowest Ssc for the nodes and will therefore produce the largest threshold bands. There is no other path that will create larger bands and because of this, the red-dotted line in figure 6.3 illustrates the worst-case scenario. It shows that if this line is used, no hunting will occur during any other thinkable path.

### 6.2 Theoretical result

The result in fig. 6.3 is taken from experiments. In this part a comparison with the theory is made.

The following plot is the voltage difference between when the node is first connected and when the shunts are connected ( $V_{before} - V_{after}$ ), with the corresponding node Ssc. According to the approximation in eq. 2.10 an inverse relation can be expected.

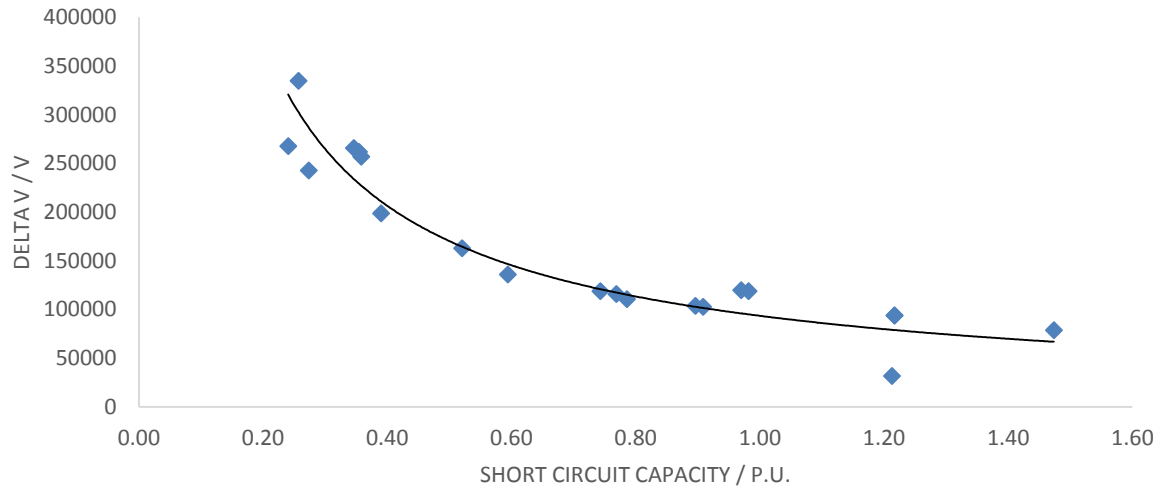


Figure 6.4 Delta V with corresponding short circuit capacity for all nodes during data gathering with trendline fitted to the datapoints.

In figure 6.4 an inverse relation can be seen. Since the shunt reactance in each node is set to the same size, the deviation of the data points is relatively small.

With the simple model of a transmission line and a shunt reactor, described in section 4.5, the voltage difference before and after the shunt is connected is plotted for different Ssc. This is shown in figure 6.5.

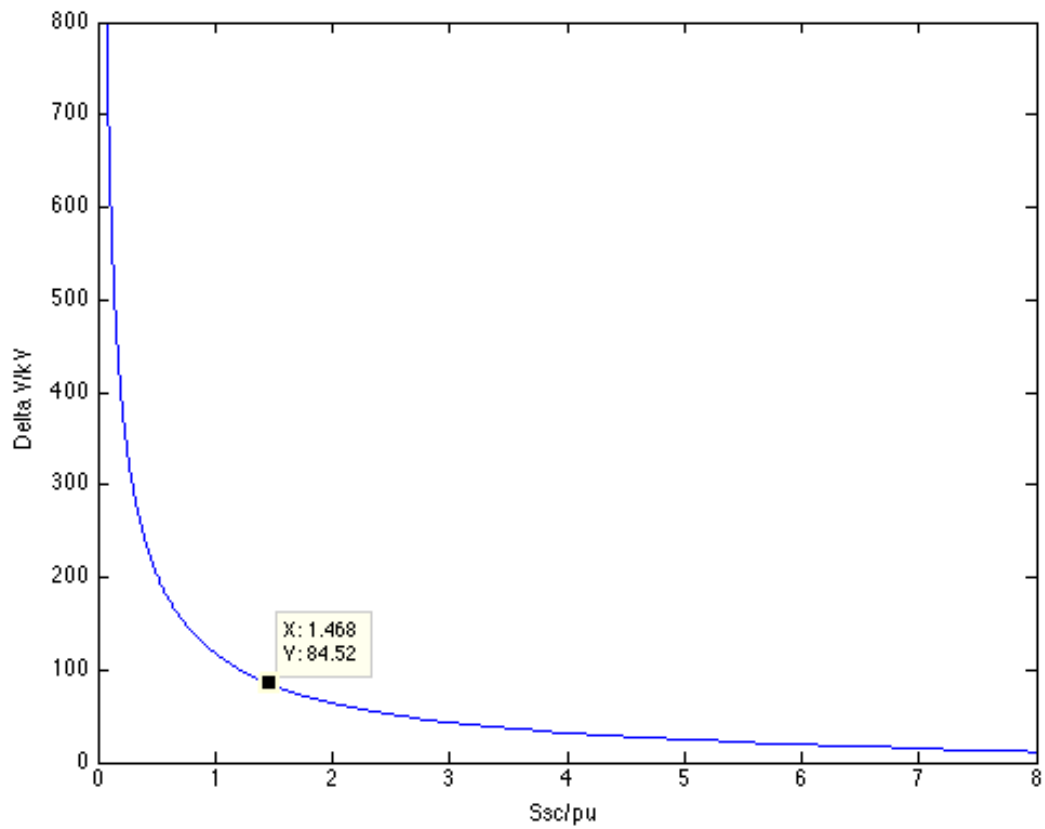


Figure 6.5 Delta V with Ssc.

In the graph the relation between delta V and Ssc behaves like an inverse, which the approximation in fig. 6.4 does as well.

The results from the PowerFactory model, when connecting a shunt reactor to a net with different strengths are demonstrated in fig 6.6-6.9.

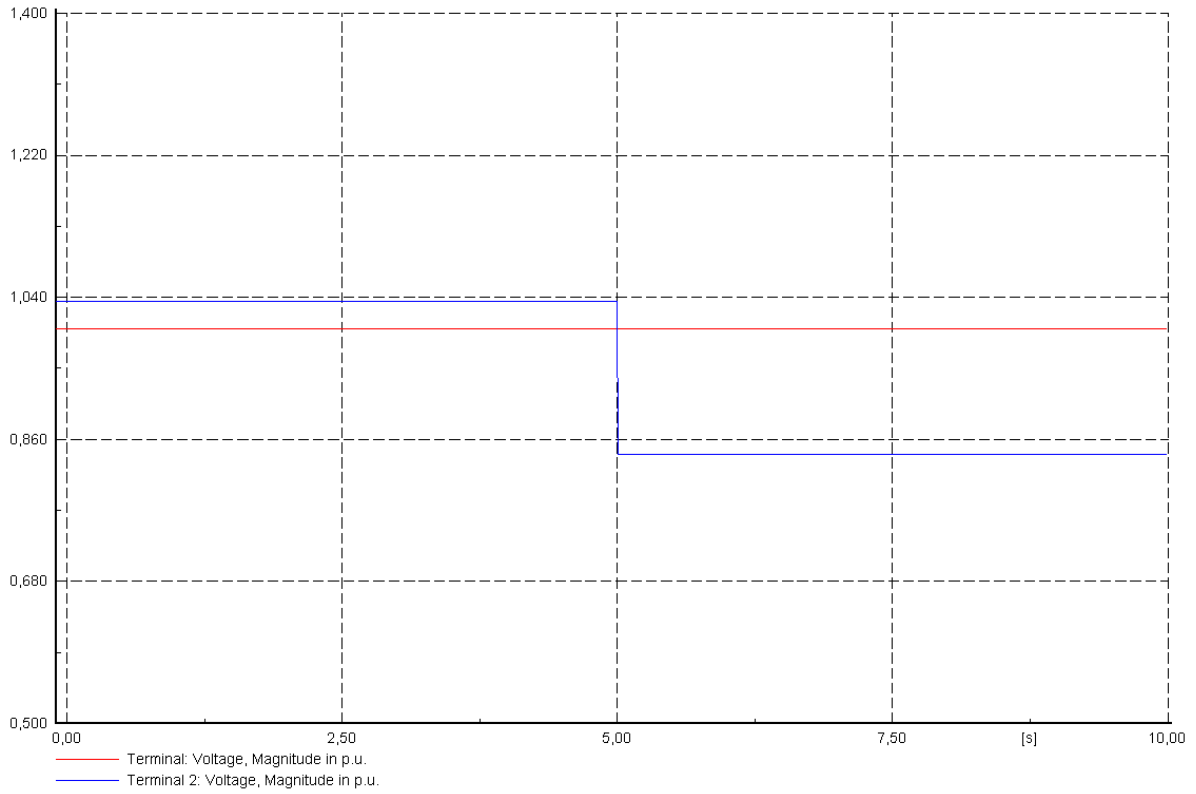


Figure 6.6 Shunt action with  $X_s=0$  in model of fig.4.5.

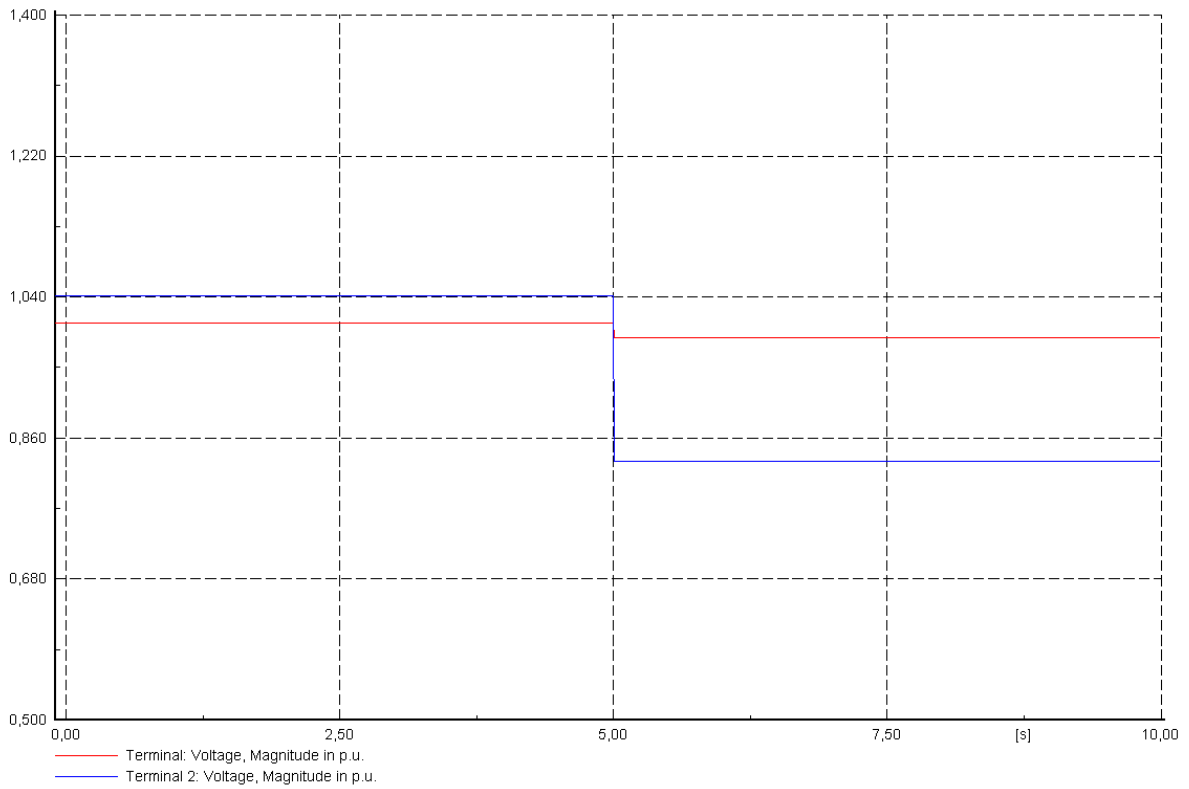


Figure 6.7 Shunt action with  $X_d=10$  in model of fig.4.5.

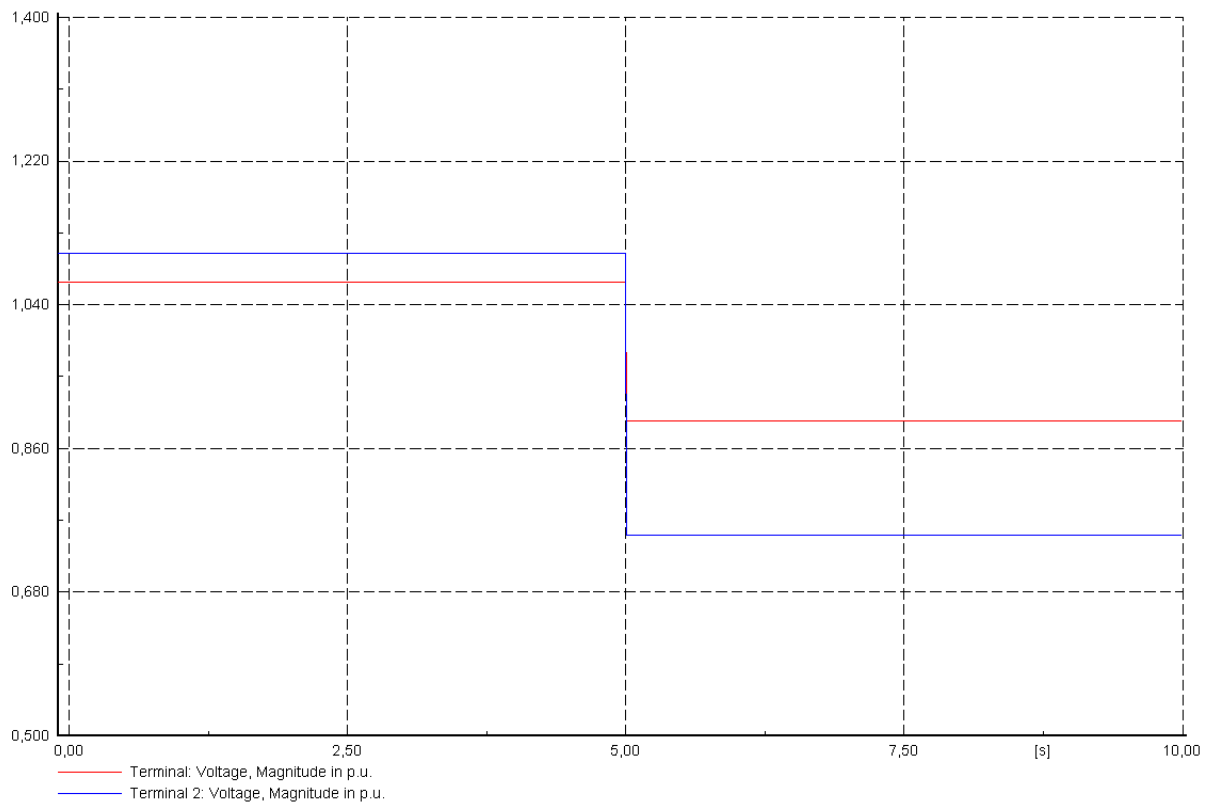


Figure 6.8 Shunt action with  $X_d=100$  in model of fig.4.5.

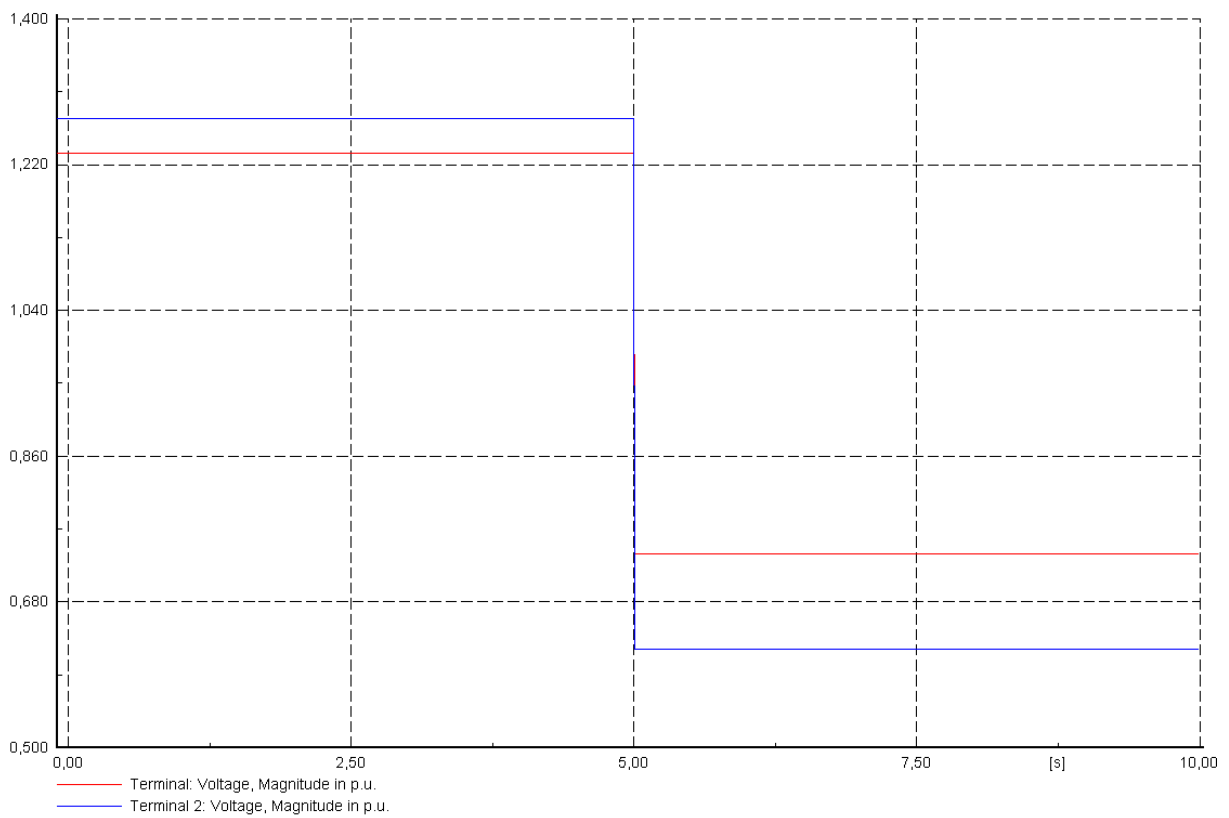


Figure 6.9 Shunt action with  $X_d=300$  in model of fig.4.5.

In fig 6.10 one can see the calculated Ssc in PowerFactory when Xd is set to 6 ohm. This has been found by trial and error to reach the Ssc as in ARISTO for this line model.

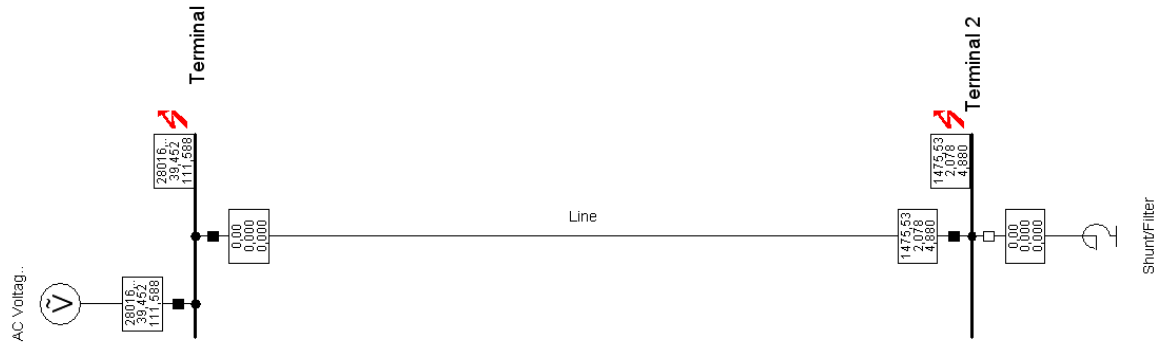


Figure 6.10 Ssc in the line model of PowerFactory when Xd=6.

The voltage difference for this case is very interesting to compare with Aristo and Matlab. It's presented in fig 6.11.

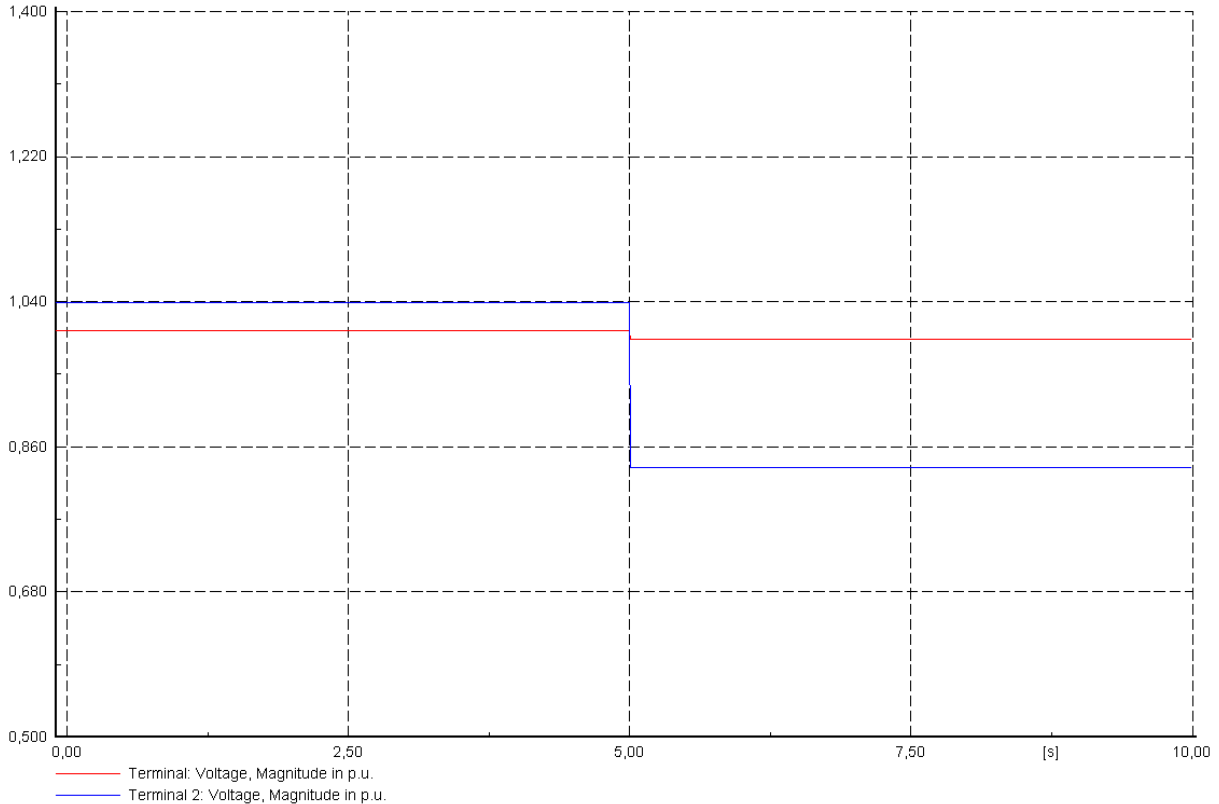


Figure 6.11 Shunt action with Xd=6 in model of fig.4.5.

The result from figures 6.6-6.11 is summarized in table 6.12. The result is pleasing and the model is acting like expected, the voltage difference increases for weaker networks. This gives accreditation that the method used when finding Ssc in Aristo is valid. That means we have an experimental method based on theory, which is backed up with these simple model experiments.

Table 6.12. Voltage differences from figures 6.6-6.9

Xd	Ssc	Voltage difference (kV)
0	1.5537	78,4
6	1.475	81,6
10	1.4276	84,4
100	0.823	140,8
300	0.4231	262,8

Ssc is calculated in PowerFactory with built in methods.

The voltage difference at Ssc=1,47 is 81,6, according to PowerFactory simulations. In the theoretical model in fig. 6.5, the voltage difference is 84.5 at Ssc=1,47. That means PowerFactory can be well used as a simulator to collect Ssc. If one compare that to the result in ARISTO when Kärnan was connected from Tornå, see table 3.3, the voltage difference was 79kV at Ssc=1.47.

# 7 HVDC Results

In the results of the HVDC investigation in this thesis, the HVDC model performance both in simulation and theory is presented.

## 7.1 HVDC performance

In the theoretical analysis in chapter 6, a PI-model together with a shunt reactor built in PowerFactory is investigated. As earlier stated in the theory, the HVDC connection can help with reactive power during for e.g. restoration. If so, the voltage difference when connection a shunt reactor should be smaller compared to the result in fig. 6.8-6.11, where no HVDC connection exists. If the voltage difference is smaller, the tolerance band needs smaller adjustment and a voltage closer to the nominal can be obtained.

The performance of the HVDC connection in the model from fig. 5.3 is presented in fig. 7.1-7.4. The Ssc is changed in the same way as in chapter 6, by changing the size of Xs in the voltage source.

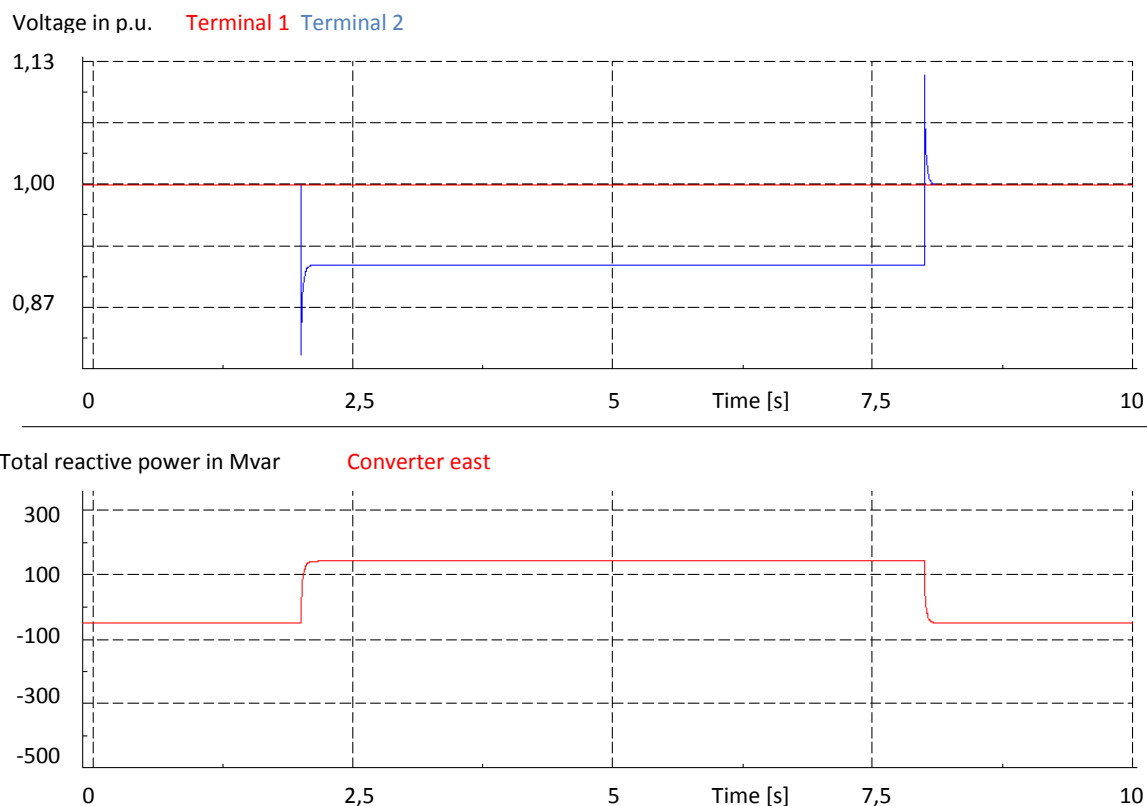


Figure 7.1 Shunt action with HVDC connection and reactive power contribution, Ssc=infinite.



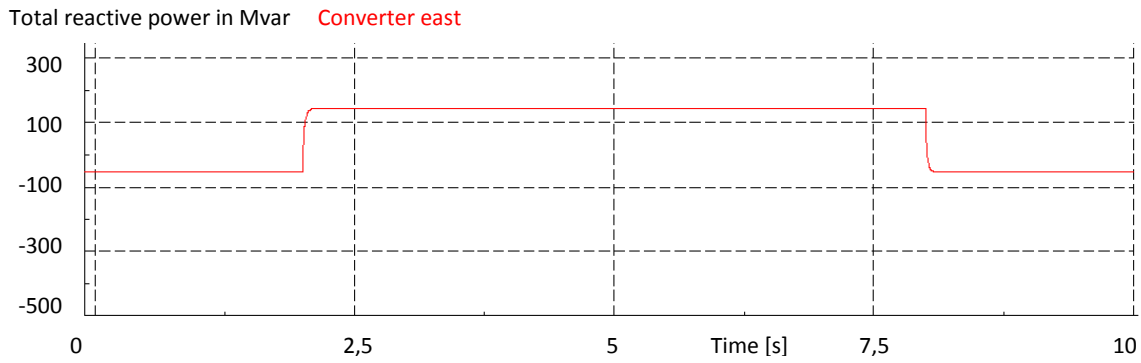
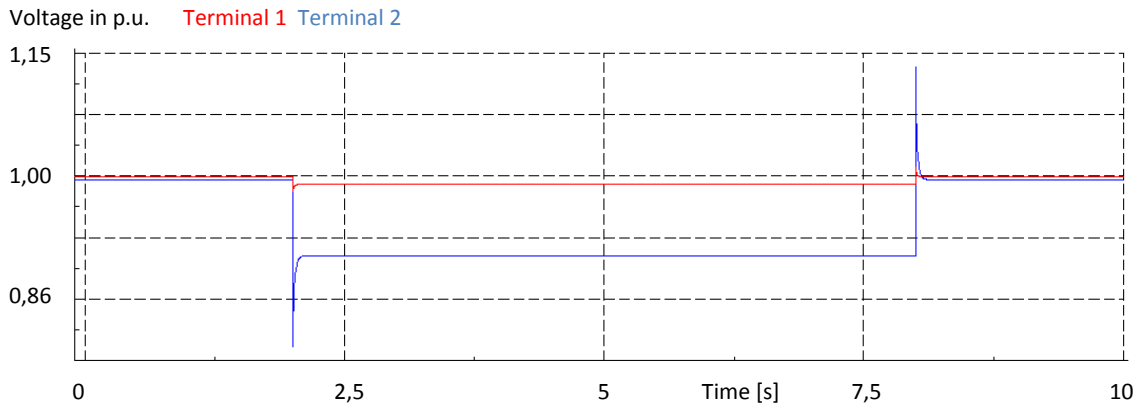


Figure 7.2 Shunt action with HVDC connection and reactive power contribution,  $S_{sc}=16$ .

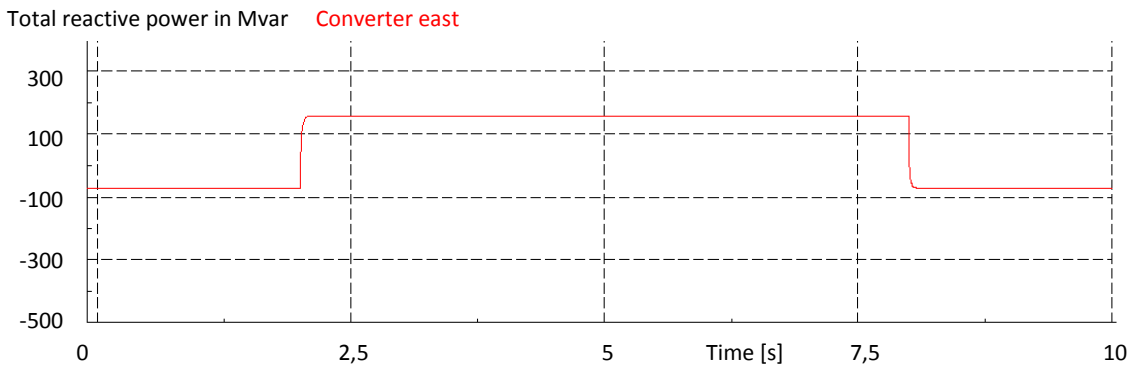
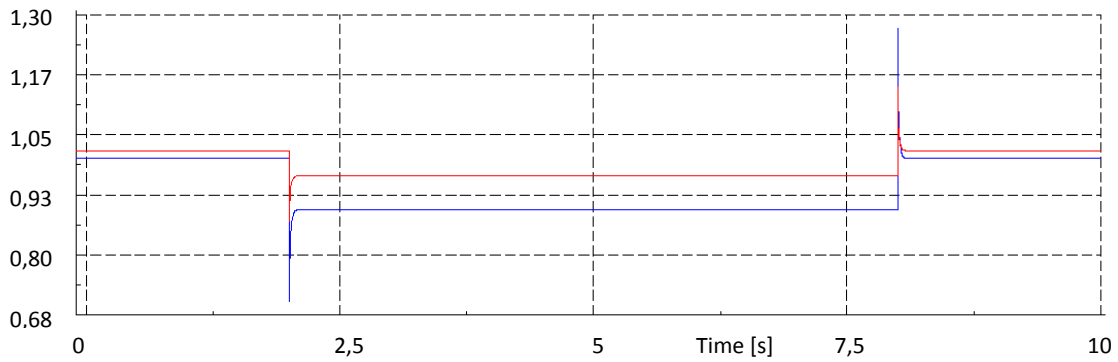


Figure 7.3 Shunt action with HVDC connection and reactive power contribution,  $S_{sc}=1,6$ .

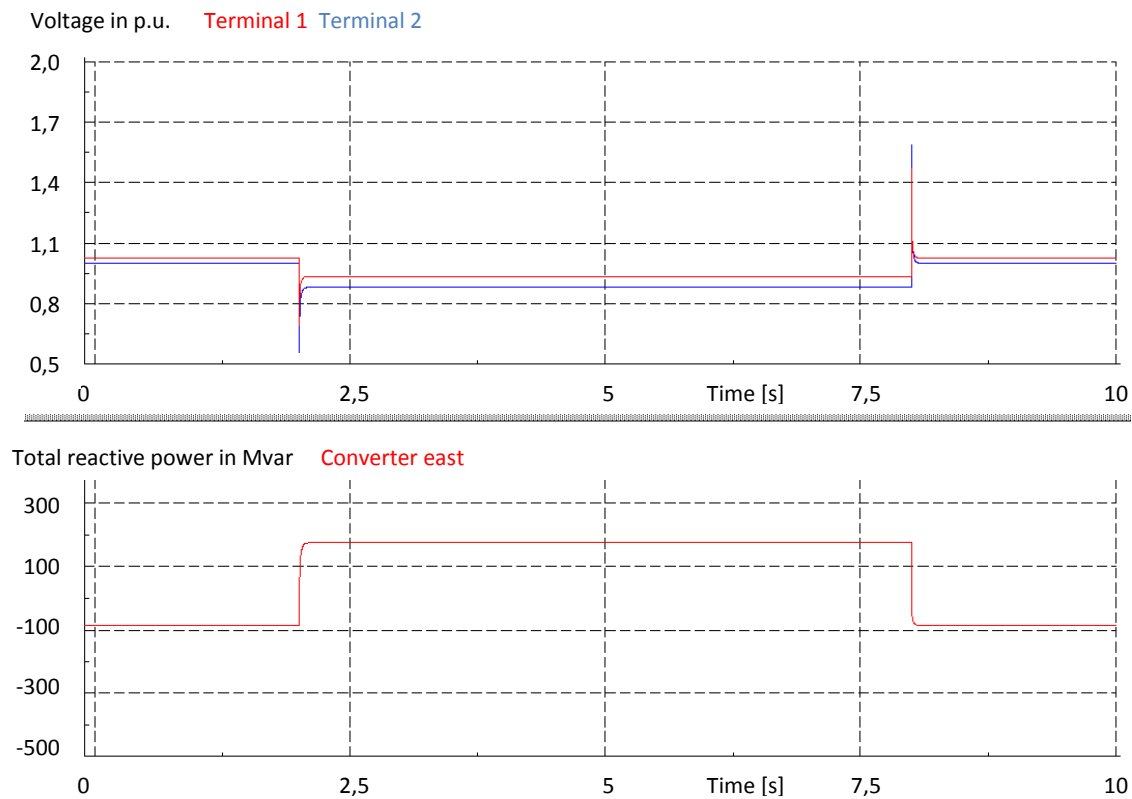


Figure 7.4 Shunt action with HVDC connection and reactive power contribution,  $S_{sc}=0,53$ .

The voltage difference is smaller now when the HVDC is connected. One can see that there is a spike every time the shunt is disconnected/connected. The spike reaches the voltage that would be reached if no HVDC were used. A short time after the shunt action, the HVDC controls the reactive power and the voltage is increases when the shunt is connected and decreased when the shunt is disconnected.

A complete comparison between the model without HVDC (fig. 4.5) and the model with HVDC (fig. 5.3) is presented in table 7.1. The voltage difference is before and after the shunt is connected.

Table 7.1 Voltage difference depending on  $S_{sc}$

$S_{sc}$	Voltage difference (kV)	Voltage difference with HVDC (kV)
Infinite	80,8	35
16	87,6	36
1,6	145,6	42
0,53	270	48

The performance of the HVDC is really present when shunt actions are made in weak system.

Below follows the result of connecting VSC-HVDC to verify the performance in terms of reactive power consumption. In this simulation the shunt reactor is not connected. The result is shown in

figure 7.5. Ferranti effect occurs in the PI model at terminal 2, see figure 5.3. After seven seconds the HVDC is connected to draw reactive power in order to stabilize the voltage.

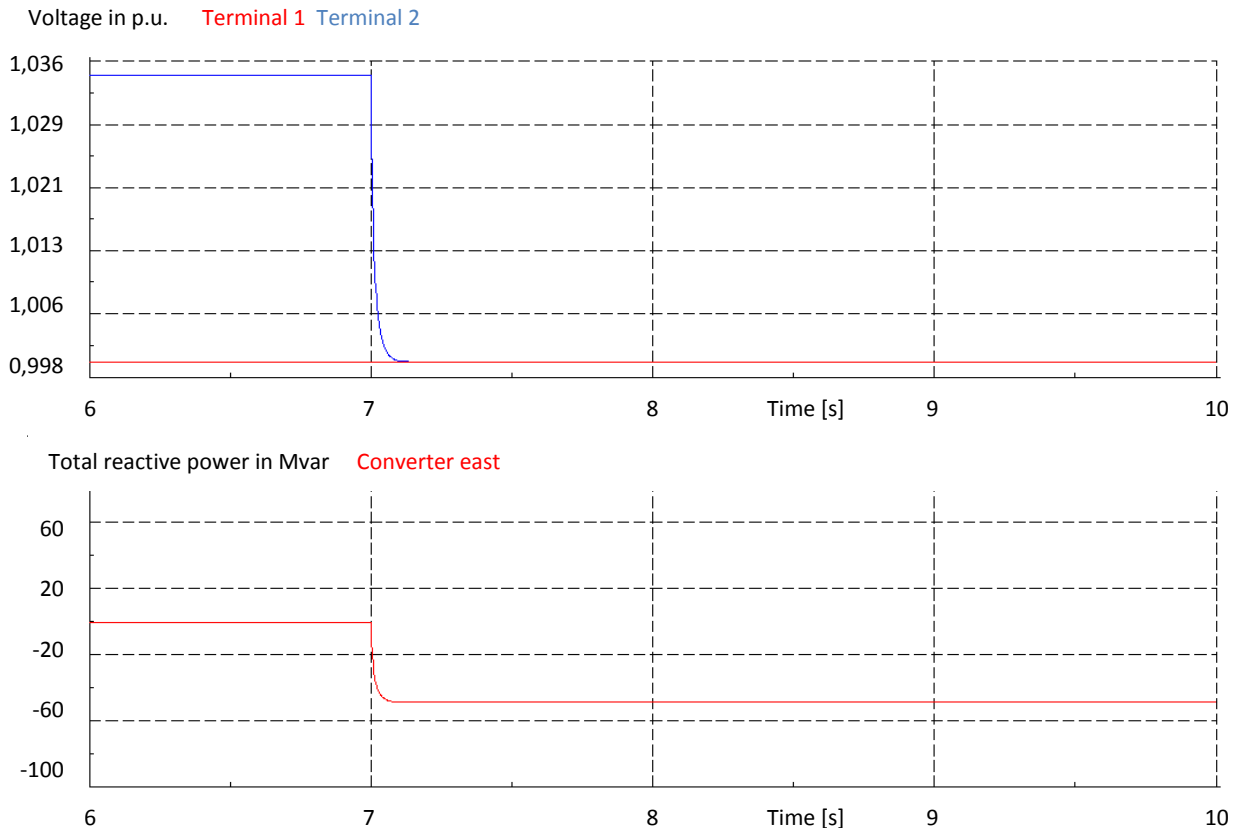


Figure 7.5 The Ferranti effect is eliminated when HVDC is connected.

The result of energizing the PI line model with HVDC is shown in fig. 7.6. It can be seen that the node that is energized increases from zero to nominal voltage when connected after 20 seconds (the blue line). The difference between the lines is due to the Ferranti effect. It can also be seen that the reactive power consumption from the HVDC converter is increased at this moment. This result shows that it is possible to energize a line from a VSC-HVDC converter station without any secondary generation.

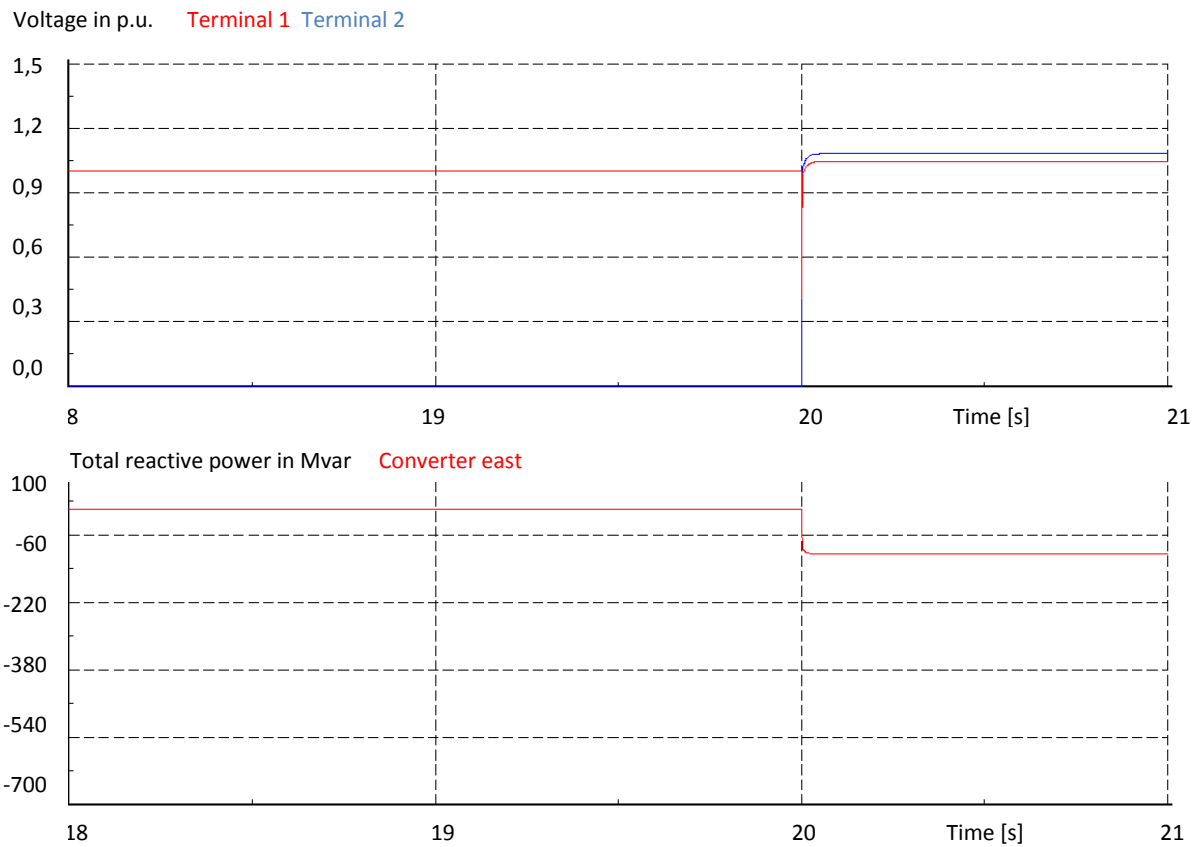


Figure 7.6 Energizing a line from VSC-HVDC

## 7.2 Energizing with VSC-HVDC and connecting shunt

In fig 7.7, the energization of a line is shown. The shunt reactor at the receiving end of the line is connected and then disconnected again. The voltage difference at the receiving end is 112 kV (before and after shunt connection). This corresponds to a  $S_{sc}$  of 0,96 with the use eq. 4.1. According to fig 6.5 this would correspond to a voltage difference of 122 kV.

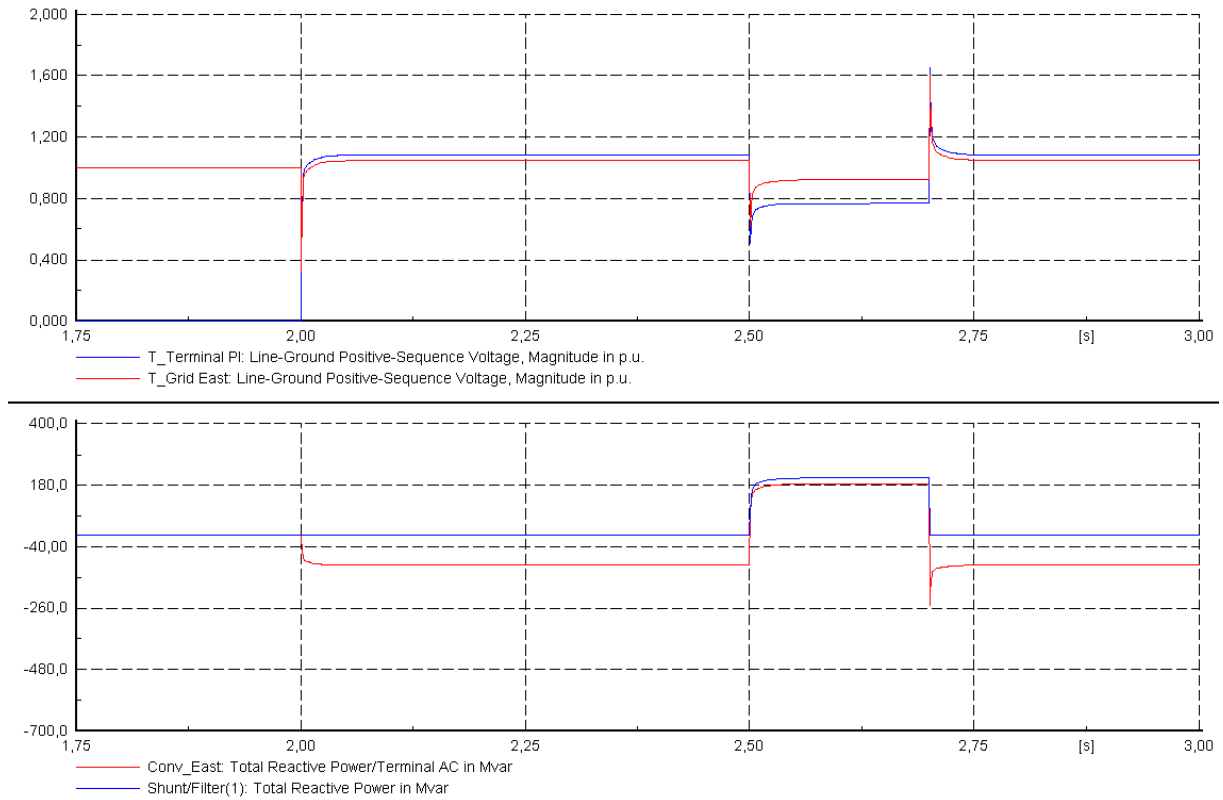


Figure 7.7. Energization of line with VSC-HVDC. Connecting line at 2 s, shunt at 2,5 s and disconnect shunt at 2,7 s

In table 7.2 one can see the difference between energization by HVDC and an AC voltage source.

Table 7.2 Comparison of voltage difference

Model	Ssc(pu)	$\Delta V(kV)$
HVDC	0.96	112
AC voltage source	0.96	122

# 8 Verification

In this chapter follows the method and results of the verification of the work on reactor hunting and Ssc. This adds satisfaction in that the results from earlier sections are reliable.

## 8.1 Verification of results in 6.1

To verify that the found relation between Ssc and tolerance band works for avoiding hunting, some random energising strategies have been made. The default tolerance band is 420 – 380 kV and  $\Delta V$  (kV) represents the change of tolerance band from the default limit to the new one, i.e. for a  $\Delta V=30$  kV the new tolerance band is 440-350 kV, as it is the lower limit that changes with  $\Delta V$  and 440 is set to the new upper limit during restoration as a default setting. The result is presented in following tables together with graphs showing case of hunting and without hunting. The voltage of the node after energization is marked in green in tables 8.1-8.5. All restorations were accomplished satisfactory expect for some cases where the voltage level is low.

Table 8.1 Short circuit capacity, change of tolerance band and resulting voltage of nodes with random restoration strategy 1

Nodes with shunts	Vb(kV)	Va(kV)	Ssc(pu)	$\Delta V$ (kV)
Norrås (Dalbo)	412	374	1,85	0
Kärnan (Njaggo)	474	358	0,97	60
Ruthuvud (Atomsberg)	433	328	0,91	64
Sydköping (Ruthuvud)	440	309	0,61	87
Blocket	375	312	0,71	79

In Figure 8.1 the hunting phenomena is illustrated when the tolerance band are set to default. Here the strategy 1 above is used. It shows the voltages after Kärnan is connected from Njaggo. The shunt reactors that are oscillating are the ones in Kärnan switchyard. The hunting also impacts the voltages in the other nodes, which can be seen in the figure 8.1

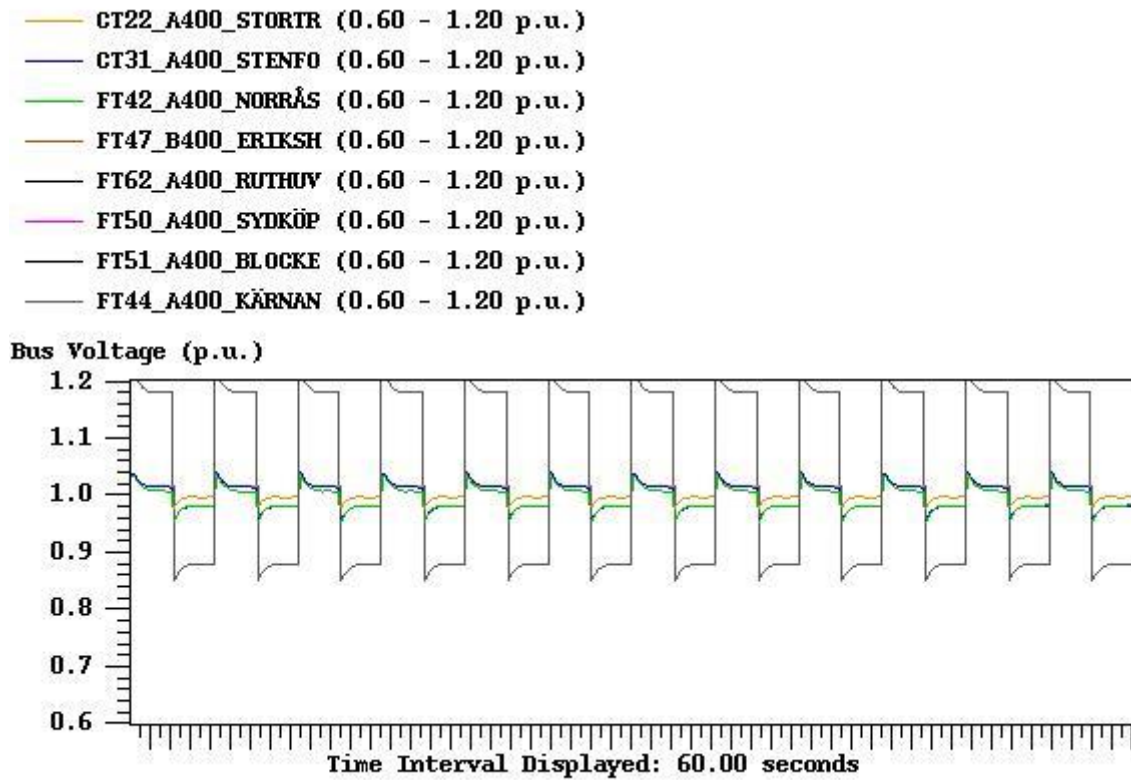


Figure 8.1 Hunting in Kärnan with default threshold bands for strategy 1

When the tolerance band is changed according to our formula, the hunting is avoided. This is shown in figure 8.2. Here the figure also shows the moment when the two nodes are connected (the two vertical lines).

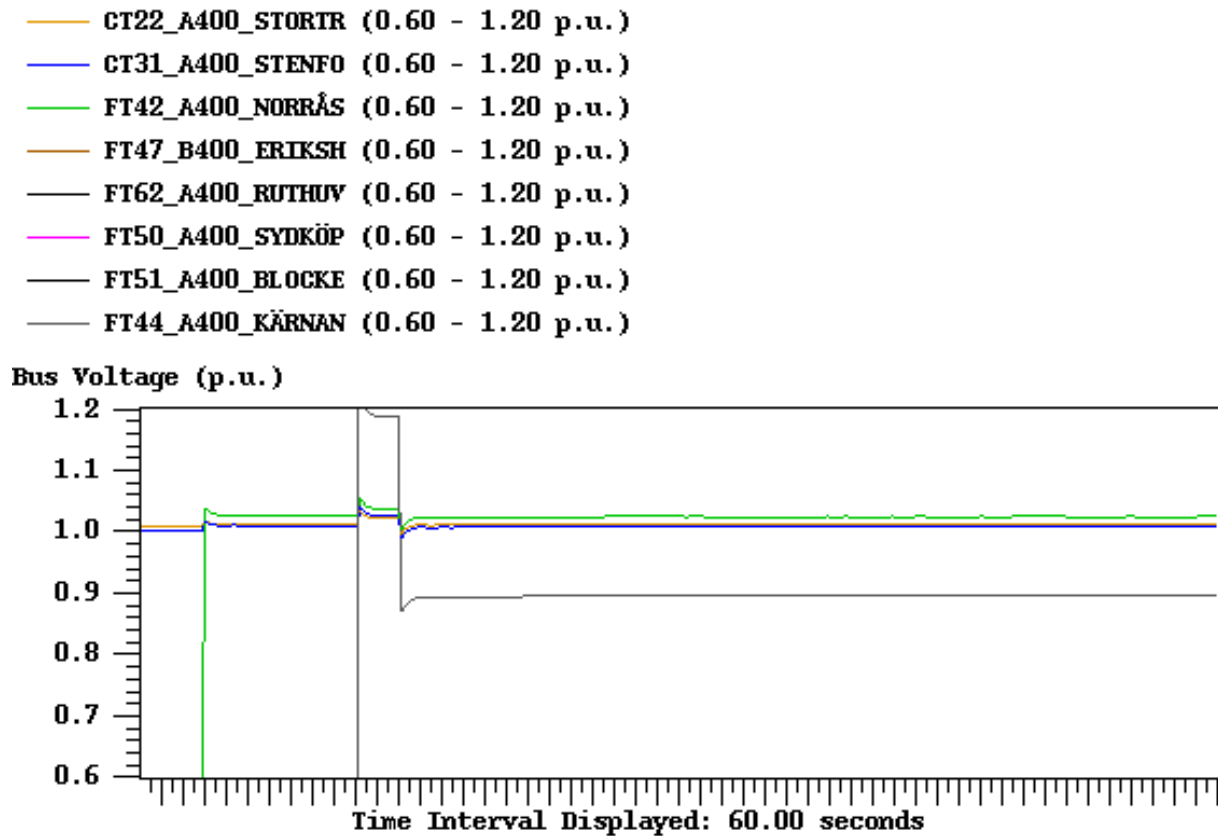


Figure 8.2 No hunting in Kärnan after adjusted threshold bands for strategy 1

Table 8.2 Short circuit capacity, change of tolerance band and resulting voltage of nodes with random restoration strategy 2

Nodes with shunts	Vb(kV)	Va(kV)	Ssc(pu)	$\Delta V$ (kV)
Kärnan (Tornå)	428	352	1,47	21
Norrås (Kärnan)	447	383	1,00	57
Ruthuvud (Atomsberg)	443	337	0,93	63
Sydköpingv(Norrås)	400	321	0,91	64
Blocket	364	322	0,93	62



- CT22\_A400\_STORTR (0.60 - 1.20 p.u.)
- CT31\_A400\_STENFO (0.60 - 1.20 p.u.)
- FT42\_A400\_NORRÅS (0.60 - 1.20 p.u.)
- FT47\_B400\_ERIKSH (0.60 - 1.20 p.u.)
- FT62\_A400\_RUTHUV (0.60 - 1.20 p.u.)
- FT50\_A400\_SYDKÖP (0.60 - 1.20 p.u.)
- FT51\_A400\_BLOCKE (0.60 - 1.20 p.u.)
- FT44\_A400\_KÄRNAN (0.60 - 1.20 p.u.)

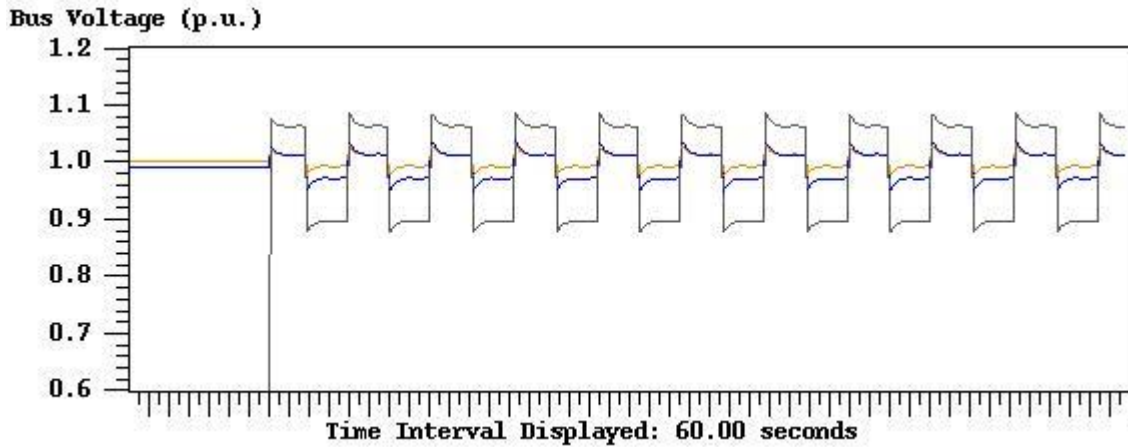


Figure 8.3 Hunting in Kärnan with default threshold bands for strategy 2

- CT22\_A400\_STORTR (0.60 - 1.20 p.u.)
- CT31\_A400\_STENFO (0.60 - 1.20 p.u.)
- FT42\_A400\_NORRÅS (0.60 - 1.20 p.u.)
- FT47\_B400\_ERIKSH (0.60 - 1.20 p.u.)
- FT62\_A400\_RUTHUV (0.60 - 1.20 p.u.)
- FT50\_A400\_SYDKÖP (0.60 - 1.20 p.u.)
- FT51\_A400\_BLOCKE (0.60 - 1.20 p.u.)
- FT44\_A400\_KÄRNAN (0.60 - 1.20 p.u.)

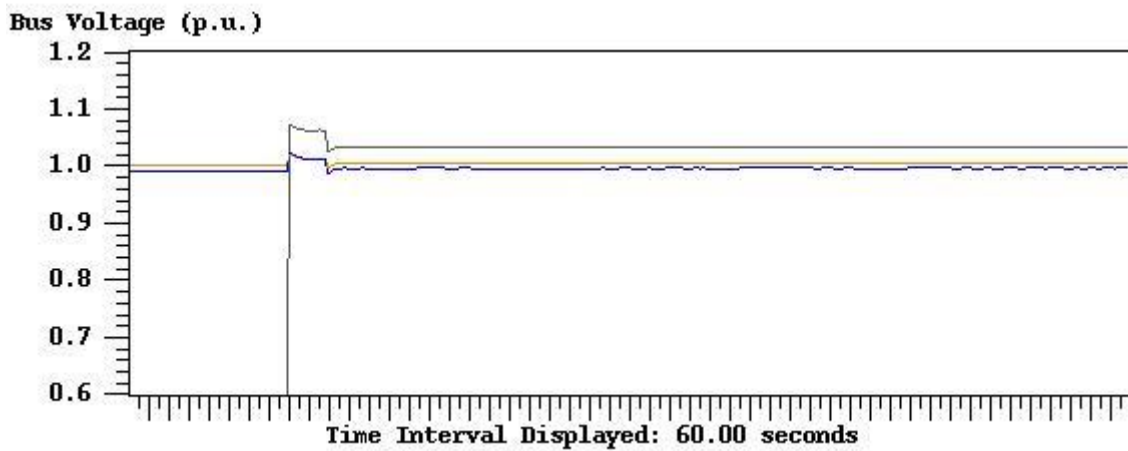


Figure 8.4 No hunting in Kärnan after adjusted threshold bands for strategy 2.

Table 8.3 Short circuit capacity, change of tolerance band and resulting voltage of nodes with random restoration strategy 3

Nodes with shunts	Vb(kV)	Va(kV)	Ssc(pu)	$\Delta V$ (kV)
Ruthuvud (Atomsberg)	442	335	0,93	62
Sydköping (Ruthuvud)	448	304	0,59	88
Blocket (Sydköping)	370	307	0,64	84
Norrås (Sydköping)	400	289	0,47	97
Kärnan (Norrås)	318	198	0,44	99

- CT22\_A400\_STORTR (0.60 - 1.20 p.u.)
- CT31\_A400\_STENFO (0.60 - 1.20 p.u.)
- FT42\_A400\_NORRÅS (0.60 - 1.20 p.u.)
- FT47\_B400\_ERIKSH (0.60 - 1.20 p.u.)
- FT62\_A400\_RUTHUV (0.60 - 1.20 p.u.)
- FT50\_A400\_SYDKÖP (0.60 - 1.20 p.u.)
- FT51\_A400\_BLOCKE (0.60 - 1.20 p.u.)
- FT44\_A400\_KÄRNAN (0.60 - 1.20 p.u.)

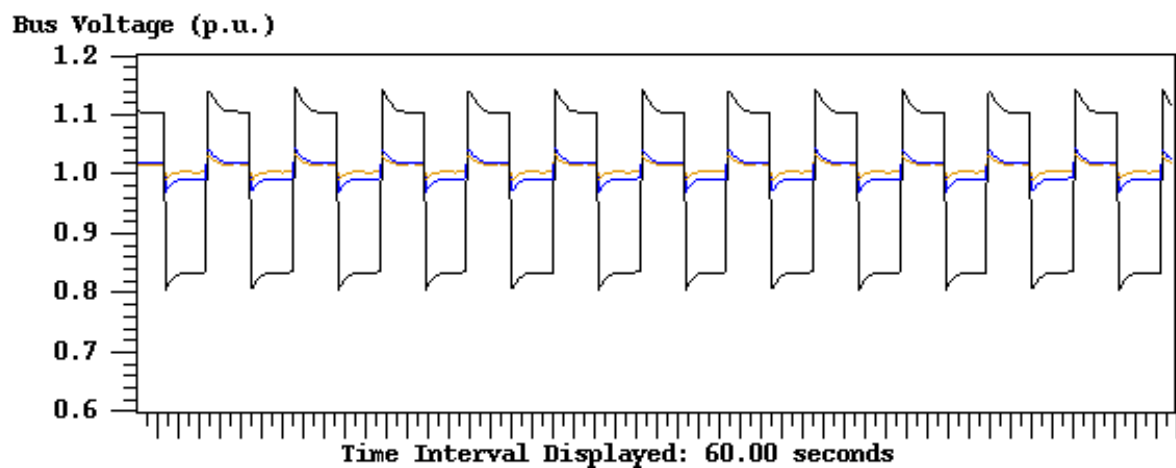


Figure 8.5 Hunting in Ruthuvud with default tolerance band for strategy 3.

- CT22\_A400\_STORTR (0.60 - 1.20 p.u.)
- CT31\_A400\_STENFO (0.60 - 1.20 p.u.)
- FT42\_A400\_NORRÅS (0.60 - 1.20 p.u.)
- FT47\_B400\_ERIKSH (0.60 - 1.20 p.u.)
- FT62\_A400\_RUTHUV (0.60 - 1.20 p.u.)
- FT50\_A400\_SYDKÖP (0.60 - 1.20 p.u.)
- FT51\_A400\_BLOCKE (0.60 - 1.20 p.u.)
- FT44\_A400\_KÄRNAN (0.60 - 1.20 p.u.)

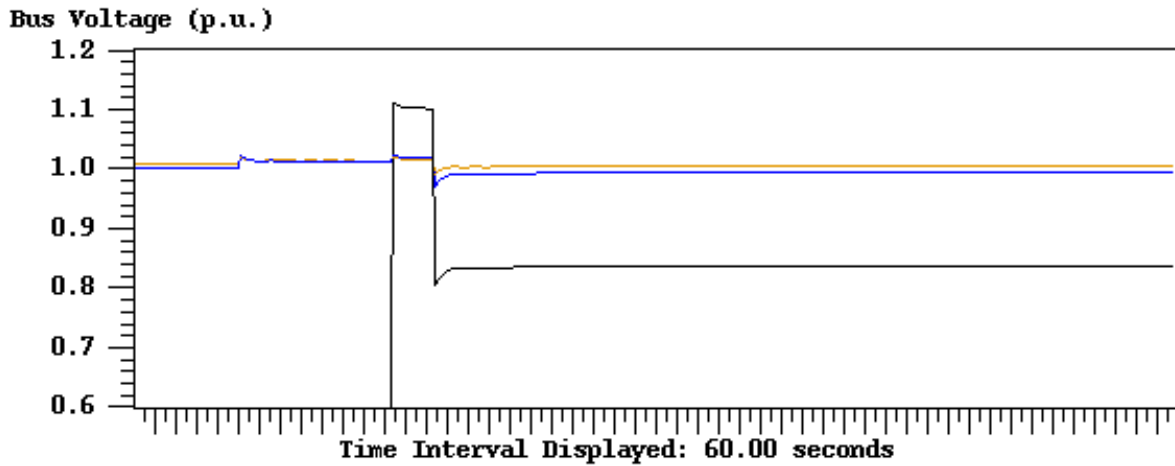


Figure 8.6 No hunting in Kärnan after adjusted tolerance bands for strategy 3.

Tables 8.4 and 8.5 are presented without graphs visualising hunting respectively no hunting, as the phenomena will look the same as in figure 8.5-8.6.

Table 8.4 Short circuit capacity, change of tolerance band and resulting voltage of nodes with random restoration strategy 4

Nodes with shunts	Vb(kV)	Va(kV)	Ssc(pu)	$\Delta V(kV)$
Ruthuvud (Atomsberg)	442	335	0,93	62
Norrås (Dalbo)	402	365	2,30	0
Kärnan (Norrås)	416	333	1,16	45
Sydköping (Norrås)	430	364	1,21	41
Blocket	402	362	1,07	52

Table 8.5. Short circuit capacity, change of tolerance band and resulting voltage of nodes with random restoration strategy 5

Nodes with shunts	Vb(kV)	Va(kV)	Ssc(pu)	$\Delta V$ (kV)
Kärnan (Tornå)	428	353	1,49	20
Norrås (Tornå)	431	402	1,56	15
Sydköping (Norrås)	391	323	1,09	50
Ruthuvud (Atomsberg)	447	340	0,92	63
Blocket (Sydköping)	442	388	0,70	79

In Figure 8.7 a graph is drawn that shows how the hunting is avoided for different nodes in the grid. This data is collected from all the strategies 1-5. The triangular and the crosses are data from all the nodes with default threshold bands. It can be seen that some of them experiences hunting (the ones with cross symbol). The square symbols show the same nodes as the cross and triangular symbols but when the thresholds has been adjusted. Here no hunting occurs at any node.

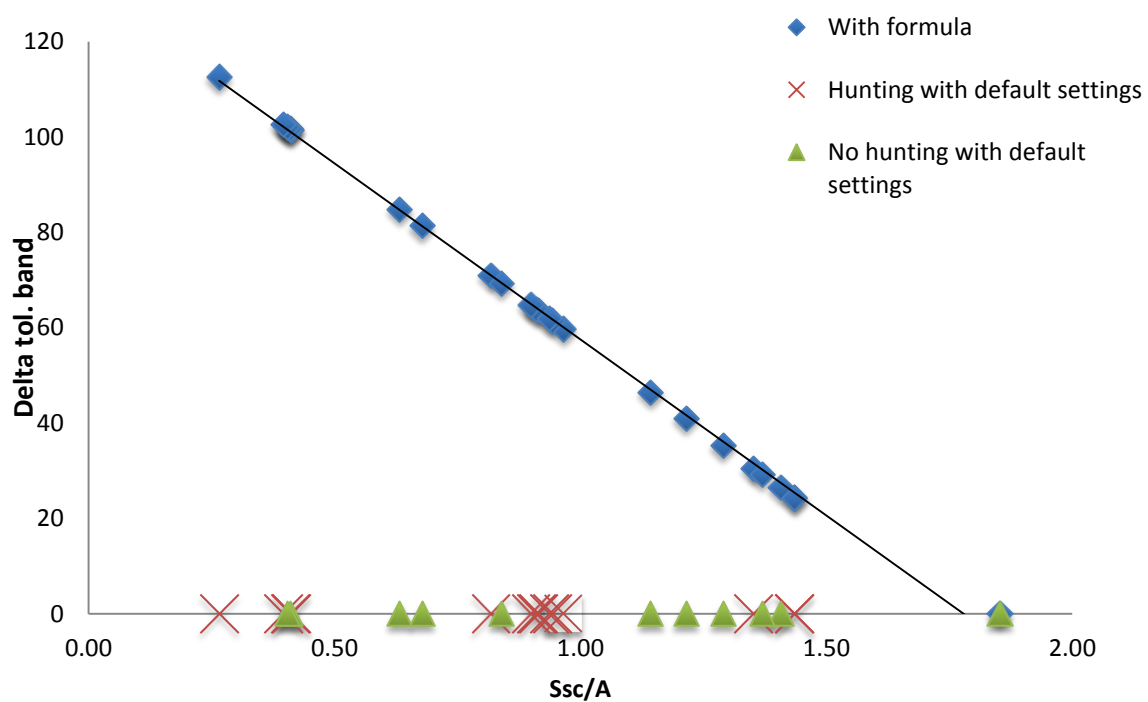


Figure 8.7 Graph showing that hunting is avoided for nodes under the line with hunting during default settings.

In this part one can make a comparison to the theory by plotting the corresponding graph to figure 6.4. One can here expect a scattered inverse relation.

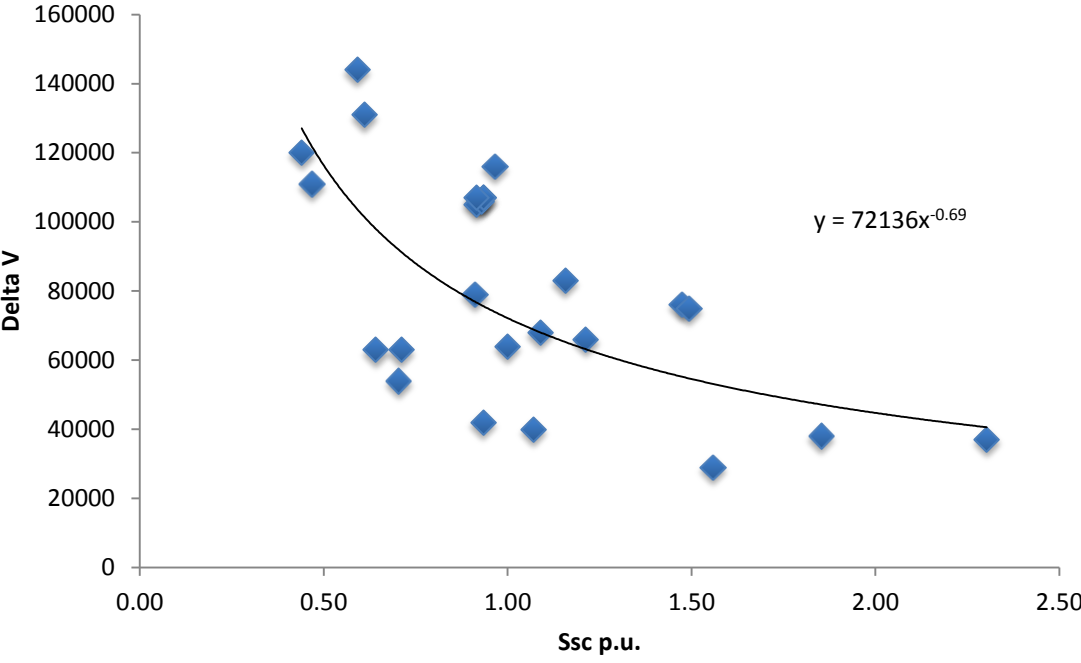


Figure 8.8 Delta V with the short circuit capacity from each node in during verification with trendline.

Compared to figure 6.4 the deviation of the points is larger. This is due to that the shunt reactor size in each node is held on its default value. That is to say, they all are not equal as in the data gathering part.





### 8.3 Larger blackout

In the previous verification scenarios the blackout are has been limited to only the southern part. Which is referred to all nodes below the mid-dotted line in nordic32. To see how well the formula work a larger blackout is simulated. This time the blackout area is the disconnect part in fig. 8.11.

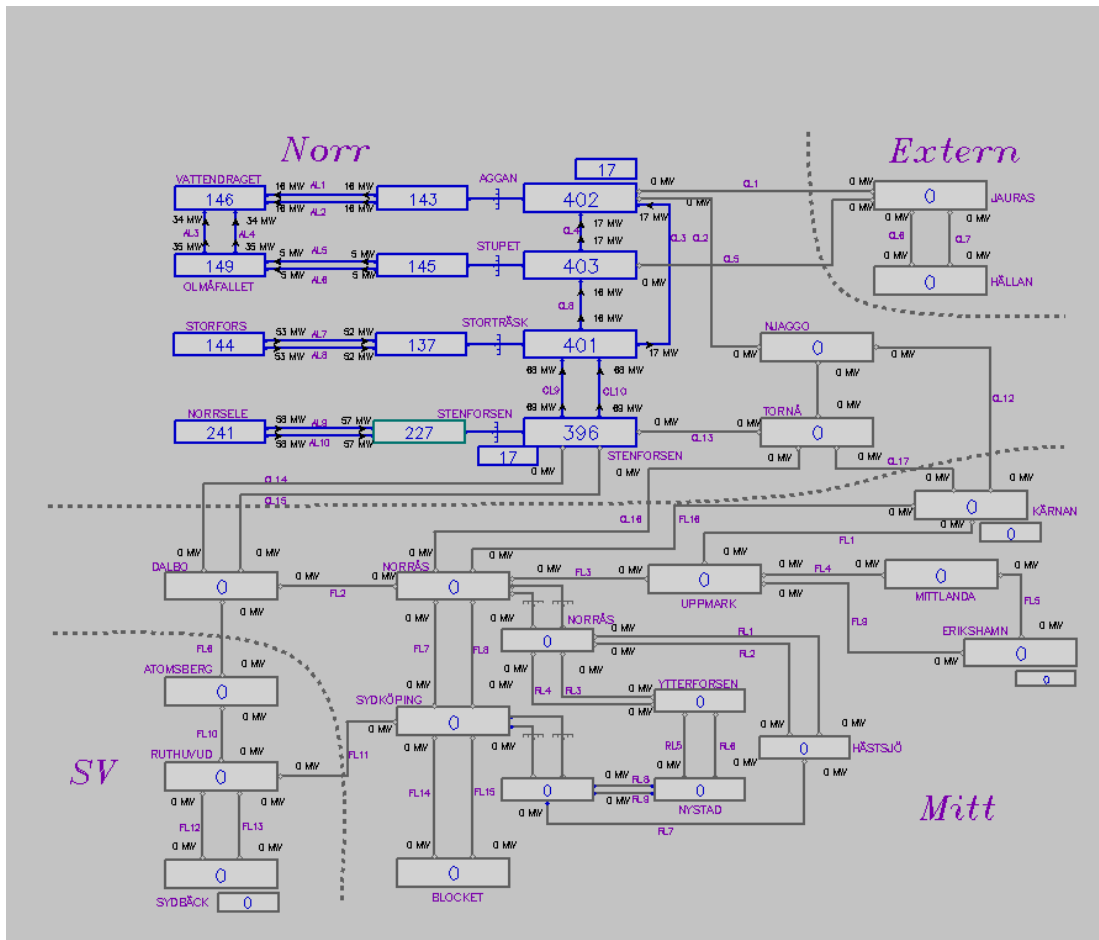


Figure 8.12 The initial large blackout scenario.

From here the energization with the formula will take place. The energization will be focused on first reach all nodes with shunt elements. In table 8.6 the build-up strategy with node voltages is presented.



Table 8.6 Short circuit capacity, change of tolerance band and resulting voltage of nodes when larger blackout

Nodes with shunts (from-to)	Vb(kV)	Va(kV)	Ssc(pu)	$\Delta V$ (kV)
Aggan-Njaggo	431	365	1,26	37
Aggan-Jauras	425	349	1,60	12
Jauras-Hällan	501	402	1,02	55
Stenforsen-Dalbo	435	410	1,68	6
Dalbo-Atomsberg-Ruthuvud	493	330	0,58	89
Dalbo-Norrås	409	347	0,97	60
Njaggo-Kärnan	501	323	0,52	94
Ruthuvud-Sydköping	449	282	0,30	110
Sydköping-blocket	353	287	0,31	109
Kärnan-Tornå	424	379	2,79	0

Again hunting is avoided. The voltages marked in green are the kept voltages after shunt action in the corresponding node. When all nodes with shunt elements are connected the node voltages can be seen in fig. 8.10.

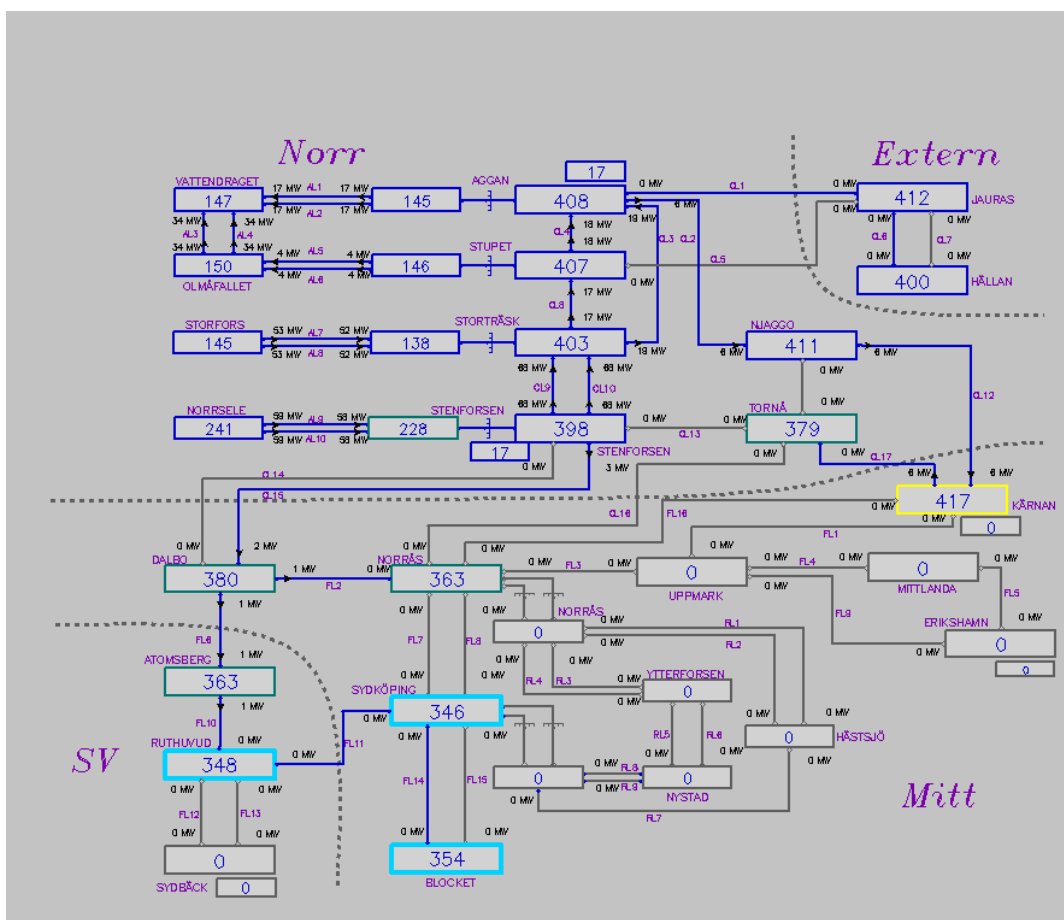


Figure 8.12 Energization of all nodes with shunt elements.

The voltages are kept at a decent level and no reactor hunting is detected so far. As the net is getting stronger and no other nodes with shunt elements will be connected, there is little risk to get hunting. From here the restoration process will look similar to the one in section 8.2, therefore a complete restoration is not necessary.

## 8.4 Northern blackout

To further investigate how well the formula works, a completely different scenario was simulated. This time with the northern part blacked out instead of the southern part. The initial scenario after the blackout can be seen in figure 8.13. The energization is made with the same method as in previous section 8.3.

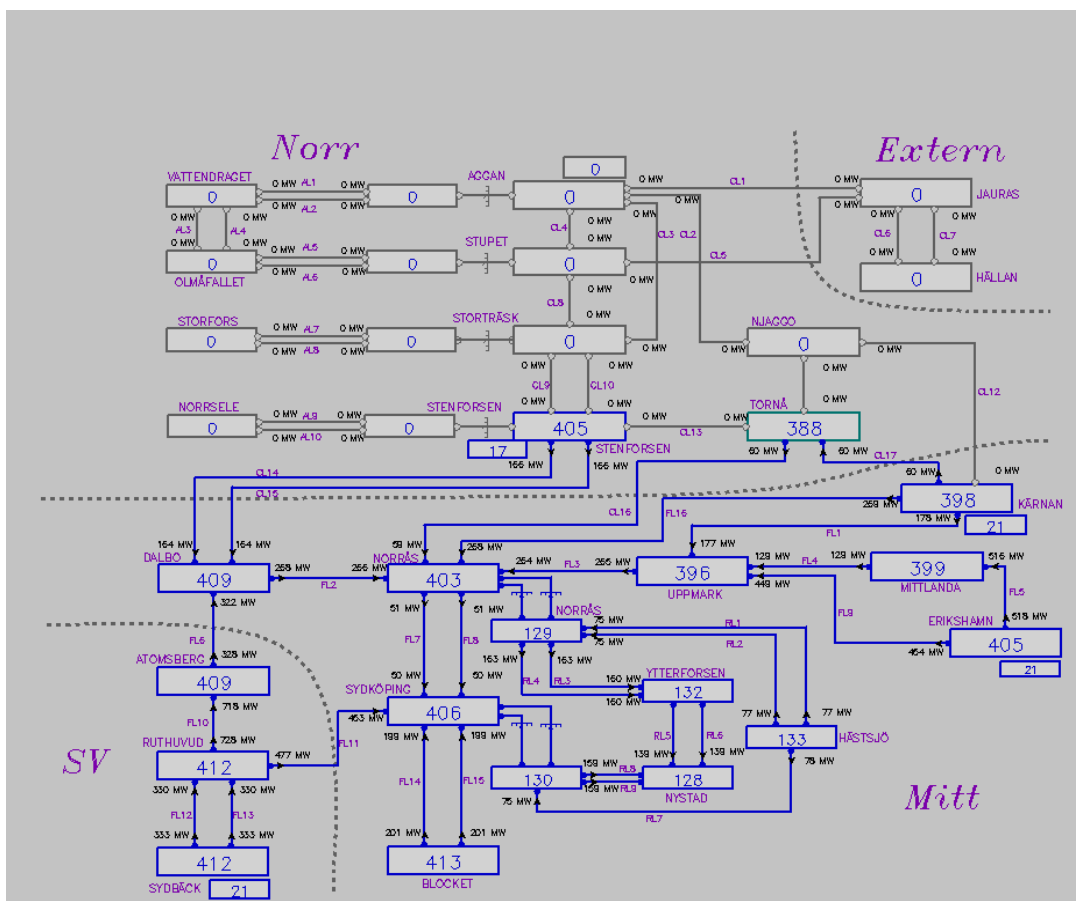


Figure 8.13 Northern blackout

The aim is to energize all nodes with shunt elements at the 400 kV level. The strategy used is shown in table 8.7.

Table 8.7 Resulting voltages, short circuit capacities and change of tolerance band after energization.

Nodes with shunts (from-to)	Vb(kV)	Va(kV)	Ssc(pu)	$\Delta V$ (kV)
Kärnan-Njaggo	450	381	1,31	34
Stenforsen-Storträsk	422	377	1,60	12
Storträsk-Stupet	408	382	2,80	0
Stupet-Aggan	390	384	12,3	0
Aggan-Jauras	389	333	1,98	0

In this simulation there were more switching events of the neighbouring shunts during the energization, compared to previous scenarios. This is due to the narrow tolerance bands, i.e. the nodes were “strong nodes” with large Ssc in this scenario. However no hunting was sustained and the voltage ended up on acceptable levels.

# 9 Discussion and conclusion

The result and verification of reactor hunting and HVDC performance is discussed in this chapter. There are comments on the theoretical analysis and the chapter finishes with thoughts on future work.

## 9.1 Reactor hunting

It can be clearly seen, in tables 5.1-5.4, that the  $S_{sc}$  is less in all the nodes during restoration compared with nodes in a complete functioning grid. This is mainly because the voltage change is larger due to less support by the rest of the grid. The reactive power difference is about the same. Since the  $S_{sc}$  changes considerably it works good as a control parameter for controlling the shunts. Meaning that for different  $S_{sc}$  the threshold levels in the shunt automatics will change with it, to avoid hunting in the weaker node.

Hunting can only occur when there is a possibility of overcompensation of reactive power. This means that the problem is more probable when the shunt reactors are of large capacity. It also means that if the voltage is high above threshold level, it is less chance of hunting than if the voltage is just a slightly above the threshold.

Since the hunting phenomenon is more likely with large reactors, a solution might be to adjust the threshold levels of the reactors so that large capacity means larger difference between maximum and minimum threshold level.

### 9.1.2 Reliability of verification

In fig 6.3 one can see how the found method works. If the tolerance band of the shunt automatics is changed due to the relation with  $S_{sc}$  on that particular line in fig. 6.3, hunting is avoided. It is a straight line and not inverse as one could expect, as there is an inverse relation between  $\Delta V$  and  $S_{sc}$  in the approximation (eq. 2.10). But the  $\Delta V$  in fig 6.3 represents needed change of tolerance to avoid hunting, which is not the same as in the approximation. There is only an inverse relation between  $\Delta V$  and  $S_{sc}$  in the approximation if  $Q$  is held constant but the reactive power drawn by the shunt reactor is not constant, the reactance ( $X$ ) is. The shunt draws less reactive power for low  $S_{sc}$ . This is because for low  $S_{sc}$  the voltage difference is high, that means  $V_a$  (after the shunt is connected) gets lower compared to if  $S_{sc}$  would be high. If the voltage  $V$  in eq. 9.1 is  $V_a$ , it can clearly be seen that  $Q$  gets lower for low  $V_a$  as  $X$  is constant.

$$X = \frac{V^2}{Q} \quad (\text{eq. 9.1})$$

That explains why there is no inverse relation in fig 6.3.

According to the verification result, hunting is avoided with the method. The relation used in the method is taken from extreme values from experiments. As a weakest path has been detected, random paths could be in somewhat pre-determined if they are weak or strong. So the experimental values of short circuit capacity and change of tolerance band are chosen to be closer to the weaker strategy. That makes the relation more reliable to prevent hunting.

The paths chosen are completely random without intention to make it weak. For all cases it works. To ensure the reliability a great number of tests should be made to receive a deviation factor for how often it works. In that way one could receive a probability of how often the method works, which would be of importance when deciding whether to use the method or not.

Even with a larger blackout hunting is avoided. The larger blackout makes the net weaker, thus it's higher risk of hunting. It is interesting to investigate on how the method works with scenarios that are very different from when the data gathering was made.

When a blackout in the north is simulated, the result is yet again that hunting is avoided. This improves the reliability that the method works in a completely different scenario. None of the energized nodes were used in previous scenarios. This gives motivation for applying the method in other power systems, e.g. in Denmark or Norway.

The resulting voltage levels in the different verification scenarios, see tables 8.1-8.5, were sometimes as low as 304 kV. According to Svenska Kraftnät this result is good but not completely enough, they would like the voltage to be 340 kV as a minimum. However, this project has been about avoiding hunting with little respect to keep the voltage at nominal level.

### **9.3 Discussion on theoretical analysis of Ssc**

The Ssc that is used in our method for power restoration is derived from eq. 2.7 and determined experimentally. This is because the system matrices for the model are not available in ARISTO. The theoretical comparison made in section 6.2 shows that the experimental method is reliable and supported by theory, as one can see that the relation between voltage difference and Ssc follows the same pattern as in fig. 6.5, which is made with circuit calculations on a PI-model.

To explain why there is a difference between fig. 6.4 and 6.5 one needs to remember that the PI-model is made with line parameters from the line between Tornå and Kärnan (in ARISTO). Whereas fig. 6.4 is created from many different nodes and therefore includes different line parameters for each point. In the approximation the source resistance is set to zero, this is not true.

It's very pleasing to see that the result from ARISTO can be confirmed in both Powerfactory and the theoretical model in Matlab. They are very close to a match. See table 9.1.

Table 9.1 Comparison between Ssc and Delta V when Kärnan is energized from Tornå

Model	Ssc(pu)	$\Delta V(kV)$
ARISTO	1.47	79
PowerFactory	1.47	82
Matlab	1.47	84.5

As the Ssc from ARISTO is a hand calculated approximation it won't be exact as in Matlab or PowerFactory (which doesn't use an approximation), but as they are very close one can rely on the method using the approximation. The reason why PowerFactory and Matlab differs is that in PowerFactory there is several different methods to calculate Ssc. Therefore it is hard to control how the Ssc is calculated.

Furthermore, in fig 6.4 it is stated that the deviation of data points is small. But as the shunt reactance in each node is the same, the deviation was expected to be zero. Apparently the nodes consume different amount of reactive power even though the capacity is the same. The reason is that when the capacity is set in each node, it is made at nominal voltage. And as the voltage is different in every node they will consume different amount of reactive power. That is why there is some deviation in fig 6.4.

During the verification part the shunt reactance was set to default setting (different for each node). That is why the deviation is larger in fig. 8.8. But as that is a realistic scenario, the result can be of more use.

What is highly desirable is of course to predict the voltage difference that will occur when the node is energized and the shunt reactor is connected. This would be possible if the Ssc is accessible e.g. through matrix calculations. By calculating the voltage difference, what is done in section 6.2, with the Ssc one can easily adjust the tolerance band of the shunt automatics. Then instead of doing it manually which is done in this thesis, one could install an automation system which take care of these calculations and set the tolerance band to the desirable limit.

The results in section 6.2, when the PI-model with a shunt reactor is investigated both in PowerFactory and numerically, are that the voltage difference is the same for each Ssc. This is expected as the models are exactly the same, but this gives validity to PowerFactory and simulations made in it. This means that simulations in PowerFactory can be used to find the Ssc in more complicated networks.

## 9.4 HVDC performance

The simulations made in PowerFactory, described in section 5.2, with a simple PI model connected with a HVDC link showed that the HVDC's reactive power injection really helped to keep the voltage at nominal level. Especially when the Ssc is low, i.e. in a weak node. Since the converter is controlled it can inject just the right amount of reactive power to raise the voltage and as what can be seen in

figure 7.3-7.6, the control is very fast. This is a big difference compared to shunt reactors, which just can be connected/disconnected with full capacity after a set time delay. In fig. 7.7 it can be seen how the VSC-HVDC consumes reactive power when a line is connected. At this point the HVDC isn't energising but it complements to prove the ability of the VSC-HVDC, that it can both consume and inject reactive power. With possibilities to control the reactive power in two directions, the VSC-HVDC converter possibly can be used during power restoration to stabilize the voltage at nodes with no load.

As a final investigation the VSC-HVDC energizes a PI-model, see fig. 5.4. The energization is successful and one can see that the voltage in the node after the PI-model, rises from 0 to 400 kV. That means HVDC now has the possibility to control the reactive power and energize nodes. This is completely necessary if to use HVDC in power system restoration. As no shunts are needed with VSC-HVDC, the restoration process can energize the net without that any hunting occurs. This will shorten the time to full power restoration.

From fig 7.7 one can see that if we energize with VSC-HVDC there is less voltage difference than with an AC voltage source. From that result one can confirm that when energizing with VSC-HVDC the risk of reactor hunting is less or at least the same as with an AC source. That means the use of shunts and EVA is not dependent on how the node is energized. Which gives the important conclusion that shunt reactors can continue to be used when restoring a power system with HVDC.

## 9.6 Future work

The work so far has been about adjusting the tolerance band in a way that hunting is avoided. That has been the purpose, without taking in consideration if the new tolerance band is realistic. Therefore a suggestion of continued work would be to see how this could be implemented in a way that only nodes that will have a realistic tolerance band will be connected. If the tolerance band is not realistic then the search should continue to find a stronger node.

In the verification, the tolerance band was adjusted back to default only when the whole net has been energized. It would be desirable to adjust the tolerance band continuously until the default setting is reached. In such way the restoration process would be less vulnerable for faults on equipment, which can prolonger a restoration even more.

The adjustment of the tolerance band is now made manually with our formula, experimentally derived. The goal is of course to implement an automatic control of the tolerance band. But for that the short circuit capacity is needed. As stated in many articles, e.g. [10], it is a non-trivial problem. Today's solutions include installed equipment in nodes and substations to measure a fault current. It's a very comprehensive to install such equipment, therefore a theoretical solution would be crucial.

Furthermore, the minimum voltage level during energization with the formula should be raised to meet the requirements from Svenska Kraftnät.

Next step regarding VSC-HVDC is to implement it in a large power grid and do power restoration with the HVDC.



# References

- [1] "Elavbrottet 23 september 2003 – händelser och åtgärder". Technical report. Svenska Kraftnät (Swedish TSO).
- [2] M. Larsson. "The impact of automatic shunt switching on voltage stability". MSc thesis. Lund University. 2012.
- [3] T. Gustafsson och D.Sipovac. "Inställning av automatiker med spänningsreglerande verkan" (in Swedish). MSc thesis. Kungliga Tekniska Högskolan. 2005.
- [4] L.Lindgren. "Automatic Power Restoration - Application of a Search Algorithm". Technical licentiate's thesis. Lund University. 2009
- [5] M. Karlsson. "Dynamisk modellering av VSC-HVDC" (In Swedish). MSc thesis. Uppsala University. 2011.
- [6] J. Duncan Glover. "Power System analysis and design". Fourth edition. Toronto: Thomson. 2008.
- [7] Woldeyesys Shire, Tamiru. "VSC-HVDC based Network Reinforcement". MSc. thesis. Delft University of Technology. 2009.
- [8] Svenska Kraftnät. Sydvästlänken (in Swedish). <http://www.svk.se/Projekt/Utbyggnadsprojekt/Sydvastlanken/>.2014. (downloaded 2014-04).
- [9] Så här funkar elnätet (in Swedish). <https://www.eon.se/privatkund/Produkter-och-priser/Elnat/Sa-har-funkar-elnetet/>. 2014. (downloaded 2014-05).
- [10] E. Ibrahim. "Experimental measurement of fault level for Sceco west". Research article. King Abdulaziz University. 2004.
- [11] List of HVDC projects. [http://en.wikipedia.org/wiki/List\\_of\\_HVDC\\_projects](http://en.wikipedia.org/wiki/List_of_HVDC_projects). 2014. (downloaded 2014-03).
- [12] Svenska Kraftnät projekt (in Swedish). <http://svk.se/Projekt/Utbyggnadsprojekt/>. 2014. (downloaded 2014-03).
- [13] "Long term dynamics part 2". Cigre Task Force 38-02-0 summary report. Cigre. 1995.
- [14] "What's new in PowerFactory version 14.1". Manual. Digsilent. 2011.
- [15] Example of the Ferranti effect. [http://nptel.ac.in/courses/Webcourse-contents/IIT-KANPUR/power-system/chapter\\_2/examp\\_2.4.html](http://nptel.ac.in/courses/Webcourse-contents/IIT-KANPUR/power-system/chapter_2/examp_2.4.html). 2014. (downloaded 2014-05).
- [16] K. Walve, A. Edström, "The Training Simulator ARISTO-Designand Experiences," IEEE PES Winter Meeting, 1999.

# Appendix A

## Paths for gathering data.

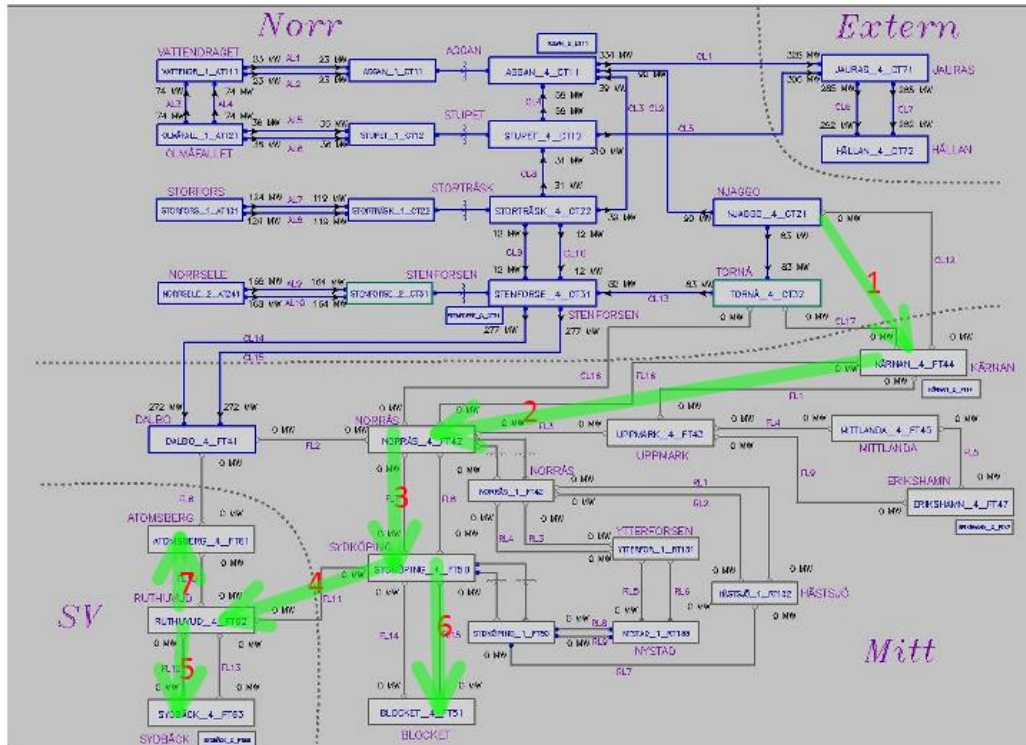


Figure A.1 Weakest path

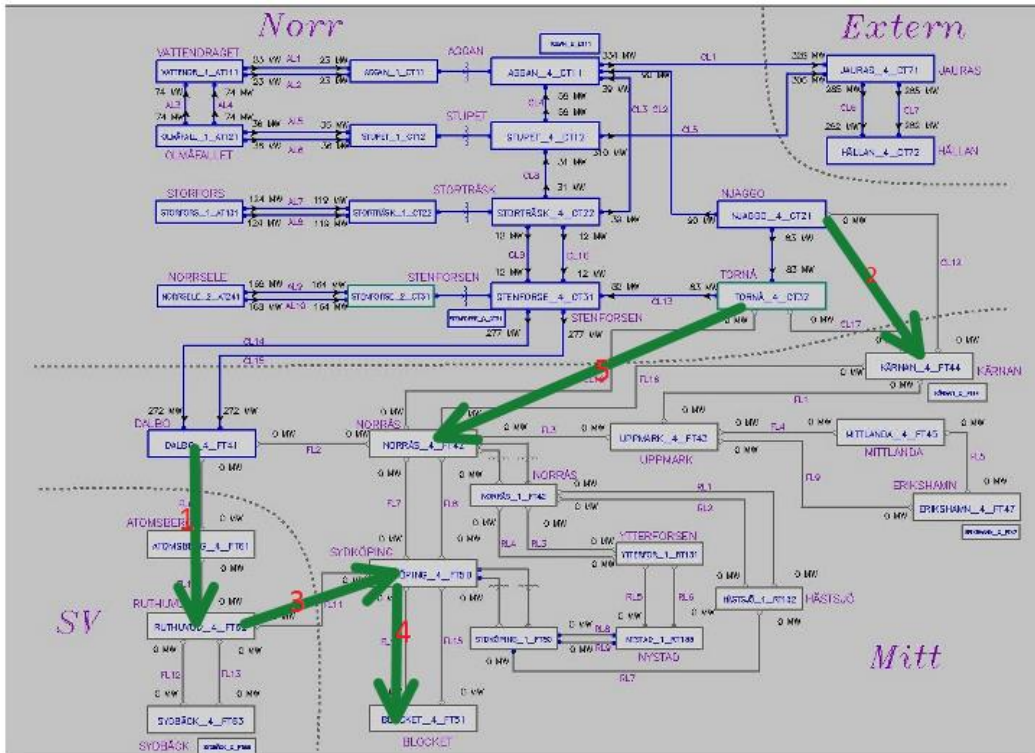


Figure A.2 Random path 1

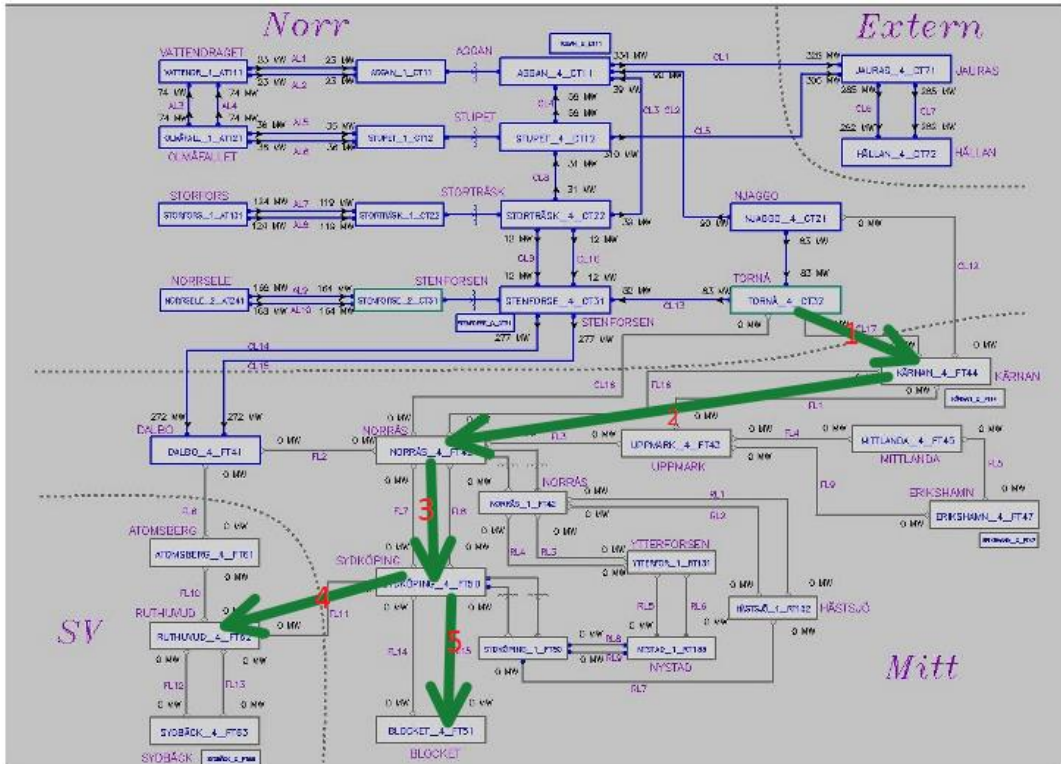


Figure A.3 Random path 2

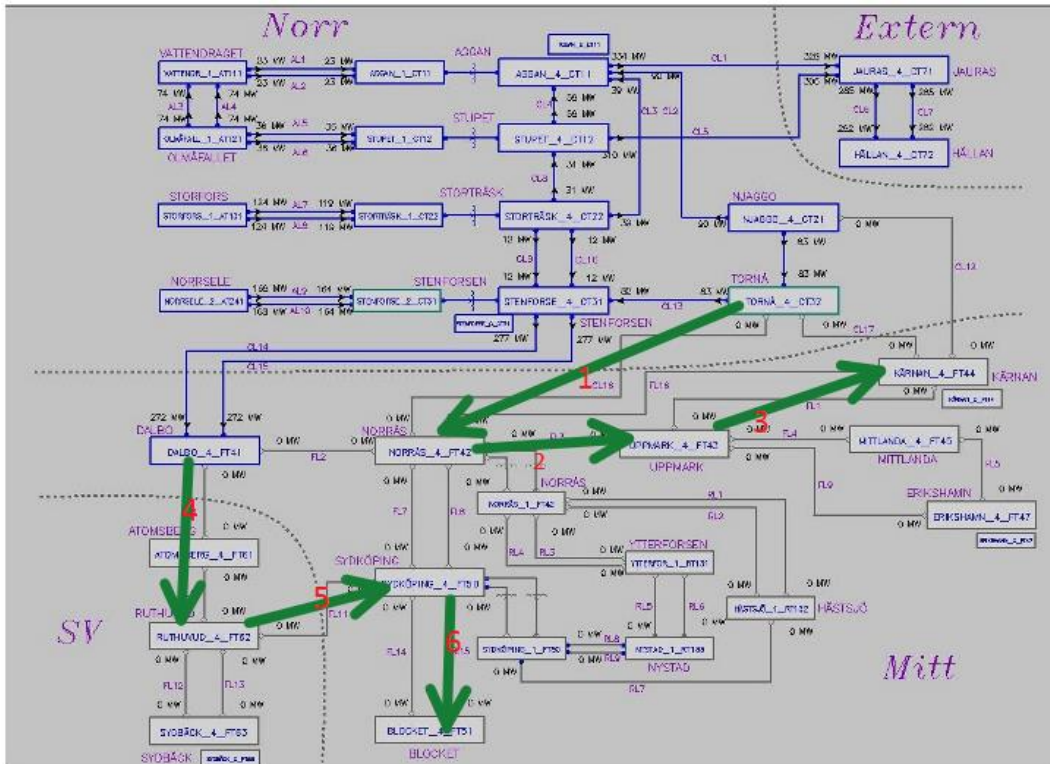


Figure A.4 Random path 3

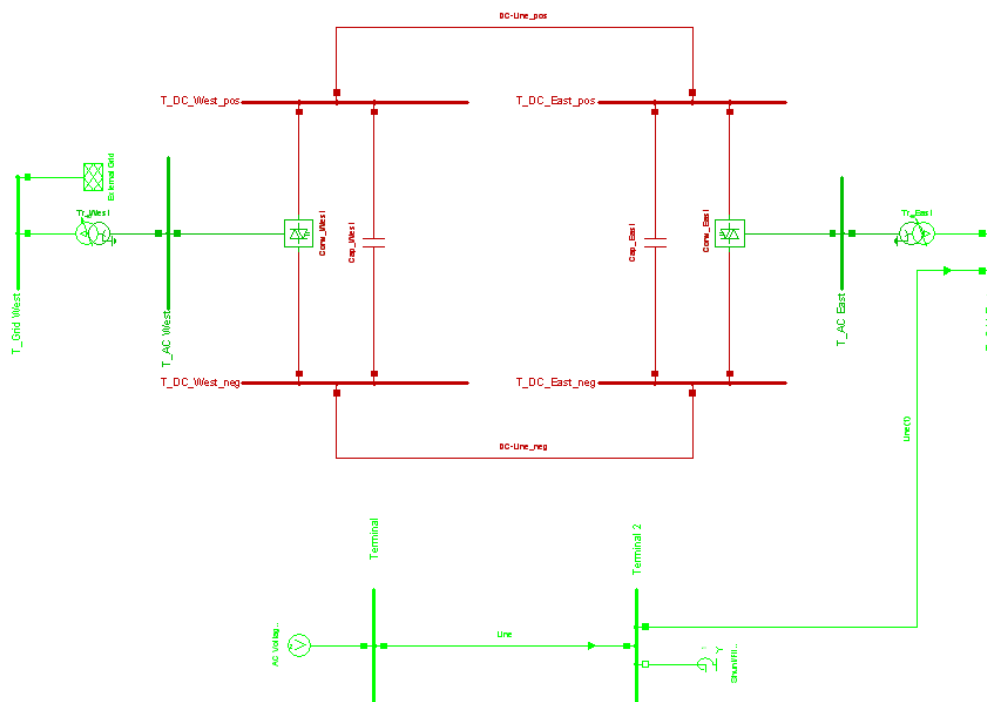


Figure A.4 Simple PI model connected with HVDC.

# Appendix B

## DC cable parameters

Length 400 km

Resistance 20 Ohm

Reactance 160 Ohm

Capacitance 0,01 micro Farad / km

Conductance 0 / km

Rated voltage 150 kV (positive and negative lines is together 300 kV)

### Matlab code:

```
% PI-MODEL with Xd and shunt reactor
```

```
close all;
```

```
DeltaV=[];
```

```
DeltaVHVDC=[];
```

```
Stesttot=[];
```

```
Stestputot=[];
```

```
B=0.1;
```

```
Vs=410000; % Voltage source.
```

```
for Xdreal=linspace(-100,1000,1000) % Using values of Xd from 0.1-10.
```

```
Vbase=400000;
```

```
Sbase=1000*10^6;
```

```
Zbase=Vbase^2/Sbase;
```

```
Xshunt=1i*457;
```

```
Rreal=16;
```

```
Xreal=107;
```

```
Z=Rreal+(1i*Xreal);
```

```
%Without shunt values
```

```
Xc1real=1/(1i*2*pi*50*(1*10^-6));
```

```
% Circuit calculations
```

```

X1=Z+Xc1real;
X2=(X1*Xc1real)/(X1+Xc1real);
Xth1=(1i*Xdreal*Xc1real)/(1i*Xdreal+Xc1real);
Xth2=Xth1+Z;
Xth=Xth2*Xc1real/(Xth2+Xc1real);
V2=abs((X2/(X2+1i*Xdreal))*Vs);
Vout=abs(Xc1real/(Z+Xc1real)*V2);

Stest=abs(Vs^2/(Xth));
Stestpu=Stest/Sbase;
Stesttot=[Stesttot Stest];
Stestputot=[Stestputot Stestpu];

%With shunt real. values

% Circuit calculations
X1s=(Xc1real*(Xshunt))/(Xc1real+Xshunt);
X2s=Z+X1s;
X3s=(X2s*Xc1real)/(X2s+Xc1real);
V2s=abs((X3s/(X3s+1i*Xdreal))*Vs);
Vsout=abs(X1s/(X1s+Z)*V2s);

DeltaV=[DeltaV (Vout-Vsout)/1000]; % Voltage difference with and without shunt.

end

figure();
plot(Stestputot,DeltaV)
xlabel('Ssc/pu');
ylabel('Delta V/kV');
axis([0 8 0 800]);
hold on;
S=Stestputot;
D=DeltaV;

```

